

**YALOVA UNIVERSITY ★ GRADUATE SCHOOL of SCIENCE ENGINEERING and  
TECHNOLOGY**

**INVESTIGATION OF BIO-OIL COMPOSITION PRODUCED FROM OLIVE  
POMACE CATALYTIC PYROLYSIS**

**M.Sc. THESIS**

**Şeyma HACIBEKTAŞOĞLU**

**Department of Energy Systems Engineering**

**Energy Systems Engineering Programme**

**JULY/2014**



**YALOVA UNIVERSITY ★ GRADUATE SCHOOL OF SCIENCE ENGINEERING AND  
TECHNOLOGY**

**INVESTIGATION OF BIO-OIL COMPOSITION PRODUCED FROM OLIVE  
POMACE CATALYTIC PYROLYSIS**

**M.Sc. THESIS**

**Şeyma HACIBEKTAŞOĞLU  
(115103007)**

**Department of Energy Systems Engineering**

**Energy Systems Engineering Programme**

**Thesis Advisor: Asst.Prof.Dr. Sibel BAŞAKÇILARDAN KABAĞCI**

**JULY/2014**



**YALOVA ÜNİVERSİTESİ ★ FEN BİLİMLERİ ENSTİTÜSÜ**

**ZEYTİN KÜSPESİNİN KATALİTİK PİROLİZİNDEN ELDE EDİLEN  
BİYO-YAĞIN BİLEŞİMİNİN İNCELENMESİ**

**YÜKSEK LİSANS TEZİ**

**Şeyma HACİBEKTAŞOĞLU  
(115103007)**

**Enerji Sistemleri Mühendisliği Anabilim Dalı**

**Enerji Sistemleri Mühendisliği Programı**

**Tez Danışmanı: Yrd.Doç.Dr. Sibel BAŞAKÇILARDAN KABAKCI**

**JULY/2014**



Şeyma HACIBEKTAŞOĞLU, a M.Sc. student of YALOVA Graduate School of Science, Engineering and Technology with student ID 115103007, successfully defended the thesis entitled “INVESTIGATION OF BIO-OIL COMPOSITION PRODUCED FROM OLIVE POMACE CATALYTIC PYROLYSIS”, which she prepared after fulfilling the requirements specified in the associated legislations, before the jury whose signatures are below.

**Thesis Advisor :** **Asst.Prof.Dr. Sibel BAŞAKÇILARDAN KABAKCI** .....  
Yalova University

**Jury Members :** **Prof.Dr. M. Halit GÖKNİL** .....  
Yalova University

**Asst. Prof. Dr. Didem OMA Y** .....  
Yalova University

**Asst.Prof.Dr. Sibel BAŞAKÇILARDAN KABAKCI** .....  
Yalova University

**Date of Submission : 12 June 2014**

**Date of Defense : 9 July 2014**





*To my loving grandfather,*



## **FOREWORD**

I would like to express my sincere gratitude to my thesis advisor, Asst. Prof. Dr. Sibel BAŞAKÇILARDAN KABAKCI; her extensive professional knowledge, constant support and encouragement helped me proceed through my studies, and also lead me to become a researcher.

I heartily would like to thank Prof. Dr. Filiz KARAOSMANOĞLU from whom I have had the honor to take the graduate courses for my master education. Also, my deepest thanks to Çağdaş ÇAĞLI and his colleagues for their technical support with the pyrolysis system. I would also like to thank Muhammet ÇAKIR for GC-MS analysis of bio-oil samples. Besides, I am grateful to my dear colleague and friend Hilal AYDEMİR for her assistance during laboratory work.

Most of all, I would like to use this opportunity to give my deepest thanks to my parents for their support, patience and understanding during the writing of my thesis.

June 2014

Şeyma HACIBEKTAŞOĞLU  
Chemical Engineer, B.Sc.



## TABLE OF CONTENTS

	<u>Page</u>
<b>FOREWORD</b> .....	<b>ix</b>
<b>TABLE OF CONTENTS</b> .....	<b>xi</b>
<b>ABBREVIATIONS</b> .....	<b>xiii</b>
<b>LIST OF TABLES</b> .....	<b>xv</b>
<b>LIST OF FIGURES</b> .....	<b>xvii</b>
<b>SUMMARY</b> .....	<b>xix</b>
<b>ÖZET</b> .....	<b>xxi</b>
<b>1.INTRODUCTION</b> .....	<b>1</b>
<b>2. FUNDAMENTALS OF BIOMASS PYROLYSIS</b> .....	<b>5</b>
2.1.1 Temperature .....	6
2.1.2 Particle Size.....	6
2.1.3 Heating Rate.....	7
2.1.4 Residence Time and Sweeping Gas Flow Rate .....	7
2.1.5 Biomass Composition .....	8
2.1.6 Catalyst Effect.....	10
2.2 Pyrolysis Mechanism .....	12
2.3 Pyrolysis Products .....	13
2.3.1 Gas .....	13
2.3.2 Char.....	13
2.3.3 Pyrolysis Oil (Bio-oil).....	14
2.3.3.1 Bio-oil Characteristics.....	14
2.3.3.2 Utilisation of Bio-oil .....	16
<b>3. UTILISATION OF CATALYSTS IN BIOMASS PYROLYSIS</b> .....	<b>19</b>
3.1 System Configurations for Catalysts Used in Biomass Pyrolysis.....	19
3.1.1 Catalyst Bed Method (In-situ).....	19
3.1.2 Catalyst Mixing Method (In-bed) .....	20
3.2 Metal Oxide Catalysts .....	21
3.3 Zeolite catalysts.....	23
3.3.1 ZSM-5 Zeolite.....	25
3.3.1.1 Shape selectivity of ZSM-5.....	26
3.3.1.2 Acidity of ZSM-5.....	28
3.4 General Effects of Catalysts on Bio-oil.....	30
3.4.1 Aromatic yield of bio-oil.....	30
3.4.2 Acidity of bio-oil.....	32
3.4.3 Viscosity of bio-oil.....	33
3.4.4 Stability of bio-oil .....	34
<b>4. DEACTIVATION AND REGENERATION OF CATALYSTS</b> .....	<b>37</b>
<b>5. EXPERIMENTAL METHODS</b> .....	<b>39</b>
5.1 Materials .....	39
5.1.1 Feedstock Characterization .....	39

5.1.3 Catalyst Properties.....	40
5.2 Experimental Procedure .....	40
5.2.1 Thermogravimetric Analysis.....	40
5.2.2 Differential Scanning Calorimetry (DSC) Analysis .....	41
5.2.3 Pyrolysis Experiments.....	41
<b>6. RESULTS AND DISCUSSION.....</b>	<b>45</b>
6.1 Thermal Behavior.....	45
6.2 Differential Scanning Calorimetry (DSC) Analysis.....	56
6.3 Kinetics of Olive Pomace Pyrolysis with ZSM-5 .....	57
6.4 Effect of Catalyst to Product Yields.....	63
6.5 Compositional Analysis of Bio-oil.....	64
<b>7.CONCLUSION.....</b>	<b>73</b>
<b>REFERENCES.....</b>	<b>75</b>
<b>CURRICULUM VITAE.....</b>	<b>85</b>

## **ABBREVIATIONS**

<b>ASTM</b>	: American Society for Testing and Materials
<b>BET</b>	: Brunauer–Emmett–Teller
<b>DCM</b>	: Dichloromethane
<b>DSC</b>	: Differential Scanning Calorimetry
<b>DTG</b>	: Differential Thermal Gravimetry
<b>IZA</b>	: International Zeolite Association
<b>LMW</b>	: Low Molecular Weight
<b>PAHs</b>	: Polycyclic Aromatic Hydrocarbons
<b>RDF</b>	: Refused Derived Fuel
<b>SEC</b>	: Size Exclusion Chromatography





## LIST OF TABLES

	<u>Page</u>
<b>Table 2.1</b> : Product yields based on pyrolysis operating parameters and reactor types... ..	11
<b>Table 3.1</b> : Physicochemical properties of zeolites most commonly used.....	25
<b>Table 5.1</b> : Main characteristics of olive pomace .....	39
<b>Table 5.2</b> : Textural properties of ZSM-5 .....	40
<b>Table 6.1</b> : Rate equations .....	58
<b>Table 6.2</b> : Kinetic parameters .....	58
<b>Table 6.3</b> : Product yields and conversion from olive pomace pyrolysis .....	63
<b>Table 6.4</b> : Methanol fraction of olive pomace bio-oil with and without the addition of catalyst... ..	70
<b>Table 6.5</b> : DCM fraction of olive pomace bio-oil with and without the addition of catalyst.....	72



## LIST OF FIGURES

	<u>Page</u>
<b>Figure 2.1</b> : Schematic of pyrolysis in a biomass particle.....	5
<b>Figure 2.2</b> : Reaction pathway for cellulose pyrolysis.....	12
<b>Figure 3.1</b> : Different frameworks of zeolites with sodalite cage structure.....	23
<b>Figure 3.2</b> : (a) pentasil unit and pentasil chain (b) framework of ZSM-5 zeolite..	26
<b>Figure 3.3</b> : Pore structure of ZSM-5 zeolite.....	27
<b>Figure 3.4</b> : An example of transition state effect of ZSM-5: suppression of trimethylbenzene formation during meta-xylene isomerization.....	27
<b>Figure 3.5</b> : An example of transition state effect of ZSM-5: suppression of trimethylbenzene formation during meta-xylene isomerization.....	30
<b>Figure 3.6</b> : The effect of CaO catalyst to viscosity of bio-oil .....	34
<b>Figure 5.1</b> : (a) Experimental setup for pyrolysis of olive pomace (b) sequential condensers for trapping pyrolysis vapors .....	42
<b>Figure 5.2</b> : (a) olive pomace in dried and grinded form (b) bio-oil samples dissolved in methanol .....	42
<b>Figure 6.1</b> : TG profiles of olive pomace at different heating rate .....	46
<b>Figure 6.2</b> : DTG profiles of olive pomace at different heating rate .....	46
<b>Figure 6.3</b> : TG and DTG profile of olive pomace at a constant heating rate of 10°C.min <sup>-1</sup> with catalyst to biomass ratio of 1:1.....	47
<b>Figure 6.4</b> : TG and DTG profile of olive pomace at a constant heating rate of 30°C.min <sup>-1</sup> with catalyst to biomass ratio of 1:1.....	48
<b>Figure 6.5</b> : TG and DTG profile of olive pomace at a constant heating rate of 40°C.min <sup>-1</sup> with catalyst to biomass ratio of 1:1.....	49
<b>Figure 6.6</b> : TG and DTG profile of olive pomace at a constant heating rate of 10°C.min <sup>-1</sup> with catalyst to biomass ratio of 1:2.....	50
<b>Figure 6.7</b> : TG and DTG profile of olive pomace at a constant heating rate of 30°C.min <sup>-1</sup> with catalyst to biomass ratio of 1:2.....	51
<b>Figure 6.8</b> : TG and DTG profile of olive pomace at a constant heating rate of 40°C.min <sup>-1</sup> with catalyst to biomass ratio of 1:2.....	52
<b>Figure 6.9</b> : TG and DTG profile of olive pomace at a constant heating rate of 10°C.min <sup>-1</sup> with catalyst to biomass ratio of 1:3.....	53
<b>Figure 6.10</b> : TG and DTG profile of olive pomace at a constant heating rate of 30°C.min <sup>-1</sup> with catalyst to biomass ratio of 1:3.....	54
<b>Figure 6.11</b> :TG and DTG profile of olive pomace at a constant heating rate of 40°C.min <sup>-1</sup> with catalyst to biomass ratio of 1:3.....	55
<b>Figure 6.12</b> :DSC profiles of olive pomace pyrolysis at heating rate of 20 °C.min <sup>-1</sup> ....	56
<b>Figure 6.13</b> :DSC profiles of olive pomace pyrolysis at heating rate of 40 °C.min <sup>-1</sup> ...	56
<b>Figure 6.14</b> :Plots obtained by Coats-Redfern method for determination of activation energy for olive pomace at the heating rate of 10 °C.min <sup>-1</sup> .....	59

<b>Figure 6.15</b> :Plots obtained by Coats-Redfern method for determination of activation energy for olive pomace at the heating rate of 30 °C.min <sup>-1</sup> .....	59
<b>Figure 6.16</b> :Plots obtained by Coats-Redfern method for determination of activation energy for olive pomace at the heating rate of 40 °C.min <sup>-1</sup> .....	60
<b>Figure 6.17</b> :Plots obtained by Coats-Redfern method for determination of activation energy for olive pomace:ZSM-5 (1:1) at the heating rate of 10 °C.min <sup>-1</sup> ... ..	60
<b>Figure 6.18</b> :Plots obtained by Coats-Redfern method for determination of activation energy for olive pomace:ZSM-5 (1:1) at the heating rate of 30 °C.min <sup>-1</sup> ... ..	60
<b>Figure 6.19</b> :Plots obtained by Coats-Redfern method for determination of activation energy for olive pomace:ZSM-5 (1:1) at the heating rate of 40 °C.min <sup>-1</sup> ... ..	61
<b>Figure 6.20</b> :Plots obtained by Coats-Redfern method for determination of activation energy for olive pomace:ZSM-5 (1:2) at the heating rate of 10 °C.min <sup>-1</sup> ... ..	61
<b>Figure 6.21</b> :Plots obtained by Coats-Redfern method for determination of activation energy for olive pomace:ZSM-5 (1:2) at the heating rate of 30 °C.min <sup>-1</sup> ... ..	61
<b>Figure 6.22</b> :Plot obtained by Coats-Redfern method for determination of activation energy for olive pomace:ZSM-5 (1:2) at the heating rate of 40 °C.min <sup>-1</sup> ... ..	62
<b>Figure 6.23</b> :Plots obtained by Coats-Redfern method for determination of activation energy for olive pomace:ZSM-5 (1:3) at the heating rate of 10 °C.min <sup>-1</sup> ... ..	62
<b>Figure 6.24</b> :Plots obtained by Coats-Redfern method for determination of activation energy for olive pomace:ZSM-5 (1:3) at the heating rate of 30 °C.min <sup>-1</sup> ... ..	62
<b>Figure 6.25</b> :Plot obtained by Coats-Redfern method for determination of activation energy for olive pomace:ZSM-5 (1:3) at the heating rate of 40 °C.min <sup>-1</sup> ... ..	63
<b>Figure 6.26</b> : GC-MS spectrum of olive pomace bio-oil dissolved in methanol .....	65
<b>Figure 6.27</b> : GC-MS spectrum of bio-oil with olive pomace: ZSM-5 mixture (1:1) dissolved in methanol .....	66
<b>Figure 6.28</b> : GC-MS spectrum of bio-oil with olive pomace: ZSM-5 mixture (1:2) dissolved in methanol.....	67
<b>Figure 6.29</b> : GC-MS spectrum of olive pomace bio-oil dissolved in DCM ... ..	68
<b>Figure 6.30</b> : GC-MS spectrum of bio-oil with olive pomace: ZSM-5 mixture (1:1) dissolved in DCM.....	69

## INVESTIGATION OF BIO-OIL COMPOSITION PRODUCED FROM OLIVE POMACE CATALYTIC PYROLYSIS

### SUMMARY

Biomass, one of the fuel alternatives of the future, is an abundant renewable energy resource. In this study, olive oil production waste (olive pomace) was used as biomass resource. Catalysed and non-catalysed pyrolysis processes were conducted in a tubular furnace with catalyst mixing method. Also, kinetics of catalytic and non-catalytic pyrolysis of olive pomace was investigated, using thermogravimetric analysis.

The thermogravimetry experiments were conducted non-isothermally at atmospheric pressure and at temperatures ranging from 20°C to 800°C under inert (N<sub>2</sub>) atmosphere. In order to find and compare the kinetic parameters (activation energy and frequency factor) for the catalytic and non-catalytic pyrolysis, three different heating rates (10, 30, 40 °C.min<sup>-1</sup>) were studied. Catalyst effect of olive pomace pyrolysis was also investigated using different biomass to catalyst ratios, which are 1:1, 1:2, 1:3 (wt., %db). In the absence of ZSM-5, olive pomace sample was pyrolyzed via thermogravimetric analyzer thus allowing us to compare the effect of ZSM-5 to traditional pyrolysis of biomass. Thermal behavior of ZSM-5, under the same process conditions, was investigated in order to evaluate the overall system. Olive pomace was pyrolyzed in one step, which was a combination of 2 stages, namely hemicellulose decomposition and cellulose decomposition. Lignin decomposition was observed in a broad range of temperature, which was above 400°C. At high heating rates and with catalyst, the decomposition of hemicellulose was not detected as a hump in the characteristic peak. Decomposition was seen as a one step reaction. Adding catalyst decreased the activation energy but did not change the peak temperatures. ZSM-5 was found to be a good catalyst to decrease the activation energy. As a result of DSC experiments, the pyrolysis reaction was found to be endothermic.

The pyrolysis experiments were carried out at 500°C, at the heating rate of 25 °C.min<sup>-1</sup>. Nitrogen gas was used as sweeping gas in the experiments and the flow rate of nitrogen was 100 L.h<sup>-1</sup> during the process. The catalytic effect of ZSM-5 was investigated using biomass to catalyst ratios of 1:1 and 1:2 (wt.,%db). With the biomass to catalyst ratio of 1:1, phenolic compounds were decreased, however, with higher catalyst amount almost all the oxygenates were eliminated. The shape selectivity of ZSM-5 was in favor of naphthalene (and its derivatives) and benzene derivatives, thus increasing the aromatic content of bio-oil.



## ZEYTİN KÜSPESİNİN KATALİTİK PİROLİZİNDEN ELDE EDİLEN BİYO-YAĞIN BİLEŞİMİNİN İNCELENMESİ

### ÖZET

Geleceğin yakıt alternatiflerinden biri olan biyokütle, yenilenebilir enerji kaynaklarının başında gelmektedir. Bu çalışmada, zeytinyağı üretim atıkları (zeytin küspesi) biyokütle kaynağı olarak kullanılmıştır. Katalizörlü ve katalizörsüz piroliz deneyler boru tipi fırın reaktörde gerçekleştirilmiştir. Ayrıca, zeytin küspesinin piroliz kinetiği (katalizörlü ve katalizörsüz) termogravimetrik analizör kullanılarak araştırılmıştır.

Termogravimetri deneyleri atmosferik basınçta azot ortamında ve 20-800 °C sıcaklık aralığında gerçekleştirilmiştir. Katalizörlü ve katalizörsüz deneyler için piroliz profili ve kinetik parametreleri (aktivasyon enerjisi ve frekans faktörü) üç farklı ısıtma hızına göre (10, 30, 40 °C.dk<sup>-1</sup>) elde edilmiştir. Zeytin küspesinin katalitik pirolizi için üç farklı katalizör:biyokütle oranıyla (1:1, 1:2, 1:3 %ağ., kb) çalışılmıştır. Zeytin küspesinin piroliz davranışı ZSM-5 kullanılmadan termogravimetrik analizörde incelenmiştir. Böylece, ZSM-5'in termal pirolize olan katalitik etkisi değerlendirilmiştir. Aynı sistem koşulları altında, ZSM-5'in termal davranışı tüm sistemi değerlendirmek açısından incelenmiştir. TGA (termogravimetrik analiz) sonuçlarına göre zeytin küspesinin pirolizi, hemiselüloz ve selüloz bileşenlerinin degradasyonunu içeren tek bir aşamayı kapsayan bozunma olarak değerlendirilebilir. Ligninin bozunması holoselüloza göre daha geniş sıcaklık aralığında (>400 °C) gerçekleşmiştir. Katalizör kullanılması durumunda, yüksek ısıtma hızında zeytin küspesinin bozunması tek aşamalı reaksiyon olarak görülmüştür, hemiselüloz bozunmasını gösteren tümsek, ilgili pikte görülmemiştir. ZSM-5'in zeytin küspesinin pirolizinde kullanılması aktivasyon enerjisini düşürücü etki göstermiştir ancak, pik sıcaklıklarını değiştirmemiştir. DSC çalışmalarında ise, hem zeytin küspesi pirolizinin hem de ZSM-5 varlığında katalitik pirolizin endotermik bir reaksiyon olduğu görülmektedir.

Zeytin küspesinden biyo-yag eldesi için yapılan deneyler ise, 500 °C sıcaklıkta ve 25 °C.dk<sup>-1</sup> ısıtma hızında azot ortamında gerçekleştirilmiştir. Boru tipi fırın reaktörde gerçekleştirilen deneylerde azot gazı 100 L.h<sup>-1</sup> hızında sistemden geçirilmiştir. ZSM-5'in katalitik etkisini görmek amacıyla 1:1 ve 1:2 oranında biyokütle: katalizör karışımları kullanılmıştır. Biyokütle katalizör oranının 1:1 olduğu deneylerde, biyo-yagda bulunan fenolik bileşikler referans biyoyağa kıyasla azalmıştır. Ancak katalizör miktarı artırıldığında oksijenli bileşiklerin tamamına yakını elimine edilmiş, ve ZSM-5 naftalin ve türevlerinin, benzen türevlerinin oluşumuna seçicilik göstererek biyoyağdaki aromatik içeriğini artırmıştır.





## **1.INTRODUCTION**

The continuous growth in economies over the world requires demand for energy at a high rate. High energy production via fossil fuels leads to an increase in CO<sub>2</sub> emissions. In addition, considering the issue in terms of the effects of global climate change and environmental responsibility, the need for renewable energy resources has become inevitable. Also, diminishing reserves of fossil fuels and the necessity of reducing CO<sub>2</sub> emissions that is emitted by fossil fuel burning processes, force us to seek environmentally and economically beneficial ways to produce energy from renewable energy resources [1-5].

Biomass, as a renewable energy resource, is regarded as CO<sub>2</sub> neutral. Because, the carbon associated with combustion of biomass is considered a part of natural cycle. Carbon emissions are released into the atmosphere and re-captured by the biomass species, thus maintaining a carbon balance. Given the fact that biomass is abundant and it accounts for 38-43% of primary energy consumption in developing countries, the use of waste based biomass sources and feedstocks is of utmost importance for research in terms of clean energy generation via thermochemical or biochemical conversion processes [6-8]. Agricultural wastes, energy crops, industrial wastes, wood and wood wastes, municipal solid waste, food processing wastes can be included in primary biomass resources [8]. Among the renewable resources, olive pomace, which is a olive oil production waste with relatively high energy value of around 18 MJ/kg, is used to convert its stored energy into biofuel materials through combustion, gasification and pyrolysis [5,9-12].

The Mediterranean area covers almost 98% of the olive production and according to statistics data obtained from International Olive Oil Council (IOOC), the annual olive oil production in Turkey is 195,000 tones per year with an increase of 2.1%. [13]. The traditional olive oil production process covers following steps: (1) separation of olives and the leaves via vibrating screen and air blowers, (2) crushing of olives in stone mills, (3) mixing of olive paste to increase the oil yield, (4)

pressing the paste and removing the oil. Final product after removing the olive oil, which is called olive pomace is mixed with hot water and pressed again. Then, olive oil is separated from the oil-water emulsion, and the pomace is dried for final disposal [12]. Approximately, 100 kg of feedstock fed into the olive oil production process yields 15-22 kg olive oil, 35-45 kg olive pomace and the rest is called olive mill waste water. In Turkey, olive pomace production is 200,000 tones per year. Most of the olive pomace produced is discarded into waste lands or used as solid fuel via combustion processes, which causes environmental problems [14]. Therefore, olive oil residues and wastes are of great concern in terms of environmental safety and energy management.

Pyrolysis is a thermochemical conversion process in the absence of an oxidizing agent and can be regarded as the initial stage of gasification and combustion. Solid char, liquid pyrolysis oil and gas are the main products of biomass pyrolysis. The amount of products and their fractions are influenced by many factors such as heating rate, pyrolysis temperature, biomass composition and catalyst effect [8,15,16]. Since biomass pyrolysis is feedstock composition-dependent process, finding suitable catalysts to regulate pyrolysis processes is an alternative way to reduce overall energy consumption [17]. Also, catalytic pyrolysis of biomass provides, with optimum catalyst/biomass ratio, chemically more homogenous fractions of pyrolysis products. In recent years, different biomass feedstock or biomass originated waste materials has been studied using several catalysts in order to understand the effects of catalyst to pyrolysis process [18-24].

Bio-oil possesses many undesirable properties, such as high content of volatile acids, water, highly oxygenated compounds, thus low heating value. In order to use bio-oil in fuel applications, upgrading of bio-oil is necessary. Catalytic pyrolysis is a promising way to improve bio-oil quality by removing of oxygenated compounds, increasing calorific value, lowering viscosity and increasing stability. Of the various catalysts studied for biomass catalytic pyrolysis, zeolites have been shown to be effective for reducing oxygenated compounds of pyrolysis oil. One of the most common zeolites have been studied is ZSM-5, which can be synthesized with different Si/Al ratios, thus having different acidity characteristics [25]. Studies have shown that using ZSM-5 as catalyst in biomass pyrolysis increased aromatic

hydrocarbons content and decreased oxygenated aromatic compounds content in bio-oil [1,21, 25-27].

The aim of this study covers (1) investigation of the catalytic effect of ZSM-5 on olive pomace pyrolysis, (2) the calculation of kinetic parameters for thermal decomposition of olive pomace with ZSM-5 and, (3) investigation of bio-oil composition produced from olive pomace catalytic pyrolysis.

The decomposition of olive pomace is studied by using thermogravimetric analysis. Pyrolysis experiments were performed in a tubular furnace system under the conditions where the heating rate was kept constant at  $25\text{ }^{\circ}\text{C}\cdot\text{min}^{-1}$ . The holding time at the final reaction temperature of  $550\text{ }^{\circ}\text{C}$  was 15 min. The catalyst effect to the kinetic behavior of pyrolysis reaction was investigated by calculating kinetic parameters via Coats and Redfern method.



## 2. FUNDAMENTALS OF BIOMASS PYROLYSIS

Pyrolysis is a thermochemical conversion process in the absence of an oxidizing agent and can be regarded as the initial stage of gasification and combustion. During pyrolysis, large hydrocarbon molecules are broken into relatively smaller ones via reactions such as depolymerization, dehydration, decarbonylation, decarboxylation, deoxygenation, oligomerization and aromatization [25,28]. Solid char, liquid pyrolysis oil, and gas are the main products of biomass pyrolysis, thus the amount and the ratio of these fractions are influenced by many factors such as heating rate, pyrolysis temperature, biomass composition and catalyst effect [8,15,16]. The initial product of pyrolysis consists of solid char, and condensable gases which are further converted into noncondensable gases (CO, CO<sub>2</sub>, H<sub>2</sub>, and CH<sub>4</sub>), liquid, and char [28].

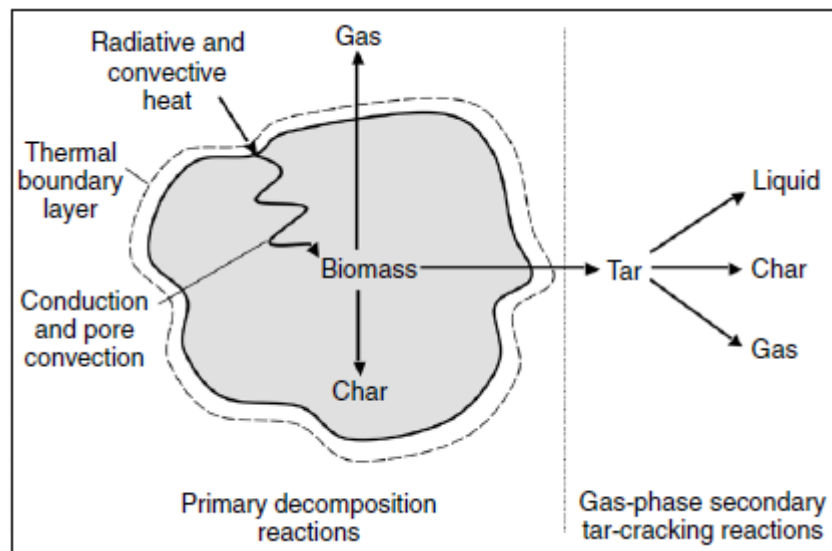


**Figure 2.1:** Schematic of pyrolysis in a biomass particle [28]

## **2.1 Pyrolysis Operating Parameters**

### **2.1.1 Temperature**

The effect of reaction temperature on amount of each pyrolysis product is regarded as one of the most important and significant parameter. Studies have shown that increasing pyrolysis temperature causes a reduction in char yields, suggesting that secondary reactions of the liquid fraction and further char decomposition reactions are promoted with increasing of temperature, resulting enhanced gas yields at temperatures over 600 °C [19,29-31]. Previous studies have confirmed that the maximum liquid yield is obtained at temperatures in the range of 500-550 °C [19,29,31,32]. In a study of Pütün [29], bio-oil yields of 41%, 46% and, 43% were obtained at temperatures 400 °C, 550 °C and 700 °C, respectively. At temperatures between 350-400 °C, char yields were close to maximum within the range of 29%-38.48% (wt.) for most cases, suggesting that biomass could not be decomposed completely [19,29,32]. Similarly, solid char formation is favored at low temperatures (<350 °C) mainly due to reason of cross-linking reaction of cellulose and lignin. However, volatiles are released at temperatures higher than 350 °C as a result of depolymerisation reactions [33].

### **2.1.2 Particle Size**

Biomass, being poor conductor of heat, often possesses heat transfer difficulties during pyrolysis. The size of particle has a direct effect on heat transfer, which in turn influences the yield and properties of bio-oil. Understanding the effect of particle size distribution on pyrolysis products yields also help to optimize residence times of the pyrolysis reactions. It is a known fact that the particle size of the feed influences the heat and mass transfer rate and release rate of volatile matter during pyrolysis process [34]. Studies have revealed that for larger particles of biomass, the yield of gaseous fraction was higher than that of obtained from smaller particles. This situation can be explained by the fact that larger biomass particles increase the residence time of volatile matter, favoring secondary cracking reactions of tar, thus increasing the gas yield. Enhanced bio-oil yield obtained using smaller particle size due to the reason that, pyrolysis process was under kinetics control with smaller particle size whereas it mainly happened on the surface of the biomass in the case of larger particle size. Due to low heat transfer rate, the temperature inside the larger

particle was lower than expected, thus causing pyrolysis process to be incomplete; resulting higher char yields and lower bio-oil yields [35,36]. Also, Asadullah *et al.* suggested that, mass transfer resistance inside the biomass particle was higher in larger particles than smaller ones, resulting increased char yield [33]. Unexpected differences between the product fractions might be due to differences in type of biomasses (for example oxygen content of the biomass has a known effect on heat transfer mechanism) [33].

### **2.1.3 Heating Rate**

As affecting heat transfer, adjusting heating rate to optimum level is of high importance regarding product yields of pyrolysis process. Increasing heating rate has an effect of enhancing liquid yields and decreasing char yields, which suggests that optimum heating rate prevents secondary reactions resulting maximum liquid yields [32,33]. Higher heating rate favors rapid formation of volatiles, while lower heating rate causes longer residence time for volatiles, thus enabling the repolymerisation reactions forming char [33]. A study on olive residue and sugar cane bagasse pyrolysis has shown that, between the heating rates of 2 and 50 K.min<sup>-1</sup>, the pyrolysis rate is increased with heating rate. It was suggested that the overlapping DTG peaks with high heating rates was a consequence of the fact that some of the constituents of the biomass samples decomposed simultaneously while at low heating rate those peaks were clear. This can be explained by the fact that, the temperature inside the biomass particle increases with an increase in heating rate and rate of decomposition is higher than the rate of formation and rate of volatile release [4]. This is the reason why optimum heating rate is necessary for an effective pyrolysis process.

As stated above, higher heating rates minimize char formation. In case of lower heating rates, which run for several days, the main product is char. This process is called carbonization. Carbonization enables the conversion of condensable vapor into char and noncondensable gases [28].

### **2.1.4 Residence Time and Sweeping Gas Flow Rate**

Sweeping gas flow rate is another important parameter which influences the residence time of volatiles and the yield of gaseous fraction of pyrolysis products. Numerous studies have shown that higher sweeping gas flow rate favors rapid

removal of vapours from the reaction medium, thereby reducing secondary reactions such as thermal cracking, repolymerization, recondensation and char formation. Hence, char yields are decreased whereas the yields of gaseous products are increased [19,29,32]. Additionally, in a study of catalytic and conventional pyrolysis of several biomass types, Huang *et al.* [30] showed that increasing gas residence time affected the yield of gaseous products of biomass pyrolysis so that secondary cracking reactions are attributable for enhanced gas yield and decreased liquid yield. Moreover, optimum sweeping gas flow is required in order to obtain maximum pyrolysis product yield from the reaction system. A study of Pütün [29] revealed that nitrogen flow rate of 200 mL. min<sup>-1</sup> was adequate for 48.30% maximum yield of bio-oil for the current system. In fact, flow rate of nitrogen does not have a significant effect on liquid yield of pyrolysis systems as it much more depends on sufficient quenching of pyrolysis vapours and downstream cooling mechanism. The study of Uzun and Sarioğlu [32], has shown that gas yields reached its maximum value of 30.08% with a nitrogen flow rate of 800 cm<sup>3</sup>min<sup>-1</sup>.

Other than the sweeping gas flow rate, the type of sweeping gas plays an important role in terms of product composition and quality. Melligan *et al.* revealed that bio-oil obtained by using H<sub>2</sub> as sweeping gas had higher heating value of 24.4 MJ/kg relatively higher than that of obtained under N<sub>2</sub> atmosphere with a higher heating value of 17.8 MJ/kg [37]. Pütün *et al.* [20] compared the outcome of biomass pyrolysis using N<sub>2</sub> and steam atmospheres as sweeping gases. The effect of nitrogen as a carrier gas was consistent with other studies in literature [32], while steam lowered the yield of char by diffusing into biomass particles, facilitating desorption and removing the volatiles.

### **2.1.5 Biomass Composition**

Biomass is composed of lignin, hemicellulose, cellulose, extractives and inorganic elements. The composition and amount of pyrolysis products vary depending on the content of biomass constituents as well as the distribution and percentages of these constituents, which vary with biomass species [38].

Cellulose, being linear-structured polymer, consists of β-1,4 linked glucose units, whereas hemicellulose is a branched-structured polymer composed of sugars such as pentoses and hexoses. Being formed by cross-linked phenylpropane units, lignin is a



more complex aromatic compound and more resistant to thermal decomposition than cellulose and hemicellulose [3,39,40]. Cellulose can be decomposed via two type of reactions: depolymerization and ring scission, which will result in the formation of different compounds. The ring scission reaction mainly results in the formation of hydroxyacetaldehyde, acetol, linear carbonyls, linear alcohols, esters. However, anhydro oligosaccharides, monomeric anhydrosugars, furans, cyclopentanones, pyrans are obtained with the depolymerization reactions [37]. Melligan *et al.* [37] revealed that, during conventional pyrolysis of biomass, cellulose decomposition follows depolymerization reaction pathway. Lignin conversion is mainly due to depolymerization reactions and fragmentation reactions, which lead to formation of aromatic compounds of the main precursors of hazardous materials present in tar [40].

During the pyrolysis of biomass, the decomposition of biomass constituents takes place after moisture evaporation. It is a known fact that, hemicellulose is the first component to decompose within the temperature range of 160-240 °C and cellulose is generally degraded at temperatures between 240-372 °C. The decomposition of lignin, however, occurs within wider range of temperature (160-625 °C) and at a low rate due to its resistant nature compared to hemicellulose and cellulose [4,41]. Ounas *et al.* compared the pyrolysis of olive residue samples and sugar cane bagasse and found out that total weight loss was higher in sugar cane bagasse (83.3%) due to its higher volatile matter content and lower ash content [4].

Biomass constituents possess different characteristics and reactivities due to their heterogenous nature, the effect of main constituents to pyrolysis products is an important parameter to take into consideration. In a study of Haykiri-Acma and Yaman [39] the behavior of sunflower shell and olive refuse was investigated during pyrolysis. It was revealed that sunflower shell with high content of volatile matter (76.0%) favored the formation of gaseous products whereas high lignin and high ash content in olive refuse samples (34.7% and 13.8% , respectively) provided enhanced yield of solid char. Huang *et al.* studied various types of biomasses with addition of catalyst at temperature of 600 °C and compared them with main biomass components. Cellulose as one of the main biomass components gave the highest yield of gaseous products (%60.7), was followed by sugar cane bagasse with yield of 57.0%. It was also found that samples with high lignin content gave more char yield

which can be explained by the presence of stable aromatic compounds present in the lignin matrix. For the major components of biomass, cellulose has the highest olefin yield whereas lignin has the lowest, which is attributable to the fact that levoglucosan is the main product of cellulose pyrolysis [30,39]. F.X.Collard *et al.* [40] compared the pyrolysis behavior of beechwood with main biomass constituents. It was noted that, cellulose produced highest amount of volatiles followed by the gas and char fractions. Also, beechwood gave high yield of tar (36.5%) due to its high content of cellulose. However, in a study of Bertero *et al.* [42] bio-oil obtained from pine sawdust, which had lower cellulose content than that of mesquite sawdust had lower yield. This shows us that the diversity of biomass species and weight percentage of biomass constituents should be further studied.

### **2.1.6 Catalyst Effect**

The presence of catalyst in pyrolysis process has been also investigated with different biomass sources [43,44]. Using catalysts in biomass pyrolysis influences the decomposition behavior of biomass, and composition and quantity of pyrolysis products. ZSM-5 zeolites were found to be effective in improving deoxygenated aromatic content of pyrolysis products while reducing liquid yield [21,45,46]. Using silica-alumina with or without deposition of alkali metals favors water formation, increases gas and char yield, consequently reducing total organic yield comparing to conventional pyrolysis [22].

Catalysts also affect the distribution and the content of chemical compounds of pyrolysis products. Zhou *et al.* investigated the effect of catalyst to biomass ratio by using zinc oxide as catalyst. With increasing the catalyst amount, approximately 6% (wt.) decrease in bio-oil yield was observed and the gas yield increased in the range of 21.38–28.74% (wt.) [19]. In a study of Huang *et al.*, HZSM-5 zeolite impregnated with 6% wt. Lanthanum showed that increasing catalyst to biomass ratio improved the chemical composition of pyrolysis liquid in terms of olefin content [30].

**Table 2.1:** Product yields based on pyrolysis operating parameters and reactor types

Reactor type	Temperature (°C)	Sweeping Gas Flow Rate	Residence Time (s)	Catalyst type	Catalyst to biomass ratio	Bio-oil (wt.%)			Gas (wt.%)	Char (wt.%)	Ref.
						Aqueous	Organic	Total (Aqueous+Organic)			
Fixed bed	600	30 cm <sup>3</sup> .min <sup>-1</sup>	10	La/HZSM-5	3	14.4	7.7	22.4	34.2	39.9	[30]
Fluidised bed	450	3.75 l.min <sup>-1</sup>	*	H-Beta	0.4	13.1	15.8	28.9	49.4	21.7	[47]
Auger reactor	500	120 l.h <sup>-1</sup>	2	ZSM-5	5	*	*	50.3	26.2	13.6	[48]
Fixed bed	500	30 cm <sup>3</sup> .min <sup>-1</sup>	4.5	Al-MCM-41	0.46	37.5	10.91	48.41	7.49	37.43	[49]
Fixed bed	500	50 cm <sup>3</sup> .min <sup>-1</sup>	0.03	CoO	0.46	22.37	34.10	56.47	21.29	22.24	[45]
Fixed bed	500	50 cm <sup>3</sup> .min <sup>-1</sup>	0.03	Co <sub>3</sub> O <sub>4</sub>	0.46	26.30	29.18	55.48	33.78	22.55	[45]
Fixed bed	500	50 cm <sup>3</sup> .min <sup>-1</sup>	0.03	NiO	0.46	24.81	22.65	47.46	27.73	24.84	[45]
Fixed bed	550	150 ml.min <sup>-1</sup>	*	ZnO	0.05	*	*	47.02	21.38	31.6	[19]
Fixed bed	490-540	50 cm <sup>3</sup> .min <sup>-1</sup>	*	ZSM-5	0.01	*	*	38.29	19.45	42.27	[50]
Fixed bed	490-540	50 cm <sup>3</sup> .min <sup>-1</sup>	*	Al-MCM-41	0.01	*	*	39.98	18.80	43.15	[50]
Fixed bed	490-540	50 cm <sup>3</sup> .min <sup>-1</sup>	*	Al-MSU-F	0.01	*	*	39.59	19.18	43.31	[50]
Fluidised bed	425-450	*	3	HZSM-5	*	20.9	11.9	32.8	46.8	20.3	[51]
Fluidised bed	400	27 l.min <sup>-1</sup>	*	ZnO	*	*	*	57	20	12	[44]
Fixed bed	450	50 ml.min <sup>-1</sup>	*	α- Al <sub>2</sub> O <sub>3</sub>	0.5	19.1	42.4	61.5	10.5	17.6	[22]
Fixed bed	500	100 cm <sup>3</sup> /min <sup>-1</sup>	*	ZnO	0.15	*	*	45.22	30.46	24.32	[34]
Fixed bed	550	100 cm <sup>3</sup> /min <sup>-1</sup>	*	Al <sub>2</sub> O <sub>3</sub>	0.1	*	*	40.95	37.69	21.36	[34]
Fixed bed	500	70 ml.min <sup>-1</sup>	4	Na <sub>2</sub> CO <sub>3</sub> /γ-Al <sub>2</sub> O <sub>3</sub>	0.5	28	9	37	23	19	[52]

\*information not available

## 2.2 Pyrolysis Mechanism

Biomass is heterogeneous, that is why it is highly essential to investigate the pyrolysis behavior and reveal a mechanism for each constituent.

Understanding of the pyrolytic behavior of cellulose is crucial due to the fact that it accounts for approximately 50% of biomass [38,53]. Levoglucosan is the main component of cellulose pyrolysis product [38,54,55]. Bai *et al.* studied the effect of levoglucosan in cellulose pyrolysis. It was suggested that during pyrolysis, cellulose conversion into levoglucosan occurred faster than its vaporization rate [54]. As demonstrated in Figure 2.2., decomposition of levoglucosan follows two competing reaction pathways: vaporization and depolymerization. It was suggested that, vaporized levoglucosan leaves reaction environment whereas, its polymerized form leads to yield low molecular weight volatiles including 5-hydroxymethyl furfural, furan, furfural, H<sub>2</sub>O, CO<sub>2</sub> and acetic acid [54].

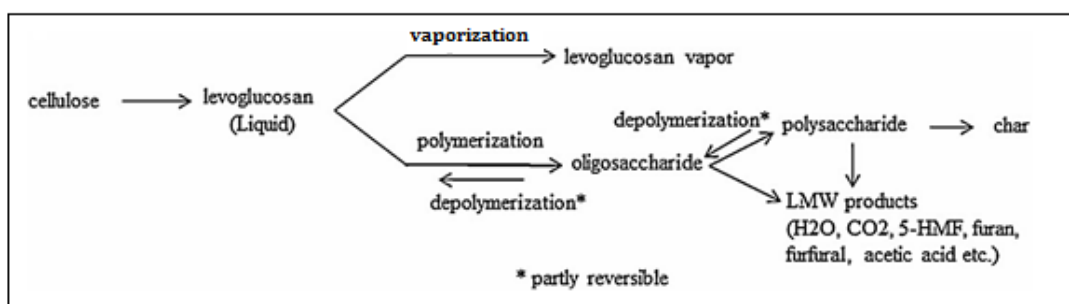


**Figure 2.2:** Reaction pathway for cellulose pyrolysis [54]

Stefanidis *et al.* investigated the pyrolysis of lignocellulosic biomass to see the effect of pyrolysis of each constituent on the overall yield [38]. Similarly, the main product of cellulose pyrolysis was found to be levoglucosan. Also, small amount of phenolic compounds which were formed as a result of secondary reactions were detected. In this study, formation of acetic acid was considered to be due to dehydration of hydroxyacetaldehyde, resulting formation of ketene which produces acetic acid via hydration [38].

In order to understand the mechanism of thermal decomposition of hemicellulose and to reveal reaction pathways for the formation of main pyrolysis products, xylan is considered to be a model compound as a replacement of hemicellulose. In a study of Stefanidis *et al.*, the main products of xylan pyrolysis were reported to be phenols and cyclic ketones, which were derived from the cleavage of the ferulic acid ester branch of xylan and cleavage of o-glucosidic bonds followed by removal of hydroxyl groups of xylose rings, respectively [38].

Lignin decomposition mainly leads to formation of phenolic compounds which are of more complicated structure than those derived from cellulose and xylan, due to their methoxy and poly substituted structure [38,55]. Xin *et al.* proposed that the primary reaction of lignin pyrolysis were depolymerization and dealkylation due to increased formation of guaiacol at 350 °C. As temperature increases to 450 or 550 °C, the decomposition of guaiacol leads to formation of phenols and CH<sub>4</sub>. Dehydroxylation of phenolic compounds followed by polymerization of ring-containing monomers lead to formation of PAHs [55].

## **2.3 Pyrolysis Products**

### **2.3.1 Gas**

The gaseous fraction of biomass pyrolysis products contains mostly hydrogen, carbon monoxide, carbon dioxide, methane, ethane and, ethylene [5,30,48,51,56]. Pyrolysis gas can be used to provide heat for pyrolysis reactor or for heat and electricity generation in a gas turbine combined cycle system [31]. Depending on the biomass feedstock and reactor configuration, primary gases of biomass pyrolysis contain 86.7 wt.% of CO<sub>2</sub>, 1.2 wt.% of CO and, 6.5 wt.% H<sub>2</sub> [42]. Dependant on the process temperature, the high heating value of gaseous products of biomass pyrolysis varies between 6.28- 14.77 MJ.m<sup>-3</sup> [31].

### **2.3.2 Char**

As solid product of biomass pyrolysis, char, which is comprised of the condensed organic residues and the inorganic phases, with an average high heating value of 28.5-29 MJ.kg<sup>-1</sup> (depending on the biomass feedstock) can be used as a solid fuel. It is also a well-known precursor for activated carbon production [31,39]. Char with

>70 wt.% fixed carbon content can be used as a raw material for production of briquettes for domestic use [5,31].

### **2.3.3 Pyrolysis Oil (Bio-oil)**

Bio-oil, is a dark brown colored liquid mixture, which is composed of an aqueous phase and an organic phase having a large number of different chemical compounds derived from depolymerization and fragmentation reactions of biomass main components: cellulose, hemicellulose and lignin [19,22,42,49,50,57]. Aqueous phase of bio-oil contains a wide variety of oxygenated organic compounds such as acetic acid, methanol, acetone. Organic phase of bio-oil contains single ring aromatic hydrocarbons such as benzene, toluene, indene, alkylated derivatives, and polycyclic aromatic hydrocarbons including naphthalene, fluorene, phenanthrene and, oxygenated organic compounds such as aliphatic alcohols, carbonyls, acids, phenols, cresols, benzenediols, guaiacol [19,42,49,50]. Due to its relatively higher organic compound content, organic phase of bio-oil has higher carbon concentration and higher calorific value than aqueous phase [23,42].

The chemical composition of bio-oil varies depending on biomass feedstock characteristics, mainly the percentages of main biomass constituents. The decomposition of cellulose leads to formation of levoglucosan and furfural which are considered valuable organic compounds in terms of fuel quality of bio-oil [50]. Phenolic compounds are the products of lignin depolymerization and cracking reactions. Among the phenolic compounds present in bio-oil, guaiacol and its alkylated compounds are the most important ones due to being thermally unstable and being able to be transformed through secondary reactions to alkylated phenols and aromatic compounds, which are desirable for bio-oil quality [57]. Acetic acid, generally the main compound in the group of acids in bio-oils, is formed by the deacetylation of hemicellulose [57].

#### **2.3.3.1 Bio-oil Characteristics**

Due to heterogeneous structure of biomass, bio-oil contains different types of acidic compounds as well as high amount of water and highly oxygenated hydrocarbons, which lead to poor combustion properties, instability, lower calorific value and higher viscosity compared to fossil fuels [26,43,58].

Water in bio-oil is primarily formed as a result of dehydration reactions and depolymerization reactions of hemicellulose, cellulose and lignin [42]. The presence of water in bio-oil is a drawback in terms of utilization of bio-oil because it lowers the heating value and delays the ignition [19]. However, high water content also leads to low viscosity so that the fluidity of bio-oil is enhanced, which is a good indicator of bio-oil quality for utilization in combustion engines [42,50]. The water yield in bio-oil varies depending upon the biomass composition and process conditions, such as 15.0 wt.% for hybrid poplar [51], 15.32 wt.% for rice husk [19], 44.3 wt.% for chañar fruit [57], 16.0 wt.% for rice straw and 18.0 wt.% for sawdust [59].

Traditionally obtained bio-oil shows high viscosity due to presence of large molecules. Levoglucosan, as a heavily oxygenated compound produced from cellulose pyrolysis, significantly affects the viscosity of bio-oil by causing crystallisation in time at room temperature [22,37,51]. Also, high level of heavy phenols which are derived from lignin depolymerization reactions, increases the viscosity of bio-oil [37]. Due to the fact that chemical reactions at higher temperatures between reactive components such as ketones and aldehydes resulting heavier compounds increase viscosity and cause instability [37,45], the storage of bio-oil becomes a major issue [22,60]. In a study of Duman *et al.*, it was reported that addition of methanol improved the stability of bio-oil such that the viscosity of bio-oil increased at 29.82% in 168 h period instead of 46.63% [60]. Bio-oils with lower content of carbonyl compounds are considered thermally more stable [22].

High oxygen content (generally 35-40 wt.% ), which means low H/O ratio, lowers the energy density of bio-oil. High oxygen content is also the reason of the immiscibility with petroleum products [22]. Oxygenated aromatic hydrocarbons decrease the heating value of bio-oil and stability but increase the viscosity due to their high molecular weight [19,45,57].

Bio-oil is considered highly acidic compared to conventional fuels and needs to be upgraded before to be utilised commercially [19,45]. Chemical composition, especially the amount of acidic compounds, determines the acidity of bio-oil. Acid

content in bio-oil leads to corrosive characteristics towards metals such as copper and iron, which makes transportation, utilisation and storage of bio-oil a major issue [37]. Biomass pyrolysis oils typically contain 3-6 wt.% volatile acids, with the main compounds being acetic and formic acids [61]. Carboxylic acids, mainly acetic acid is formed from the cleavage of acetyl groups in the hemicellulose components of biomass [22,61], and from ring scission of cellulose [37]. For non-catalytic bio-oil, acidity accounts for its pH in the range of 2.0-3.0 [51,57,60].

### **2.3.3.2 Utilisation of Bio-oil**

Bio-oils can be used in many applications. It can be used as a substitute in chemical industry as food flavorings, fertilizers, emission control agents [32], as an energy carrier in stationary applications for heat and electricity generation in boilers, furnaces, engines and turbines [18,32].

Furans are valuable chemical compounds present in bio-oil because they can be used for organic solvent production and for substituting fossil fuels [37]. Aromatic hydrocarbons in bio-oils with lower molecular weight is more favorable than the ones with higher molecular weight, in terms of utilisation as fuel additives because they have lower boiling points [18]. Oxygenated compounds decrease the stability and energy density [57] and thus the quality of bio-oil [37]. However, low level of oxygenated molecules such as (alkyl)-furans compounds are favorable due to the reason that high octane number of these compounds enhance energy density of bio-oil, thereby facilitating the utilisation of bio-oil as fuel additive [22]. Phenolic compounds in bio-oil (particularly phenolic ethers such as vanillin, guaiacol and syringol) are the precursors for the synthesis of pharmaceutical and polymeric compounds or adhesives [57].

Using the bio-oil as a fuel without upgrading results in several significant problems such as poor volatility, high viscosity, high water content, low repolymerization temperature (<100 °C), corrosiveness for engine equipments [62]. Emulsification and blending are amongst the most preferred methods to upgrade the bio-oil when substituting conventional diesel [62-64]. Van de Beld *et al.* investigated the performance of bio-oil derived from pine wood in a modified diesel engine connected to a generator to convert mechanical power to electricity. It was noted that, at air inlet temperatures in the range of 100-120 °C and at an engine compression



ratio of 17.6, bio-oil/ethanol blends were found to reduce CO emissions and increase NO<sub>x</sub> emissions. Adding up to 30 wt.% of ethanol to the bio-oil improved combustion performance due to better atomization of the fuel, resulting in lower CO emissions [62]. Similar results were obtained by Yang *et al* [65]. In a study of wood pyrolysis oil, it was revealed that using pure bio-oil in diesel engines leads to the widening of spray channels, thus damaging the injector. The results of this study showed that at 200 °C tip temperature, the needle of nozzle was stuck in a short period of operation time [66]. Sugarcane bio-oil was blended with gasoline in the range of 5-14 vol.%. The results showed that blending up to 10 vol.% of bio-oil with gasoline did not affect the operation of Otto engine of 4kW capacity connected to a 2 kWe generator suggesting that power and fuel consumption were similar with that of gasoline operated engine [67]. However, specific modifications of diesel engines are necessary for using the bio-oil or bio-oil derived fuels in diesel engine systems. Dedicated fuel feeding system parallel to diesel feeding line, a pilot diesel fuel injection, use of cleaning fuels such as methanol, and corrosive resistant or stainless steel fuel pump and injector design are amongst the modifications adapted by researchers [63,65,66]. Furthermore, in order to reduce viscosity of the fuel, short preheating at temperatures <90 °C is needed and direct heating is not recommended [68].

Boucher *et al.* investigated softwood bark pyrolysis oil with the addition of methanol as a possible liquid fuel for gas turbines. The results of this study showed that the viscosity of bio-oil was close to the gas turbine requirements with the value of 5.3 cSt at 90 °C and the net heating value of 32 MJ.kg<sup>-1</sup> was recorded as relatively high. However, due to the fact that the ash and solid content present in the bio-oil will eventually cause degradation in gas turbines, filtering and upgrading of bio-oil is required [69]. López Juste and Salvá Monfort [70] conducted a preliminary study on combustion performance of a gas turbine operated with bio-oil (80.0 wt.%)/ethanol (20.0 wt.%) mixture. At high air flow rate, considerable increase in CO emission was observed suggesting that using bio-oil/ethanol mixture leads to inefficient operation of the combustor. In order to utilise bio-oil for gas turbine applications, fuel preheating at temperatures 70-90 °C is necessary to keep viscosity lower than that of 10 cSt. Resistant materials to acidity of bio-oil should be selected in order to prevent wear corrosion damage [68]. Modifications must also include nozzle adaptations for

bio-oil specific properties because using standard nozzles does not allow for full load (thus causing power decrease). It is of high importance that start-ups and shut-downs must be done using standard fossil fuels in order to warm up combustion chamber facilitating bio-oil ignition [68].

### **3. UTILISATION OF CATALYSTS IN BIOMASS PYROLYSIS**

Depending on the biomass type used; the low calorific value, high water content, high viscosity (due to large molecules), high oxygen content (due to oxygenated hydrocarbon content) as well as instability, immiscibility with other fossil fuels make bio-oil difficult to use directly as a fuel without upgrading [26,58]. In order to upgrade bio-oil to use in fuel applications, two different methods have been utilised: hydrodeoxygenation and catalytic cracking. In hydrodeoxygenation, bio-oil compounds react with hydrogen under high pressure and moderate temperature to produce hydrocarbon compounds and water. Catalytic cracking is used to upgrade bio-oil through a catalytic medium, removing oxygen from bio-oil compounds in the form of H<sub>2</sub>O and CO<sub>2</sub>, involving the chemical reactions of rupturing the C-C bonds via dehydration, decarboxylation and decarbonylation [1,18,26,58]. Catalytic cracking has several advantages over hydrodeoxygenation including operating at atmospheric pressure and in an environment with no need of extra hydrogen supply [1].

#### **3.1 System Configurations for Catalysts Used in Biomass Pyrolysis**

There are two methods for catalytic pyrolysis in use: catalytic bed and catalyst mixing. In catalytic bed method, which is also referred to as “in-situ” upgrading or ex-bed method, pyrolytic vapors coming from the first reactor pass through a catalytic reactor which is called catalytic bed, resulting bio-oil, char and gaseous products. In catalyst mixing (in-bed) method, however, biomass and catalyst samples are mixed physically before being inserted in pyrolysis reactor [1,29,49].

##### **3.1.1 Catalyst Bed Method (In-situ)**

Catalyst bed method, also called *in-situ* pyrolysis, involves catalytic upgrading subsequent to thermal conversion of biomass resulting pyrolysis vapors [1]. In general, *in-situ* catalytic pyrolysis of biomass can be performed using different reactor configurations: single stage and two stage reactor configurations. Single stage pyrolysis involves catalytic pyrolysis of biomass in the same reactor with catalyst,

whereas two-stage configuration involves fixed bed/ fluidized bed reactor followed by a fixed bed catalytic reactor. The former produces more coke than the latter [51]. A study by Mante and Abglevor [51] using two stage reactor configuration for catalytic pyrolysis of hybrid poplar wood with HZSM-5 reported low yield of coke with 3.8% of value which was relative to the weight of biomass. Advantage is that catalytic pyrolysis of evolved vapors from biomass can be operated at a different temperature than that of the main pyrolysis reactor in case of two stage reactor configuration is employed [20]. However, compared to catalyst mixing, the catalyst bed method also leads to high amount of char resulting clogging of catalysts pores which prevents the diffusion of vapors through the pores [1].

In a study of Thangalazhy-Gopakumar *et al.*, it was noted that some non-catalytic bio-oil compounds was detected when using catalysts bed method, suggesting that primary tar compounds were converted into secondary and tertiary tar compounds before reaching the catalyst-bed to be cracking into aromatics [1]. Uzun and Sarioğlu reported that using catalyst bed method with several type of catalysts decreased the liquid yield compared to catalyst mixing method [32]. Iliopoulou *et al.* studied catalytic pyrolysis of lignocellulosic biomass and explained the *in-situ* effect of metal modified ZSM-5 with various percentages. It was suggested that transition metals favored the formation of hydrogen which leads to hydrocarbon reactions on the zeolite acid sites via catalyst bed mode [45].

### **3.1.2 Catalyst Mixing Method (In-bed)**

Catalyst mixing method can be done by either addition of catalyst to biomass with defined amounts or by wet impregnation of biomass. Due to better physical surface contact between biomass and catalyst in pyrolysis reactor, mixing allows immediate interaction of evolved pyrolysis vapors with the catalyst suggesting that evolved vapors can be adsorbed on the catalyst surface to be diffused into the pores for catalytic cracking [1,32]. Disadvantage is that the catalytic conditions are irreversible so that biomass and catalyst should be operated under the same conditions [20].

Aromatic content of bio-oil is of utmost importance and utilizing catalysts is one alternative way to increase aromatization reactions (thus enhance bio-oil quality).

Studies have shown that catalytic mixing method provides better mass transfer for cracking of bio-oil compounds in terms of aromatization and deoxygenation [1,32]. Thangalazhy-Gopakumar *et al.* investigated the catalytic effect of ZSM-5 zeolite in pyrolysis of pine wood chips under helium environment. It was revealed that using catalyst mixing method with 1:9 biomass to catalyst ratio gave 41.5 % of aromatic yield compared to that of 9.8% using catalyst bed method with 1:5 biomass to catalyst ratio. In this study, the absence of guaiacol compounds in bio-oil shows that catalyst mixing is an effective method for cracking of lignin derived compounds to aromatics [1]. Pütün *et al.* studied pyrolysis of cotton seed with the addition of MgO with defined proportions to the biomass samples. Compared to conventional pyrolysis results, aromatic and aliphatic content was enhanced to the values of 35% and 23%, and the oxygen content was reduced from 9.56 to 4.90% [29]. The results of rice husk pyrolysis with ZnO studied by Zhou *et al.* showed that catalyst mixing with various amounts significantly improved bio-oil quality in terms of hydrogen content, H/C ratio, higher heating value, and reducing carboxylic acid content of bio-oil [19]. Thus, in order to design large scale pyrolysis plants, effective and homogenous mixing systems are necessary.

### 3.2 Metal Oxide Catalysts

Metal oxide catalysts have been extensively studied in literature, using miscellaneous biomass species, with regard to their effect on the quality and quantity of pyrolysis products. It is a known fact that metal oxides as any catalysts, influence the decomposition temperature. Accordingly, in a thermogravimetric study conducted by Chattopadhyay *et al.* using Cu/Al<sub>2</sub>O<sub>3</sub> as a catalyst, it was noted that transition metal supported alumina had a strong effect on decreasing the devolatilization temperature of volatiles [17]. Zabeti *et al.* applied amorphous silica alumina (ASA) supported with alkali or alkaline earth metals in pyrolysis of pinewood. Maximum bio-oil was obtained with non-supported amorphous silica alumina with the value of 42.4 wt.%. However, the fraction with Cs/ASA showed the best performance in terms of oxygen elimination in aromatic hydrocarbons thus increasing the heating value of bio-oil [22]. Wang *et al.* [71] investigated the catalytic effect on pyrolysis of lignocellulosic biomass using catalysts including NiMo/Al<sub>2</sub>O<sub>3</sub>, CoMo/Al<sub>2</sub>O<sub>3</sub>, CoMo-S/Al<sub>2</sub>O<sub>3</sub>, activated alumina, and porous silica. In order to enhance the production of pyrolysis intermediates (benzene, toluene, xylene, naphthalene), it was suggested that CoMo-

S/Al<sub>2</sub>O<sub>3</sub> was most favorable of amongst all. However, NiMo/Al<sub>2</sub>O<sub>3</sub> gave highest yield of CH<sub>4</sub> with the value of 51.82%. Shadangy and Mohanty [72] studied CaO and Al<sub>2</sub>O<sub>3</sub> in pyrolysis of *Hyoscyamus niger L.* and confirmed that, consistent with other studies mentioned above, adding catalysts to pyrolysis process considerably decreased the bio-oil yield however, eliminated the oxygenated groups present in bio-oil thus improving its fuel quality. Aysu and Küçük investigated the pyrolysis of eastern giant fennel (*Ferula orientalis L.*) comparing the effect of ZnO and Al<sub>2</sub>O<sub>3</sub> catalysts [34]. Al<sub>2</sub>O<sub>3</sub>, with the value of 79.94%, was found to be more effective than ZnO in terms of conversion of biomass. However, the effect of the catalyst on the bio-oil yield was different from each other. ZnO increased the bio-oil yield with increasing catalyst to biomass ratio whereas bio-oil yield decreased with increasing Al<sub>2</sub>O<sub>3</sub> addition. This indicated that Al<sub>2</sub>O<sub>3</sub> promoted gas formation. In a study of Yorgun and Şimşek, activated alumina was used in pyrolysis of *Miscanthus x giganteus* and it was noted that, at high heating rates, 60 wt.% of catalyst loading to biomass is effective for maximum liquid production with the value of 51 wt.%. The oxygen content of bio-oil was found to be higher than that of non-catalytic bio-oil [73]. Nguyen *et al.* investigated the pyrolysis vapors of pine wood chips over 20 wt.% Na<sub>2</sub>CO<sub>3</sub>/γ-Al<sub>2</sub>O<sub>3</sub>. It was reported that liquid yield was lowered but decarboxylation of carboxylic acids was favored with the catalyst, resulting a pH value of 6.5 suggesting that the sodium based alumina catalyst is effective on improving acidity of bio-oil. Hydrocarbon concentration was increased from 0.5% to 17.5% indicating a higher energy density of bio-oil [52]. Chen *et al.* presented the gaseous product distribution of biomass (rice straw and saw dust) pyrolysis, at a temperature of 800 °C, utilising different metal oxides such as Cr<sub>2</sub>O<sub>3</sub>, MnO, FeO, Al<sub>2</sub>O<sub>3</sub>, CaO, and CuO. It was noted that except for CuO and Al<sub>2</sub>O<sub>3</sub>, all the catalysts noticeably improved gas production [59]. Zhou *et al.* [19] studied the pyrolysis of rice husk with the addition of ZnO. The results of this study indicated that ZnO showed a trend to decrease bio-oil yield with increasing biomass to catalyst ratio. However, ZnO improved the bio-oil compositional quality in terms of low weight molecular compounds including alkanes, alkenes, styrene and alkyl phenols (thus increasing bio-oil stability). Nokkosmäki *et al.* also studied the same catalyst for the conversion of pyrolysis vapors of pine sawdust and the viscosity of catalytic bio-oil was shown to be reduced by 40% compared to non-catalytic pyrolysis results [44].

Pütün *et al.* [29] revealed that utilising MgO as a catalyst in cotton seed pyrolysis in a fixed bed reactor improved the bio-oil quality by removing oxygenated compounds, enhancing higher heating value and increasing aromatic content of bio-oil.

### 3.3 Zeolite catalysts

Zeolites, having a tetrahedral structure and acidic nature, are three dimensional aluminosilicates linked through oxygen atoms and supported with channels and cavities, resulting porous structure of exceptional catalytic activity. Each type of this tetrahedral zeolites with overall charge balance of minus one, have Si or Al at the center, and oxygen atoms at the corners of the structure [74].

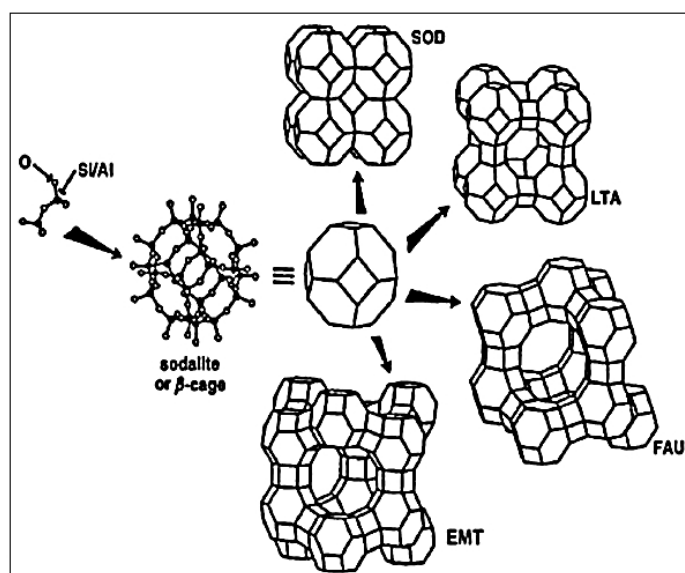


**Figure 3.1:** Different frameworks of zeolites with sodalite cage structure [75]

Zeolites possess following characteristics: (1) cracking of deoxygenated compounds via shape selectivity, (2) high surface area, (3) varied dimensions of channels and pores, (4) high adsorption capacity [24,76]. The physical properties of zeolites depend on the synthesis conditions including temperature, gel precursors, structure-directing agent [77]. The pore size and framework of zeolites tend to affect the product composition via several reactions restricting formation of hydrocarbons larger than that of pore size of zeolites. This is called shape selectivity and is one of the most important factors distinguishing zeolites from other type of catalysts. Selectivity is based on whether the aromatics derived from pyrolysis vapors can enter, form in, and diffuse out of the pores of the zeolite [24,25]. Shape selectivity of

zeolites is elaborately discussed in section 3.3.1.1 demonstrating ZSM-5 as a zeolite type.

The main reason why zeolites are commonly used in biomass pyrolysis is that their varied acidity and shape-selectivity provide advantage over silica-alumina catalysts of amorphous structure, in terms of aromatization reactions. Acidity depends on the Si/Al ratio of zeolite structure and can be caused by Brønsted and Lewis acid sites [24]. Acidity affects the catalytic reactions by providing enhanced cracking activity with decreasing Si/Al ratio [25]. Hence, the distribution of acid sites in the pores of zeolites is of high importance in terms of preventing coke-forming reactions in internal pores of zeolite. Low of Si/Al ratio causes higher amounts of acid sites with close proximity. Due to this reason, coke forming reactions which convert aromatic hydrocarbons into coke compounds will increase. Therefore, an optimum acidity is required for zeolites if it is used in biomass pyrolysis [21].

Aside from the distribution of acid sites, the pore structure of the individual zeolite plays an important role for selectivity of products and in terms of aromatic content of bio-oil. The pores of zeolites are characterized by the size of the ring defining the pore, that is, the n-number of the ring, which is referred to as the number of Si or Al atoms in the ring [78]. Hydrocarbon chain length of pyrolysis products, thus the size distribution of aromatic compounds, depends on the zeolite pore size and internal pore surface area. In general, larger pores and surface area leads to long chain structured hydrocarbons. Microporous surface area of the catalyst determines the yield of gaseous products of pyrolysis, whereas macroporous area determines the liquid yield [26,29]. A range of zeolites with different pore sizes have been studied in literature [32,79,80]. Y zeolite (faujasite), having a cubic structure with a pore system composed of 12-membered circular ring channels has the largest average pore size (7.4 Å) and internal pore space (11.24 Å) [24,25]. Such relatively large pore size affects the catalyzed reactions resulting less contact between pore surface and pyrolysis vapors, thereby leading to less cracking of biomass-derived oxygenates. Also, straight channels with larger pore size do not provide shape selectivity compared to other zeolites, which have smaller and sinusoidal channels that enable shape selectivity [25]. Despite having large pore size [77], Beta zeolite is of tetragonal crystal structure and has 12-membered straight channels crossed with 10-



membered ring channels, which makes it more effective for production of aromatic hydrocarbons, than Y-zeolites [25]. Ferrierite, as a medium pore size zeolite, have orthorhombic structure with 8 and 10 membered channels with internal pore space 6.31 Å [25,77].

Due to having two parallel channels connected with 12-membered rings and 8-membered rings, Mordenite is classified as a large pore sized zeolite and have orthorhombic structure [24,25,77]. ZSM-5, consisting of a MFI orthorhombic structure, is composed of 10-membered straight channels connected by 10-membered sinusoidal channels [74]. General physicochemical properties of zeolites are presented in Table 3.1.

**Table 3.1:** Physicochemical properties of zeolites most commonly used [24] [75] [76] [80]

<b>Catalyst</b>	<b>ZSM-5</b>	<b>Mordenite</b>	<b>Beta Zeolite</b>	<b>Y Zeolite</b>	<b>Ferrierite</b>
<b>IZA Code</b>	MFI	MOR	BEA	FAU	FER
<b>Pore Dimension</b>	3	2	3	3	2
<b>Channel System</b>	10-10	12-8	12-12	12-12	8-10
<b>Pore size (Å)</b>	5.1×5.5	7.0×6.5	7.6×6.4	7.4×7.4	4.2×5.4
	5.3×5.6	5.7×2.6	5.6×5.6		3.5×4.8
<b>Internal Pore Space(Å)</b>	5.2-5.5	4.2-6.7	6.1-6.68	11.24	6.31
<b>BET surface area(m<sup>2</sup>/g)</b>	395.5	558.7	643.1	809.1	*

\*information not available

Zeolites with medium and large pore size facilitate faster reactant diffusion compared to zeolites with smaller pore size, thus yielding more aromatics in liquid fraction of pyrolysis product. However, large-pore size zeolites produce less aromatics than medium-pore size zeolites because large pores promotes coke formation [24]. Accordingly, a recent study confirmed that ZSM-5 of medium pore size and medium internal pore surface area favors higher aromatics production and lower coke yield [21].

### 3.3.1 ZSM-5 Zeolite

ZSM-5, as one of the most common used zeolites in biomass pyrolysis [25], consists of pentasil units and have orthorhombic structure [78]. Being composed of 10-membered straight channels connected by 10-membered sinusoidal channels enables

ZSM-5 to have significantly more cracking activity than the other zeolites [25,30]. ZSM-5 has been widely used as catalyst in petroleum industry due to its shape selectivity, exceptional pore size with steric hindrance, thermal stability and solid acidity [81].

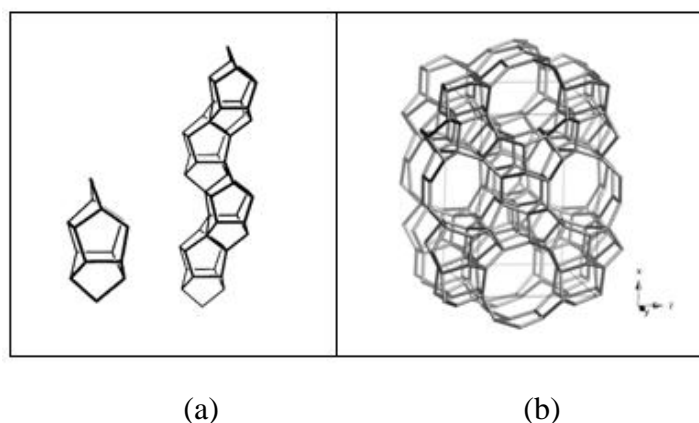


**Figure 3.2:** (a) pentasil unit and pentasil chain [78] (b) framework of ZSM-5 zeolite [82]

Compared to other zeolites, medium scaled pore size of ZSM-5 makes it difficult for larger aromatic coke precursors to form inside the pores [83]. Studies have shown that, regardless of feedstock, utilising ZSM-5 in biomass pyrolysis reduces the oxygenated compound content in bio-oil and simultaneously increases aromatic species [84-88]. Deoxygenation of oxygenated organic compounds occurs inside the ZSM-5 zeolite pores via reactions such as dehydration, decarboxylation and decarbonylation [30,45,50]. At lower temperatures, oxygen is found to be removed in the form of  $H_2O$ , whereas, in case of higher temperatures  $CO$  and  $CO_2$  are the main products of oxygen removal [45]. Oxygen removal, primarily in the form of  $CO$  and  $CO_2$ , is more preferable as it leads to less carbon deposition on the zeolite and, more hydrogen formation and consequently less water content in bio-oil [45].

### 3.3.1.1 Shape selectivity of ZSM-5

The phenomenon of shape selectivity can be explained by the combined effect of molecular sieve and catalytic reaction that occurs at the external and internal acidic sites of zeolites [89]. ZSM-5, having porous structure, can be used for shape-selective catalysis providing that not only the pore size but also dimensions of reacting and diffusing molecules are similar to zeolite pores [21]. Thus, the effect of pore size and steric hindrance of ZSM-5 on the catalytic reactions must be

investigated if zeolites with better performance are to be designed for biomass conversion [77].

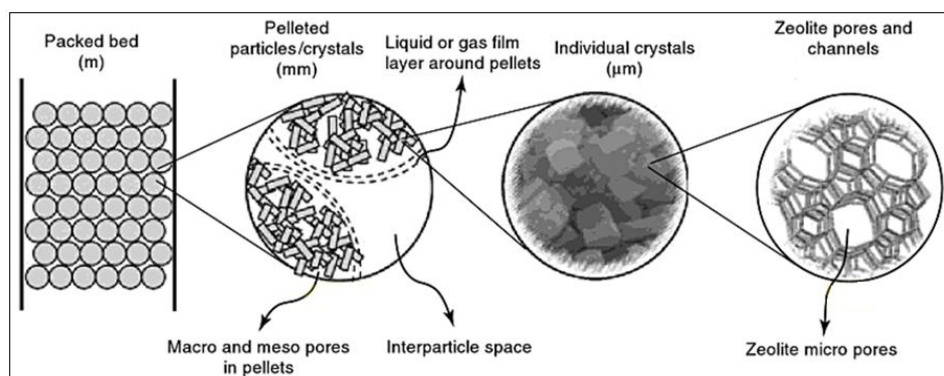


**Figure 3.3:** Pore structure of ZSM-5 zeolite [90]

The formation of pyrolysis products with shape selective catalysis depends on two types of selectivity: (1) reactant and product selectivity and, (2) transition state selectivity, which are described with their mass transfer effects and intrinsic chemical effects, respectively [24,77,89]. The main idea behind reactant and product selectivity lies behind the fact of hindered diffusion of reactants and products inside zeolite pores. Specific pore size of ZSM-5 affects the diffusion of reactants inside the pores excluding the ones with dimensions larger than the pore openings of ZSM-5, thereby preventing them from reaching the catalytic active sites and consequently allowing catalytic decomposition only at the external active sites [77,89]. Due to pore geometry of ZSM-5, formation of certain products are restricted affecting the chemical reaction and thus causing selectively homogenization of pyrolysis products [89].

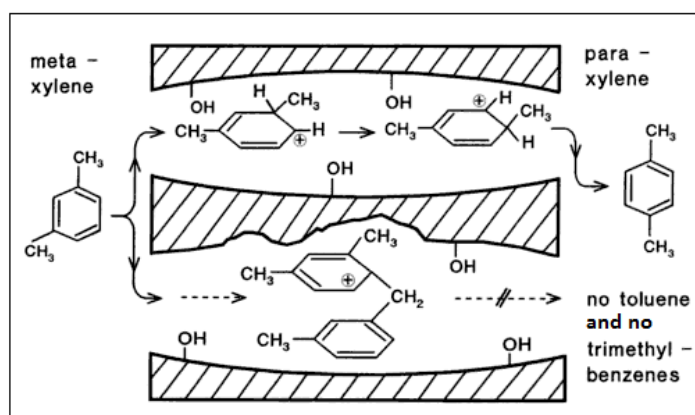


**Figure 3.4:** An example of transition state effect of ZSM-5: suppression of trimethylbenzene formation during meta-xylene isomerization [89]

Selectivity of ZSM-5 have been extensively studied and it is more commonly found to cause selectivity over aromatic compounds [46]. Mihalcik *et al.* [25] studied different zeolites for the conversion of several types of biomass and biomass components. According the results of this study, ZSM-5 was found to promote the formation of *p*-xylene in abundance for every case of biomass pyrolysis. In a study of Foster *et al.* [21], HZSM-5 for furan conversion showed a tendency for aromatic selectivity giving higher yield of aromatics as naphtalene having the highest percentage of 30.4% of overall aromatic species. Fogassy *et al.* [91], investigating the shape selectivity of zeolites for lignin fragments, revealed that majority of the phenolic compounds derived from lignin decomposition are too large to enter through zeolite pores, therefore, the conversion of these compounds occurs at the external active sites. As Yu *et al.* [24] suggested, however, at higher temperatures effective pore size of ZSM-5 increases, enabling bigger molecules than that of ZSM-5 pore size to reach the internal catalytic active sites. Jae *et al.* investigated the role of pore size of several types of zeolites in glucose pyrolysis (using kinetic diameters for products and reactants as affecting parameters) to determine whether the catalytic reaction occurs inside the pores or at the external surface [77]. Kinetic diameter was estimated from the properties at the critical point. It was revealed that ZSM-5 allowed pyrolysis intermediates and products (such as benzene, toluene, indene, ethylbenzene, *p*-xylenes) to diffuse into pores due to their significantly small kinetic diameters than that of ZSM-5 pore size. As temperature increases to 600 °C, due to thermal distortion, compounds like naphtalene which gave the highest yield in aromatics are likely to be formed inside the pores as well as on the surface. According to this study, it was concluded that, in addition to pore size, internal pore space of ZSM-5 affects the catalytic reaction. This suggests that biomass conversion with ZSM-5 is affected by mass transfer limitations as well as transition state effects [77].

### 3.3.1.2 Acidity of ZSM-5

Aside from the shape selectivity, the acidity of ZSM-5 plays an important role for the conversion of oxygenates into aromatics. It is generally accepted that, Brønsted acid sites are the active sites that converts oxygenated compounds into aromatics rather than Lewis acid sites. Cracking of large oxygenated occurs at the acid sites of external surface of ZSM-5, whereas, conversion of smaller ones into aromatics takes

place at the acid sites inside the pores [24,92]. Therefore, the abundance of both external and internal acid sites must be investigated in order to design a better process for aromatics formation.

As explained by Van Santen (1994), Brønsted acid sites are generated as a result of replacement of silicium which has a valency of four, by a metal atom, most commonly aluminum with a valency of three [90]. Thus, this makes Brønsted acid sites proton donors. Si and Al are connected with a proton-attached oxygen atom which leads to a chemically more stable structure [90,93]. On the other hand, Lewis acid sites are electron pair acceptors and the nature of these sites is related to aluminum atoms positioned in the framework [93,94].

In addition to nature of the acid sites, the molar ratio between  $\text{SiO}_2$  and  $\text{Al}_2\text{O}_3$  in zeolite framework also influences the reactivity and performance of ZSM-5. Optimum Si/Al ratio is necessary to provide high availability of Brønsted acid sites for adequate acidity and to maintain the distance between acid sites in order to limit coke-forming reactions [21]. As Si/Al ratio decreases (increase the acidity of ZSM-5) the acid sites will be in close proximity to each other, resulting in secondary reactions for conversion of aromatic compounds to coke species [21].

Foster *et al.* [21] investigated the effect of ZSM-5 with varying Si/Al ratio on pyrolysis of glucose. This study showed that decreasing Si/Al ratio contributed formation of the additional acid sites for ZSM-5 with increasing coke yields. Coke and product yields, based on varying acidity, obtained from the study is demonstrated in Figure 3.5. In a study of Carlson *et al.* [83], ZSM-5 ( $\text{SiO}_2/\text{Al}_2\text{O}_3=15$ ) promoted coke formation mostly on the catalyst surface giving the highest yield of 33% for coke ( where the catalyst to biomass ratio was 19). It was also indicated that coke formation on the external pores of ZSM-5 did not significantly decrease the yield of aromatics but affected the selectivity towards light hydrocarbons, resulting lower yields for benzene and toluene, higher yields for naphthalenes and indanes.

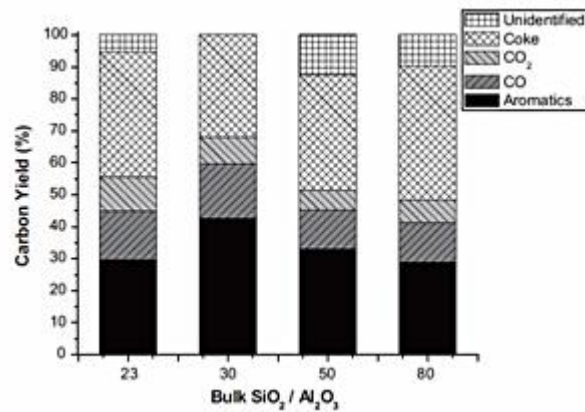


**Figure 3.5:** Effect of varying SiO<sub>2</sub>/Al<sub>2</sub>O<sub>3</sub> composition to fractional yield of pyrolysis products [21]

### 3.4 General Effects of Catalysts on Bio-oil

It is a known fact that catalysts have strong influence on pyrolysis in terms of product distribution, chemically homogenization, enhancing fractional product yield, upgrading the pyrolysis products to better quality. Among catalysts, zeolites and metal oxides have been mainly investigated for biomass conversion and found to be effective in changing the composition of bio-oil by reducing the oxygenated compounds via deoxygenation reactions and enhancing the aromatic yield, thus producing a more homogeneous and stable organic fraction that can be upgraded to diesel grade fuels [32,49]. To consider pyrolysis products, particularly bio-oil, for stationary fuel applications or heat/electricity generation, properties including acidity, viscosity, stability, and aromatic content of bio-oil are needed to be evaluated [22]. Therefore, the effects of catalysts to bio-oil must be addressed, as elaborately discussed below, in order for better understanding of biomass conversion.

#### 3.4.1 Aromatic yield of bio-oil

Aromatic content of bio-oil is of high importance in terms of producing diesel grade fuels from biomass feedstocks and biomass originated waste materials. Among aromatics, the amount of benzene, toluene, ethyl-benzene and xylenes (BTEX components) are the most significant feedstock materials to take into consideration for petroleum chemical industry [71,92].

Utilising catalysts has been shown to increase the yield of bio-oil as well as the content of aromatics in bio-oil which is a good indicator fuel quality. Kim *et al.* [92] studied catalytic pyrolysis of mandarin residues with high lignin content and found that using HZSM-5 of 23 and 80 acidity increased yield of monoaromatics from 3.4% to 36.0% and 41.0%, respectively. From the study of Zheng *et al.* [80], changing crystal size of ZSM-5 affected the aromatic yield and BTX selectivity so that smaller crystal size gave maximum aromatic yield and lowest BTX selectivity with the values of 38.4% and 36.3%, respectively. However, larger crystal size exhibited lowest aromatic yield and highest BTX selectivity with the values of 31.1% and 42.6%, respectively. Thus, smaller crystal size (200 nm) was found to be optimum for high aromatic yield. Zhang *et al.* [87] compared the behavior of pyrolysis of aspen lignin under the effect of H-Y and HZSM-5 catalyst. At catalyst to feed ratio of 3:1, production of aromatics exhibited a maximum value of 23% using HZSM-5 as catalyst, where the oxygen content of the aromatics decreased to about 4% and the HHV of the fraction was estimated to be approximately 46 MJ/kg, which is closer to that of gasoline and diesel. It was indicated that HZSM-5 was more effective than H-Y in converting phenolic compounds to aromatic hydrocarbons [87] due to its higher acidity and smaller pore size compared to HY [87]. Similarly, Pattiya *et al.* [79] studied ZSM-5 and two mesoporous materials including Al-MCM-41 and Al-MSU-F to investigate the fast pyrolysis of cassava rhizome. It was revealed that, of all the catalysts tested in the study, ZSM-5 gave the highest yield of aromatic hydrocarbons in order of toluene > benzene > 4,7-dimethylindane > *p*-ethyl-styrene > 5-methylindane > xylenes.

Aside from zeolites, the effect of metal oxides towards aromatization has been studied by researchers [7,46,95,96]. From the results of the study of Ateş & Işıkdağ [95], using alumina as catalyst on corncorb pyrolysis exhibited a trend to promote the formation of 1,1,3,3-tetramethylindane, benzene and 1-methyl-4-(penylmethyl) being most significant monoaromatic compounds. The formation of naphthalene, 1-(2-propenyl)-, a PAH compound, was found to be increased at moderate temperature using catalyst. Smets *et al.* [97] compared various catalysts including HZSM-5,  $\gamma$ -Al<sub>2</sub>O<sub>3</sub>, Na<sub>2</sub>CO<sub>3</sub>. Sodium carbonate was the most effective catalyst to increase the yield of aromatics following HZSM-5. Wang *et al.* [96] also conducted a comparative study for catalytic conversion of herb residues over alumina, ZSM-5

and Al-SBA-15, where alumina was found to give the highest bio-oil yield. Thus, the researchers of this study investigated the effect of alumina to the aromatic yield in terms of toluene, ethylbenzene and *p*-xylene compounds and revealed that the percentage of aromatic fractions increased from 8.02% to 10.93%.

### 3.4.2 Acidity of bio-oil

The acidity of bio-oil is due to volatile acids, mainly carboxylic acids, i.e., formic acid and acetic acid [61]. Phenolic compounds also contribute the acidity of bio-oil [22]. Determination of acidity in bio-oil is performed either by measuring pH value or total acid number. pH value is an indicator for evaluating the corrosiveness of bio-oil, whereas, total acid number is used as a quality indicator for bio-oil utilisation in co-processing of petroleum refining facilities and it relates to the level of acidic components in the oil [61].

Studies have clearly shown that organic acids are reduced by utilising catalysts [52], thereby, facilitating the utilisation of bio-oil in fuel applications. The main question is to find the most suitable catalyst-biomass match, taking the process conditions into account for pyrolysis systems, in order to replace bio-oil with fossil fuel equivalents (such as diesel and gasoline).

Zabeti *et al.* [22], studied amorphous silica alumina modified with alkali or alkali earth metals such as Na, K, Cs, Mg and Ca. It was concluded that, amongst all the catalysts tested in the study, K/ASA was the most effective catalyst to reduce the carboxylic acids and carbonyl substituted-phenols content in bio-oil. Zhou *et al.* [19] investigated the effect of ZnO to physicochemical properties of rice husk bio-oil. pH value of catalytic bio-oil was recorded as 4.35 whereas non-catalytic bio-oil had 4.15 of pH value. Thus, this indicated the effect of ZnO catalyst towards reduction of acidic compounds in bio-oil. Abu Bakar & Titiloye [50] studied rice husk pyrolysis over various catalysts including ZSM-5, Al-MCM-41, Al-MSU-F and (Brunei rice husk ash) BRHA. Catalysts have been shown to reduce the acid number from 55 mg/KOH to 39-47 mg/KOH, with ZSM-5 and BRHA having the lowest value. Also, pH value of the catalytic rice husk bio-oil was recorded in the range of 2.7-3.0. Majority of acidic compounds were carboxylic acids, as acetic acid having the highest percentage. Mante & Agblevor [51] studied HZSM-5 as deoxygenating catalyst to convert hybrid poplar wood to biosyncrude oil. As indicated in the study,



the pH value of light biosyncrude oil containing mainly aromatic hydrocarbons, was increased from 2.60 to 4.05 in result of reducing effect of HZSM-5.

### 3.4.3 Viscosity of bio-oil

High viscosity of bio-oil, compared to conventional fuels, is one of the drawbacks for its utilisation in fuel applications. Most importantly, in case of bio-oil using combustion engines, high viscosity increases the droplet size from the injector spray thereby affecting the ignition of droplets [98]. Therefore, decreasing viscosity of bio-oil to improve fuel properties is essential. Scientists revealed that use of catalysts improved fuel properties of bio-oil by decreasing viscosity [56,99].

Azargohar *et al.* conducted non-catalytic pyrolysis experiments for several biomass waste materials and it was observed that the viscosity of bio-oil, ranging between 63-418 cP, was much more higher than that of crude petroleum oil (~ 23 cP), requiring a further a upgrading process. It was also revealed that the reason of high viscosity was mainly due to lignin derived hydrocarbons of large molecular weight [100]. However, in a study of Fan *et al.* on rape straw pyrolysis over nanocrystalline HZSM-5, the dynamic viscosity was reported to be 5.12 mm<sup>2</sup>/s which was between the accepted limits for diesel fuel as indicated in the study [99]. Mante *et al.* investigated the hybrid poplar wood pyrolysis with the additive effect of Y-zeolite based FCC catalyst to ZSM-5. FCC/ZSM-5 catalyst was found to be more effective than pure ZSM-5 in decreasing viscosity of bio-oil samples, indicating synergistic effect of hybrid catalyst, also suggesting that lower weight hydrocarbons was attributed to be formed by presence of catalyst [56]. Mante & Abglevor [51], studied hybrid poplar wood pyrolysis with the addition of ZSM-5. They classified the liquid fraction of pyrolysis product as LBS (low biosyncrude) oil containing mainly aromatic hydrocarbons and HBS (high biosyncrude) oil which consists of mainly phenols, methyl-substituted phenols, naphthalenes, benzenediols, and naphthalenol. The viscosity of LBS oil, which was significantly lower than that of non-catalytic bio-oil (285 cSt), was reported to be 4.90 cSt. It was suggested that lower viscosity was attributed to the catalytic cracking of levoglucosan and depolymerization of lignin derived products [51]. Shadangy & Mohanty conducted several studies using various biomass species over CaO, Kaolin and Al<sub>2</sub>O<sub>3</sub> [72,101,102]. Regardless of the biomass type, CaO was found to produce bio-oil of lower viscosity than that of non-

catalytic bio-oil compared to other catalysts used for their studies. The viscosities of bio-oil obtained by using CaO were 0.019629 Pas [102] and 9.007 cP [72], indicating that utilising catalyst favored a decrease in viscosity about 62% and 74.5%, respectively.

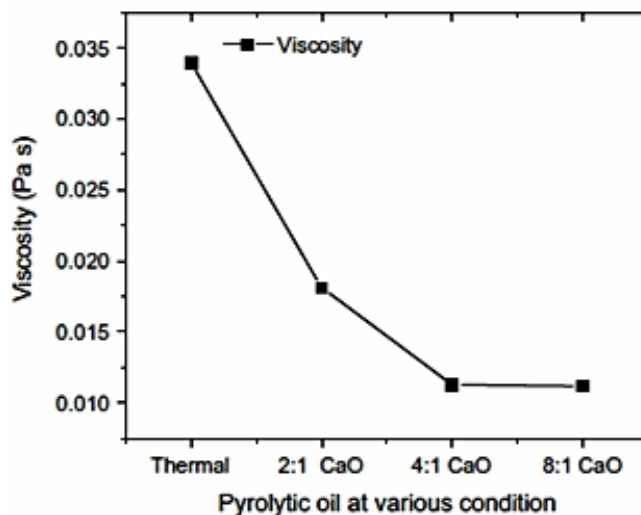


**Figure 3.6:** The effect of CaO catalyst to viscosity of bio-oil [102]

Abu Bakar & Titiloye studied ZSM-5, Al-MCM-41, Al-MSU-F and BRHA (brunei rice husk ash) for the conversion of rice husk to bio-oil and the viscosities of bio-oils were, as indicated, 1.55, 1.65, 1.49, and 1.57 cSt, respectively. All the catalysts used in the study decreased viscosity about 1.7-11.3% and slightly increased water content, which indicates that the catalysts favored dehydration reaction [50].

### 3.4.4 Stability of bio-oil

Bio-oil is not as chemically or thermally stable as fossil fuels due to its high content of oxygenated compounds [98]. At high temperatures above 40 °C or during long term storage situations, the viscosity of bio-oil is reported to increase due to chemical reactions between components such as ketons and aldehydes, leading to formation of compounds of heavy molecular weight [22]. Thus, it is expected that bio-oil with lower content of carbonyl groups would be more stable. Utilising catalysts, in order to facilitate transportation and storage of bio-oil, leads to enhanced cracking reactions of heavy molecules as well as removal of oxygenated compounds, thus leading to production of bio-oil with high stability [103]. There is no standard method for determination of stability of bio-oil, however, in result extensive studies on this matter, several methods have been developed by researchers [104-106].

In a study of Zabeti *et al.*, where Cs/ASA was found to be most effective catalyst to eliminate oxygenated compounds and increase aromatic yield compared all the catalysts tested in the study. The results of Size Exclusion Chromatography (SEC) showed that bio-oil molecular weight shifted to higher weight regions after aging [22]. Mante and Agblevor conducted a stability test for the catalytic bio- oils (low and high biosyncrude oil) produced from hybrid poplar wood. The stability and aging test was performed in a gravity oven at 90 °C for 24 hours. Also, the viscosities of the bio-oil samples stored at 40 °C for over 10 months were also measured and the change in viscosity was found to be 5% for low biosyncrude oil and 27.9% for high bio syncrude oil. It was concluded that, catalytic bio-oils were thermally stable and could be stored in room temperature for over 10 months without any significant increase in viscosity [51]. Nokkosmäki *et al.* studied pine sawdust pyrolysis with the addition of ZnO as catalyst. The stability test was performed at 80 °C for 24 h and showed that viscosity was changed with the use of ZnO. The change in viscosity was 55%, which was significantly lower than that of non-catalytic bio-oil(129%) [44]. Duman *et al.* investigated the effect of methanol addition to the stability of bio-oil produced from safflower oil cake using FCC as catalyst. Addition of methanol reduced the viscosity. The viscosity was much lower at higher temperatures, thus indicating a more stable bio-oil. After aging test at 40 °C for 168h, the viscosity increased by 46.63% and 21.08% in case of raw bio-oil and methanol amended bio-oil, respectively [60].



#### 4. DEACTIVATION AND REGENERATION OF CATALYSTS

Catalyst deactivation, the loss of catalytic activity and selectivity over time, is one of the major problems concerning industrial application of catalysts in pyrolysis process [27,56].

The causes of deactivation are mainly due to chemical, mechanical and thermal mechanisms of catalyst delay [107], but, in this section only physical deactivation is addressed. Physical deactivation is done either by coke deposition on the catalyst pores or by covering active catalytic sites preventing pyrolysis vapors to enter through the pores for catalytic reactions such as aromatization, depolymerization and isomerization [56,107,108]. As suggested by Forzatti and Lietti [108], catalyst deactivation reactions proceeding via carbonium ion intermediates involve series of chemical reactions which vary by the variety of components of reaction mixture, catalyst type, reactions conditions.

Coke is deposited on catalyst pores, in the form of carbon oxides via oxidation. In case of deactivation, if irreversible, regeneration of catalysts under more severe conditions than that of main process is necessary to remove coke [109]. Mante *et al.* compared the catalytic activity of different zeolites in terms of coke deposition, and reported that Y-zeolite was more prone to produce coke than ZSM-5 because of its faujasite structure, larger pore size and acidity [56]. In a study of Iisa *et al.*, ZSM-5 zeolite was regenerated via oxidation and after five regeneration cycles, no reduction in catalytic activity was recorded [27]. Nokkosmaki *et al.* [44] observed catalyst deactivation at 400 °C. The catalyst affected the degradation of polysaccharids, so that between the first and the fifth pyrolysis cycles, the ratio of levoglucosan was raised from 1.0% to 2.0%. Zabeti *et al.* studied regeneration of Cs/ASA catalyst by calcinating under air atmosphere at 600 °C for five hours operation [22]. The regenerability of catalyst was evaluated measuring the BET surface area and bio-oil yield obtained after regeneration. It was reported that BET surface area of regenerated catalyst decreased by 10.6% whereas bio-oil yield remained the same

with 45.0 wt.%, suggesting that Cs/ASA catalyst is regenerable. Similar results were obtained by Aho *et al.* investigating the effect of regenerated catalyst to pyrolysis of biomass with H-Beta zeolite with Si/Al ratio of 25. After regeneration, surface area of catalysts decreased, though, the bio-oil yield increased [47].

## 5. EXPERIMENTAL METHODS

### 5.1 Materials

#### 5.1.1 Feedstock Characterization

Olive pomace was obtained from a local olive oil producer, Körfez Oil Production Plant which is located in South Marmara Region. Olive pomace samples were oven dried at  $104\pm 3$  °C for 24 h to remove the moisture, then grounded to pass through a 60 mesh sieve (250  $\mu\text{m}$ ) using a RETSCH AS 200 vibrating sieve prior to thermal analysis. Gross calorific value of the samples were determined using an adiabatic mode bomb calorimeter (IKA C5000) as described in ASTM D 5865. The samples were also analyzed for their ash content by muffle furnace at 575 °C as described in ASTM E 1755-01. Volatile matter content was determined in accordance with ASTM E872-82. Elemental composition of olive pomace was investigated using LECO CHN628 elemental analyzer and the properties of olive pomace are reported in Table 5.1.

**Table 5.1:** Main characteristics of olive pomace

Properties		Olive Pomace
Gross Calorific Value (kJ/kg)		20,300
Elemental Analysis (wt.%)	Carbon	48,7
	Hydrogen	7,1
	Nitrogen	2,9
Proximate Analysis (wt.%)	Volatile Matter	75.6
	Moisture	2,5
	Ash	3

Previous study of Başkan [14], revealed that lignin, cellulose and hemicellulose contents of the olive pomace were in the range of 323-557, 140-249, 273-416  $\text{g.kg}^{-1}$  pomace, respectively. Thus, in this study, these values were accepted to be the compositional distribution of olive pomace.

### 5.1.3 Catalyst Properties

Ammonium form of ZSM-5 powder provided by Zeolyst International Inc. was used as catalyst in this study. It is a low acidity zeolite having a silica to alumina molar ratio of 280. The physicochemical properties of ZSM-5 zeolite is summarized in Table 5.2. Prior to experiments, the catalyst was calcined in a muffle furnace at 550 °C for two hours. Olive pomace and ZSM-5 samples were prepared in ratios of 1:1 (wt,% db), 1:2 (wt, % db) and 1:3 (wt, % db), where the abbreviations “wt, %db” denotes the percentages on dried weight basis.

**Table 5.2:** Textural properties of ZSM-5

Catalyst	ZSM-5
BET Surface Area (m <sup>2</sup> /g)	400
SiO <sub>2</sub> /Al <sub>2</sub> O <sub>3</sub> Molar Ratio	280
Nominal Cation Form	Ammonium

## 5.2 Experimental Procedure

### 5.2.1 Thermogravimetric Analysis

In this study, catalytic pyrolysis characteristics of olive pomace (reaction rate and weight loss due to decomposition) were investigated using thermogravimetric analysis by an Exstar SII TG/DTA 6300 analyzer. The experiments were conducted non-isothermally at atmospheric pressure and temperatures ranging from 20 °C to 800 °C under inert (N<sub>2</sub>) atmosphere. In order to find and compare the kinetic parameters of catalytic olive pomace pyrolysis, three different heating rates (10, 30, 40 °C.min<sup>-1</sup>) were studied. The effect of catalyst on olive pomace pyrolysis was also investigated using different biomass to catalyst ratios, which are 1:1, 1:2, 1:3 (wt, %db). In the absence of ZSM-5, olive pomace sample was pyrolyzed via thermogravimetric analyzer thus allowing us to compare the effect of ZSM-5 to traditional pyrolysis of biomass. Thermal behavior of ZSM-5, under the same process conditions, was investigated in order to evaluate the overall system.



### **5.2.2 Differential Scanning Calorimetry (DSC) Analysis**

Differential Scanning Calorimetry was used in order to determine whether the pyrolysis process have endothermic or exothermic nature. DSC curves were measured by heating up to 10 mg of sample in covered platinum pans using Exstar SII DSC 7020 analyzer. The analyses were conducted at atmospheric pressure and temperatures ranging from 20 to 600 °C at two different heating rates; 20 °C.min<sup>-1</sup> and 40 °C.min<sup>-1</sup> under nitrogen atmosphere.

### **5.2.3 Pyrolysis Experiments**

In order to study the catalytic effect of ZSM-5 on bio-oil composition, the furnace application of olive pomace pyrolysis was necessary. Pyrolysis of olive pomace was evaluated with and without the addition of ZSM-5 as catalyst. All the pyrolysis reactions with or without ZSM-5 catalyst were carried out in a modified PROTHERM 12/50/450 model tubular furnace under N<sub>2</sub> atmosphere. After an extensive literature review, the optimum conditions for highest bio-oil yield was determined to be 550 °C of pyrolysis temperature and 25 °C.min<sup>-1</sup> of heating rate and 15 minutes of retention time excluding the heating up and cooling down. Experimental set up of the system is demonstrated in Figure 5.1(a) and 5.1(b). Olive pomace with a particle size smaller than 250 µm was used as feedstock in the experiments. Prior to experiments, nitrogen with 100 L.h<sup>-1</sup> flow rate was passed through the furnace for 30 minutes in order to eliminate the oxidizing environment. For non-catalytic runs, raw biomass of 0.5-1.0 gr was weighed in a ceramic crucible and inserted inside the furnace. For catalytic runs, biomass to catalyst ratio of 1:1 and 1:2 (wt.%, db) was selected in order to evaluate the effect of catalyst to olive pomace conversion. The pyrolysis vapors leaving reaction medium passed through two sequential condensers, placed in a separate unit filled with ice-salt mixture, where the condensable vapors were allowed to condense. Condensable fraction of pyrolysis products was then dissolved in dichloromethane and methanol for further compositional analysis by using GC-MS.



**Figure 5.1:** (a) Experimental setup for pyrolysis of olive pomace  
 (b) sequential condensers for trapping pyrolysis vapors

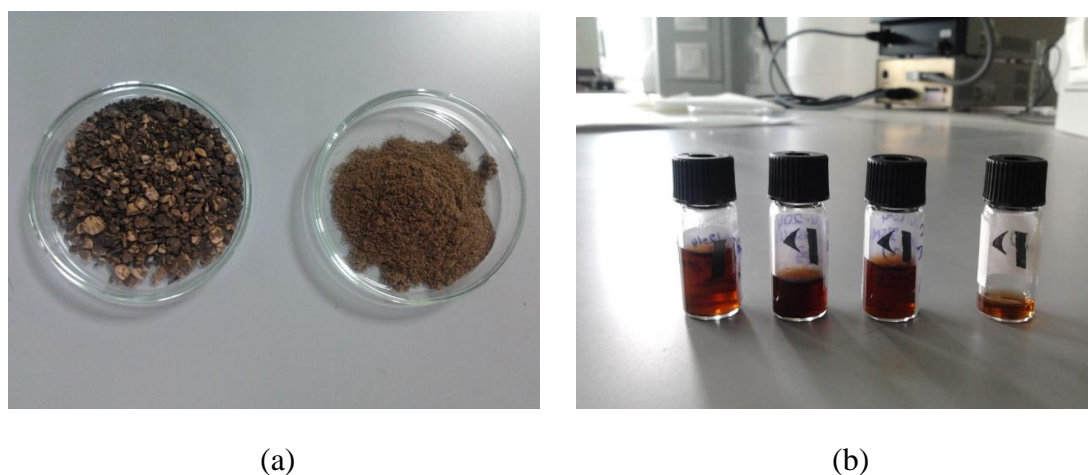


**Figure 5.2:** (a) olive pomace in dried and grinded form  
 (b) some bio-oil samples dissolved in methanol and DCM

#### 5.2.4 Analysis of Bio-oil

To understand the catalytic effect of ZSM-5 on bio-oil composition, GC-MS (Gas Chromatography-Mass Spectrometry) was used as an analytical method in order for detection and identification of bio-oil components. The bio-oil samples, which were collected from condensers, dissolved in methanol and dichloromethane were delivered to Redoks Lab for compositional analysis by using GC-MS. Composition of bio-oil was measured by Trace 1300 ISQ GC-MS (Thermo Scientific) equipped with TR-5MS capillary column (30.0 m  $\times$  0.25 mm inner diameter  $\times$  0.25  $\mu$ m thickness). Helium was employed as the carrier gas at a constant flow rate of 1.5 ml.min<sup>-1</sup>. Initial oven temperature was set at 313 K, held for 5 min, then increased to

573 K with a heating rate of 278 K.min<sup>-1</sup> and held for further 10 min. Splitless injection was carried out at 573 K and a sample volume of was injected. Data were acquired in scan mode, and a  $m/z$  range from 30 to 500 Da was scanned. Chromatographic peaks were identified with NIST mass spectral data library.



## 6. RESULTS AND DISCUSSION

### 6.1 Thermal Behavior

There are several studies investigating kinetic behavior of olive residues and olive pomace via thermal pyrolysis. Ounas *et al.* investigated kinetic behavior of olive residue and sugar cane bagasse samples under nitrogen atmosphere at specific heating rates in the absence of catalyst. When the heating rate was  $10 \text{ K}\cdot\text{min}^{-1}$ , hemicellulose was decomposed in the range of 433-513 K; cellulose was degraded at relatively higher temperature range of 513-633 K and lignin was pyrolyzed at temperatures 433-900 K [4]. In the study of Başakçılardan-Kabakçı and Aydemir, olive pomace and RDF blends were traditionally pyrolyzed using thermal analysis at three different heating rates. At each heating rate thermal pyrolysis of olive pomace showed that pyrolysis reaction occurred in one stage having one small shoulder, which shows the decomposition of hemicellulose, just before the peak temperature [12]. Therefore, in order to understand the catalytic effect of ZSM-5 on pyrolysis of olive pomace, it is essential to study the kinetics of catalytic pyrolysis via thermal analysis. Thermogravimetric analysis (TGA), as a technique to study decomposition reactions, provides us to evaluate the effects of catalysts on pyrolysis process by providing the data of sample's weight loss versus time and temperature [10,17].

Figure 6.1 and 6.2 show the TG and DTG profiles of olive pomace. Profiles display two peaks; the first peak indicating the moisture removal ( $<110^\circ\text{C}$ ), and the second peak indicating the degradation of cellulosic fraction. It is evident from the profiles that the second peak is an overlapping stages of hemicellulose and cellulose degradation.

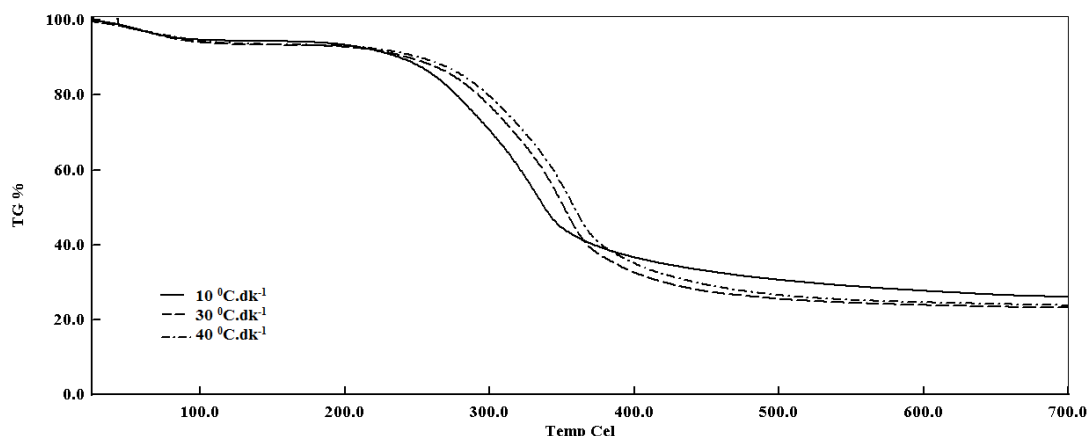


**Figure 6.1:** TG profiles of olive pomace at different heating rates

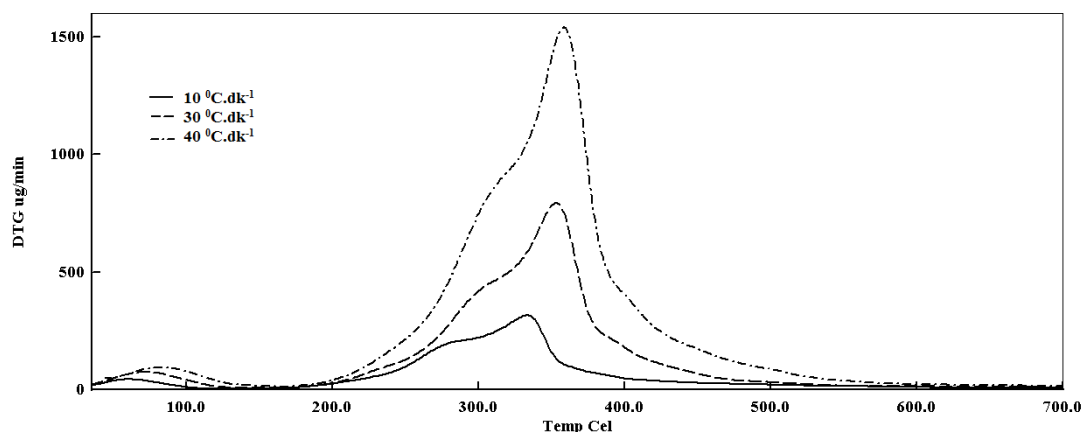


**Figure 6.2:** DTG profiles of olive pomace at different heating rates

Hemicellulose and cellulose were decomposed around 200-300 °C and 350-400 °C, respectively. The long tail after the peak denoted the degradation of lignin, which usually degraded at temperatures between 280-500 °C. At conditions where the constant heating rate was set as 10 °C.min<sup>-1</sup>, the first peak around 60,2 °C corresponded to 5,6% of weight loss; the second peak around 333<sup>0</sup>C corresponded to 67,2% of weight loss. As the heating rate increased to 30 °C.min<sup>-1</sup> and 40 °C.min<sup>-1</sup>; 7% of weight loss was seen due to moisture removal. The weight loss due to decomposition of cellulosic fraction was 69,5% and 70% respectively. Obviously, increasing the heating rate shifted the peak temperatures to higher.

From the TG and DTG profiles of samples, adding catalyst did not alter the peak temperatures of the decomposition reaction. Only the weight loss due to decomposition was changed. At the heating rate of 40°C.min<sup>-1</sup>, the hump (or stage 1) due to hemicellulose degradation in the DTG profiles were ceased. Figures between 6.3 and 6.11 show the TG and DTG profiles of olive pomace pyrolysis with the addition of ZSM-5 at different heating rates.

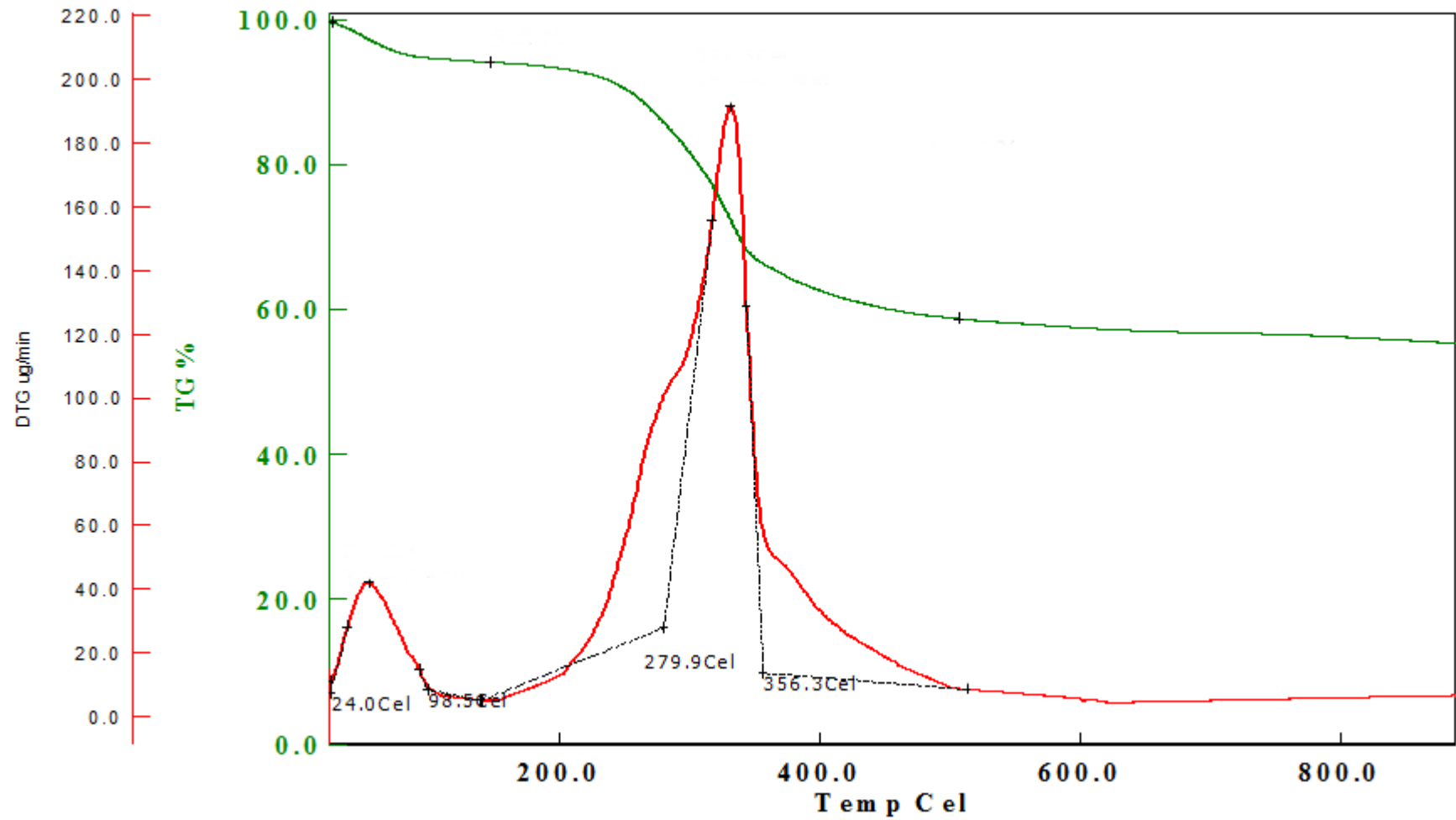


**Figure 6.3:** TG and DTG profile of olive pomace at a constant heating rate of  $10^{\circ}\text{C}\cdot\text{min}^{-1}$  with catalyst to biomass ratio of 1:1

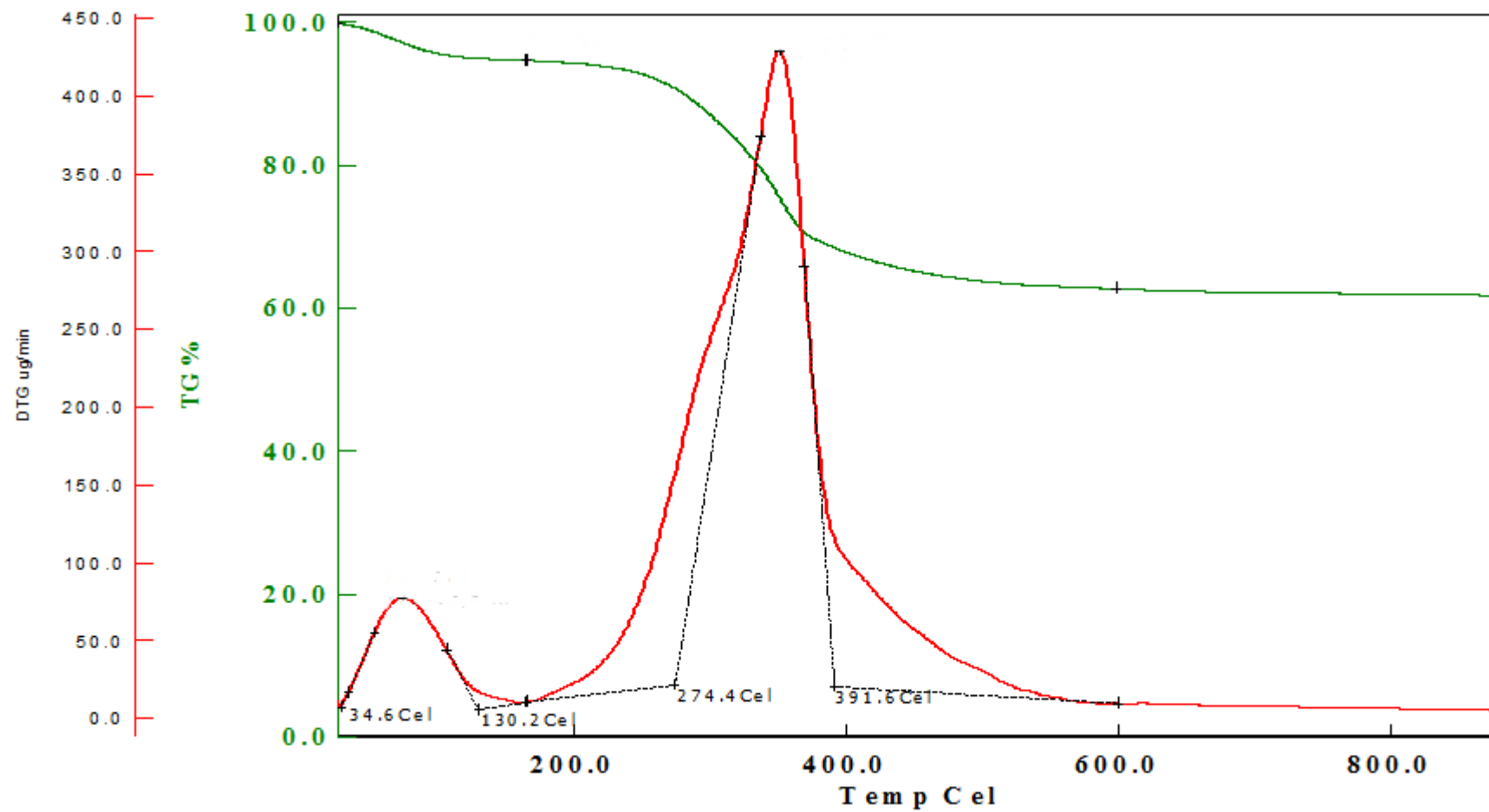


**Figure 6.4:** TG and DTG profile of olive pomace at a constant heating rate of  $30^{\circ}\text{C}\cdot\text{min}^{-1}$  with catalyst to biomass ratio of 1:1



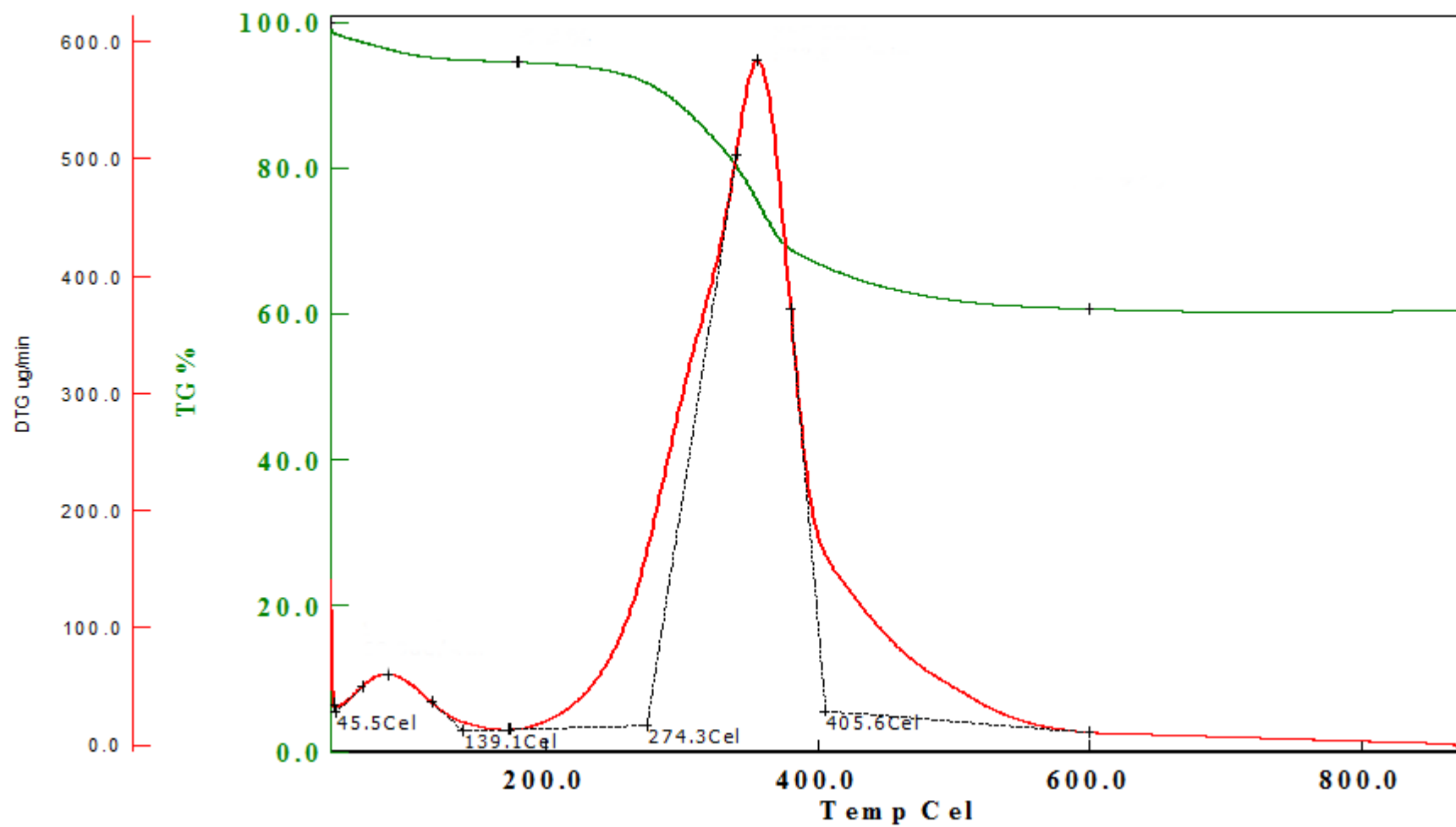


**Figure 6.5:** TG and DTG profile of olive pomace at a constant heating rate of  $40^{\circ}\text{C}\cdot\text{min}^{-1}$  with catalyst to biomass ratio of 1:1

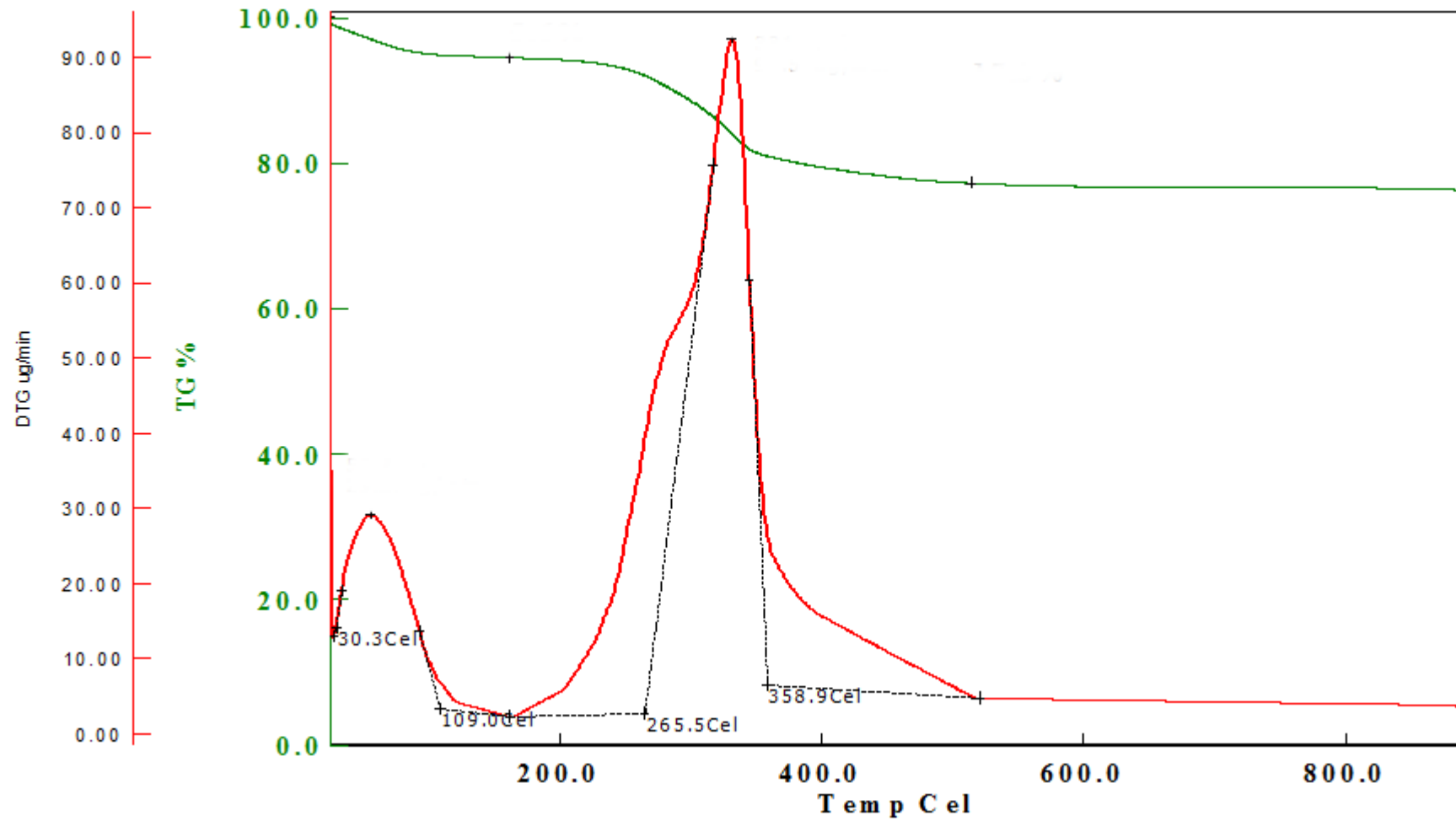


**Figure 6.6:** TG and DTG profile of olive pomace at a constant heating rate of  $10^{\circ}\text{C}\cdot\text{min}^{-1}$  with catalyst to biomass ratio of 1:2

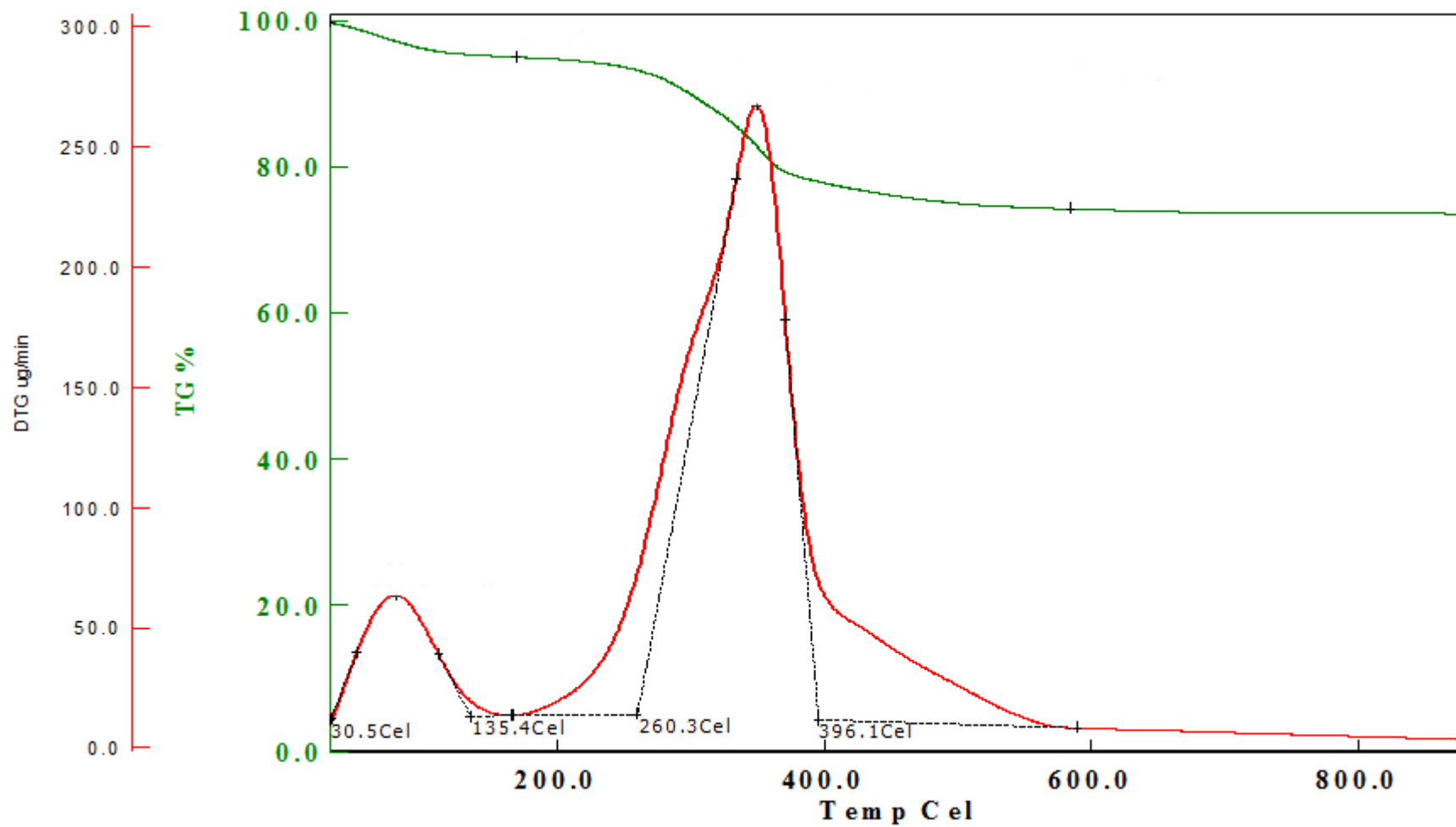


**Figure 6.7:** TG and DTG profile of olive pomace at a constant heating rate of  $30^{\circ}\text{C}\cdot\text{min}^{-1}$  with catalyst to biomass ratio of 1:2

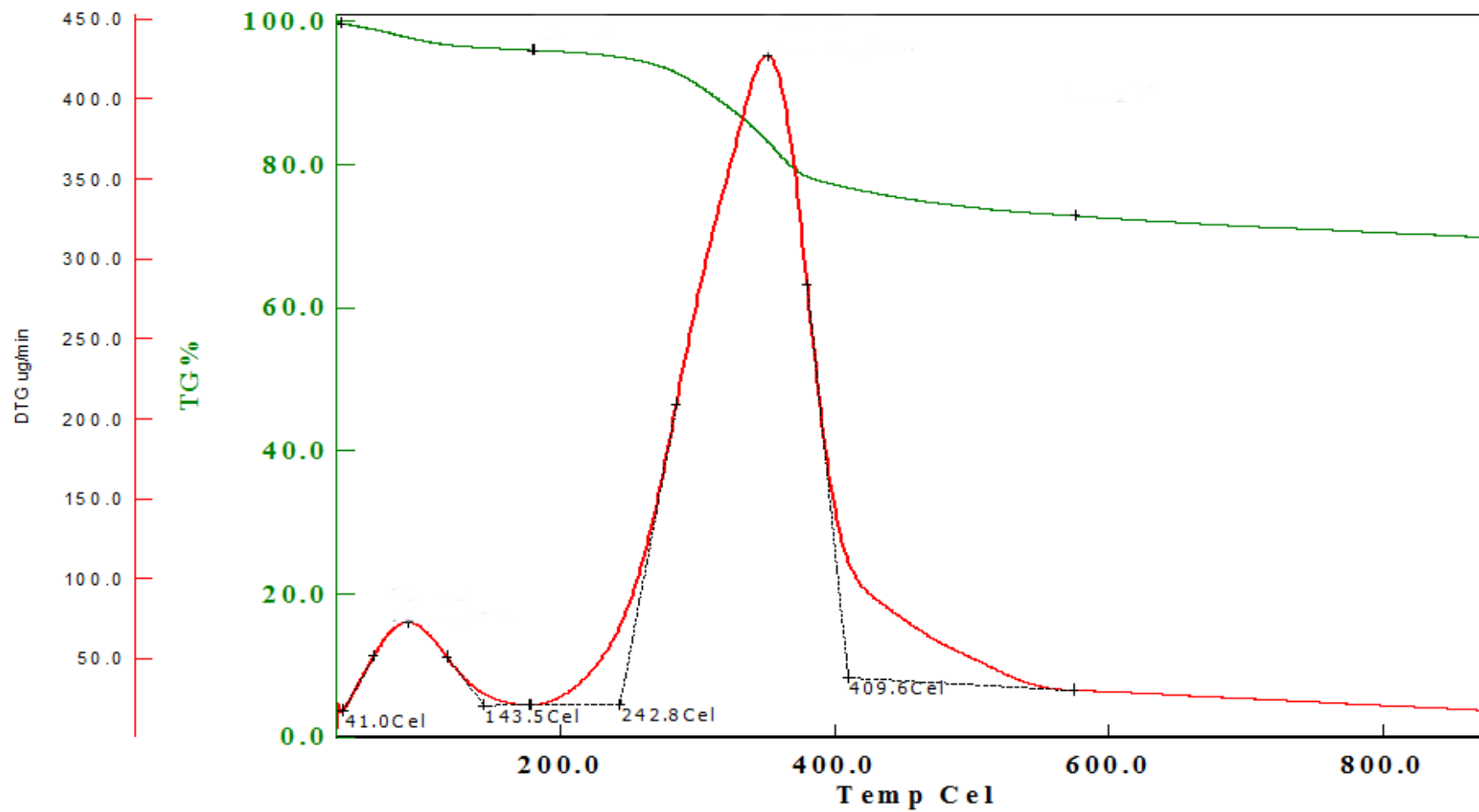


**Figure 6.8:** TG and DTG profile of olive pomace at a constant heating rate of  $40^{\circ}\text{C}\cdot\text{min}^{-1}$  with catalyst to biomass ratio of 1:2

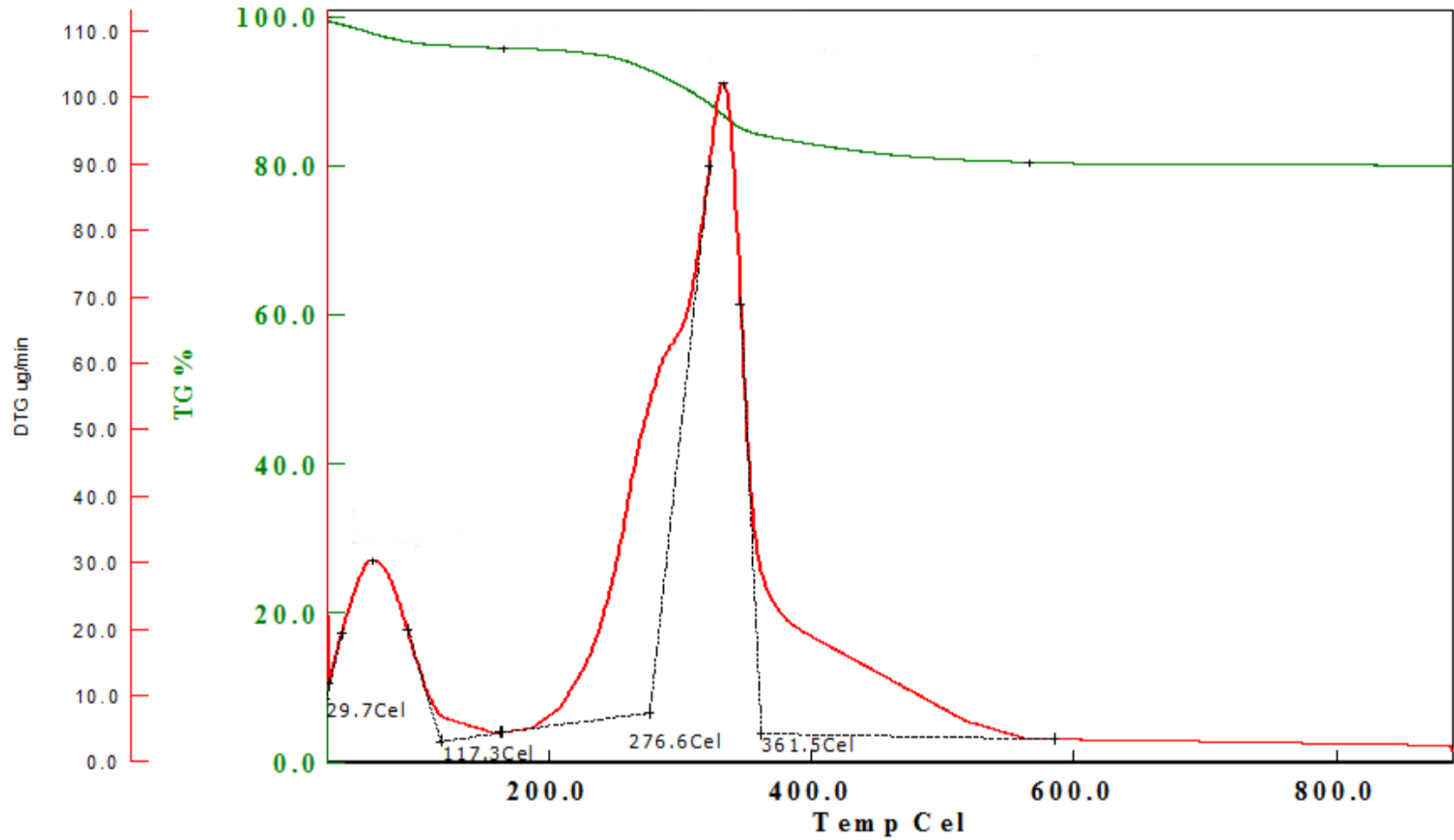


**Figure 6.9:** TG and DTG profile of olive pomace at a constant heating rate of  $10^{\circ}\text{C}\cdot\text{min}^{-1}$  with catalyst to biomass ratio of 1:3

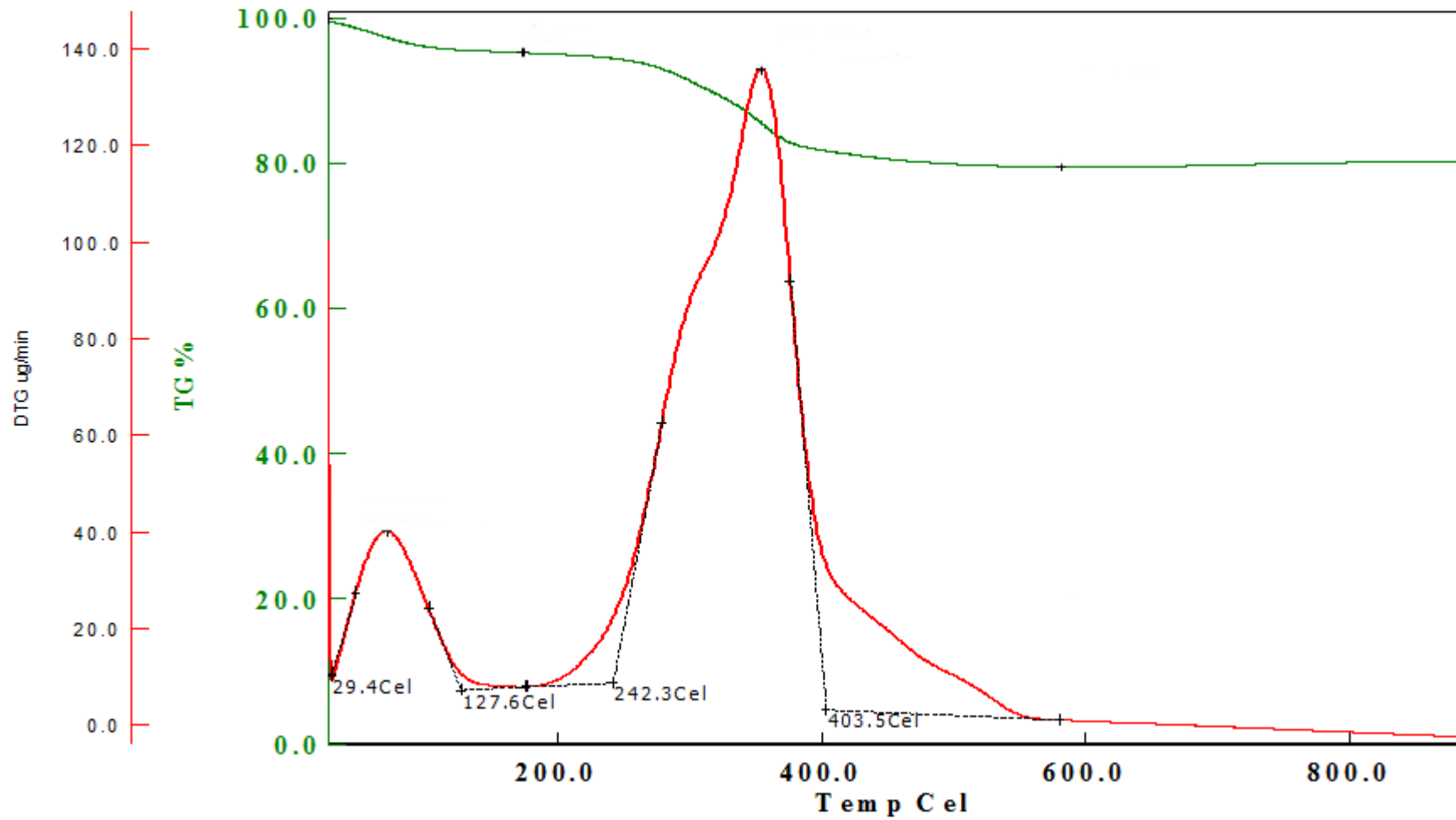


**Figure 6.10:** TG and DTG profile of olive pomace at a constant heating rate of  $30^{\circ}\text{C}\cdot\text{min}^{-1}$  with catalyst to biomass ratio of 1:3

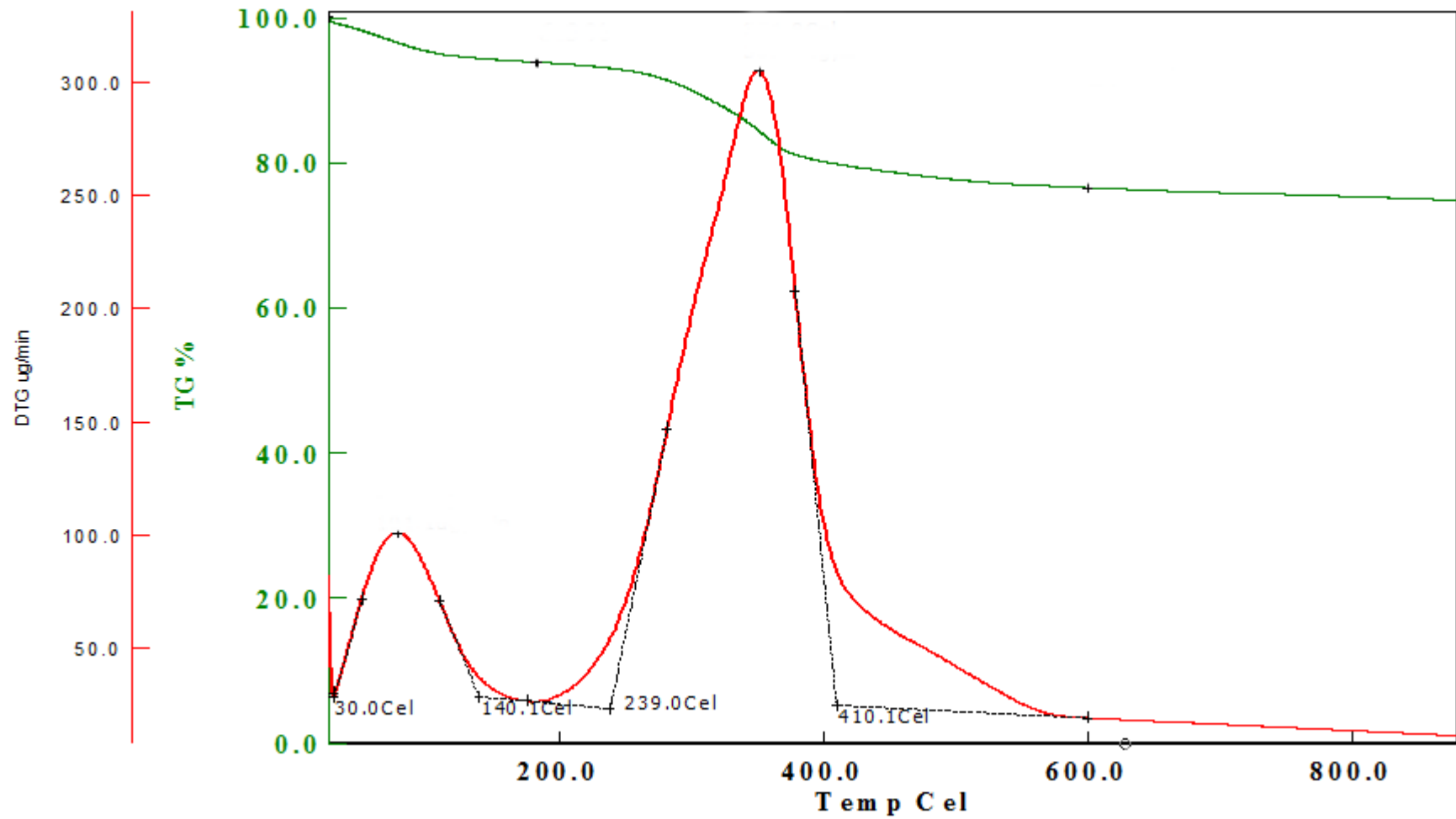


**Figure 6.11:** TG and DTG profile of olive pomace at a constant heating rate of  $40^{\circ}\text{C}\cdot\text{min}^{-1}$  with catalyst to biomass ratio of 1:3

## 6.2 Differential Scanning Calorimetry (DSC) Analysis

Figure 6.12 and 6.13 show the DSC profiles of olive pomace with or without the addition of ZSM-5 at two respective heating rates: 20 and 40 °C.min<sup>-1</sup>. It was clearly seen that, the DSC profiles and DTG profiles showed consistent degradation mechanism for olive pomace. The degradation of hemicellulose and cellulose were found to be overlapped while lignin was decomposed in a wider range of temperature. Non-catalytic pyrolysis of olive pomace was evidently an endothermic reaction, though, use of ZSM-5 did not altered this situation resulting a catalytic pyrolysis with endothermic nature. A high endothermic peak was seen below 100 °C. The wide endothermic peak observed between 250-275 °C showed the pyrolysis of cellulose fraction.

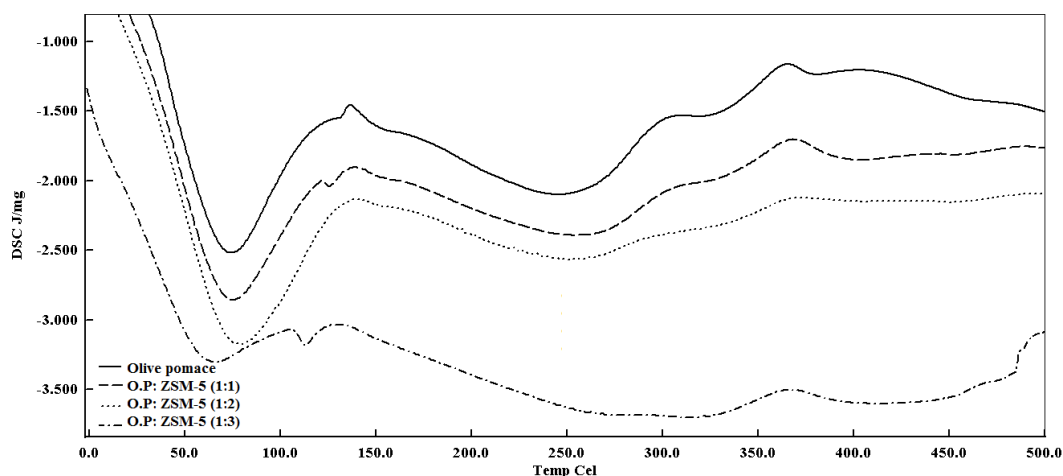


**Figure 6.12:** DSC profiles of olive pomace at heating rate of 20 °C.min<sup>-1</sup>

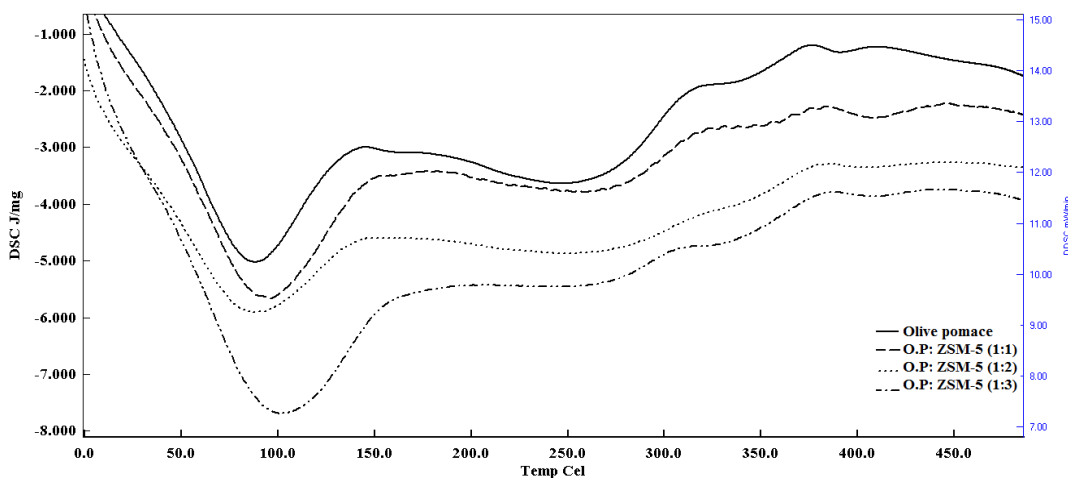


**Figure 6.13:** DSC profiles of olive pomace at heating rate of 40 °C.min<sup>-1</sup>



### 6.3 Kinetics of Olive Pomace Pyrolysis with ZSM-5

The kinetic parameters, mainly activation energy and pre-exponential factor were obtained from TGA data by using Coats and Redfern method. Application of Coats and Redfern method of TGA data is extensively summarized below.

For the thermal decomposition of component A to a component B, conversion or the fraction of the reacted component A is given by

$$x = \frac{m_0 - m}{m_0 - m_f} \quad (6.1)$$

Where  $m$  is the weight of the sample at a given time  $t$ ,  $m_0$  and  $m_f$  are the weights at the beginning and at the end of the relevant reaction. The rate of conversion is described as,

$$\frac{dx}{dt} = k(T) \cdot f(x) \quad (6.2)$$

where  $f(x)$  and  $k(T)$  are functions of conversion and rate constant respectively. In a thermogravimetric analysis, constant rate of temperature change,  $\beta$ , is defined as  $\beta = dT / dt$ . By using  $\beta$  in equation 6.3,

$$\frac{dx}{dt} = \beta \cdot \frac{dx}{dT} \quad (6.3)$$

The temperature dependence of the rate constant, which is also given by Arrhenius equation ( $k(T) = A \cdot e^{-E/RT}$ ), is written in equation 6.3 to obtain,

$$\frac{dx}{dt} = \frac{A}{\beta} \cdot e^{(-E/RT)} \cdot f(x) \quad (6.4)$$

where  $A$  (the pre-exponential factor) and  $E$  (activation energy) are Arrhenius parameters. Coats and Redfern developed an integral method and derived a simplified mathematical expression that used the asymptotic series expansion to obtain an approximation for equation 6.4,

$$\ln\left(\frac{g(x)}{T^2}\right) = \ln\left[\frac{A \cdot R}{\beta \cdot E} \left(1 - \frac{2 \cdot R \cdot T}{E}\right)\right] - \frac{E}{RT} \quad (6.5)$$

$f(x)$  and  $g(x)$  in equations 4 and 5 are defined for different reaction models and are given extensively given in literature. Due to the reason that the term  $\left(1 - \frac{2 \cdot R \cdot T}{E}\right)$  is approximately constant and equal to unity, the plot of  $\ln\left(g(x)/T^2\right)$  versus  $(1/T)$  gives

a straight line whose slope is activation energy and intercept is the pre-exponential factor. If the reaction order is well estimated, the plot gives a straight line with a maximum value of correlation coefficient. Several reaction models using  $f(x)$  and  $g(x)$  are listed in Table 6.1 [110].

**Table 6.1:** Rate equations

Reaction Model	$f(x)$	$g(x)$
First order	$1-x$	$-\ln(1-x)$
Second order	$(1-x)^2$	$(1-x)^{-1}-1$
Contacting cylinder	$2(1-x)^{1/2}$	$1-(1-x)^{1/2}$
Contacting sphere	$3(1-x)^{2/3}$	$1-(1-x)^{1/3}$

In the present study the pyrolysis reaction was first assumed to be first order. The effect of catalyst on decomposition was seen clearly in the kinetic parameters.

**Table 6.2:** Kinetic parameters

Sample	Constant heating rate ( $^{\circ}\text{C}\cdot\text{dk}^{-1}$ )	Stage	E ( $\text{kJ}\cdot\text{mol}^{-1}$ )	Pre-exponential factor ( $\text{dk}^{-1}$ )	$R^2$
<b>Olive Pomace</b>	10	S <sub>I</sub>	29,3	18,97	0,989
		S <sub>II</sub>	47,3	1613,4	0,997
	30	S <sub>I</sub>	30,5	70,23	0,992
		S <sub>II</sub>	42,8	1402,57	0,999
	40	S <sub>I</sub>	29,4	60,11	0,981
		S <sub>II</sub>	54,3	20900	0,993
<b>Olive Pomace:ZSM-5 (1:1)</b>	10	S <sub>I</sub>	23,2	5,24	0,973
		S <sub>II</sub>	45,5	1248	0,992
	30	S <sub>I</sub>	15,1	1,368	0,973
		S <sub>II</sub>	44,3	2125	0,989
	40	S <sub>I</sub>	11,5	0,559	0,977
		S <sub>II</sub>	44,6	2665	0,988
<b>Olive Pomace:ZSM-5 (1:2)</b>	10	S <sub>I</sub>	12,9	0,433	0,993
		S <sub>II</sub>	33,7	107,4	0,980
	30	S <sub>I</sub>	9	0,085	0,999
		S <sub>II</sub>	35,6	111,8	0,984
	40	S <sub>I</sub>	34,3	253,61	0,987
		S <sub>II</sub>	37,5	236,6	0,989
<b>Olive Pomace:ZSM-5 (1:3)</b>	10	S <sub>I</sub>	20,1	3,08	0,994
		S <sub>II</sub>	37,5	236,6	0,989
	30	S <sub>I</sub>	10,6	0,63	0,987
		S <sub>II</sub>	36,5	511,95	0,982
40	S <sub>I</sub>	26	46,7	0,978	

Figures between 6.14 and 6.25 show the plots of  $\ln(g(x)/T^2)$  versus  $1/T$ . Table 6.2 shows the kinetic parameters, which were calculated by using Coats-Redfern method. The correlation coefficients indicated that the first order reaction model fitted the experimental data. The catalytic pyrolysis of olive pomace comprised of two stages (except moisture removal) and all stages represented different kinetic parameters. At the same heating rates investigated, adding catalyst lowered the activation energy and changed the frequency factor. The catalyst significantly increased the rate of reaction.

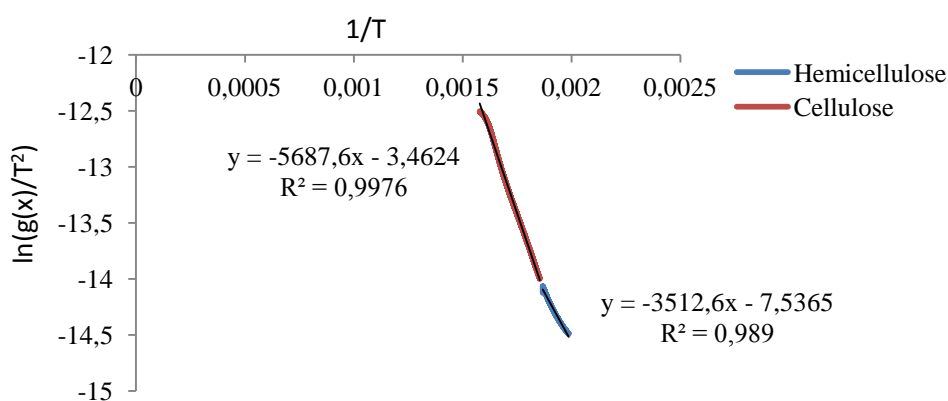


**Figure 6.14:** Plots obtained by Coats-Redfern method for determination of activation energy for olive pomace at the heating rate of  $10\text{ }^{\circ}\text{C}\cdot\text{min}^{-1}$

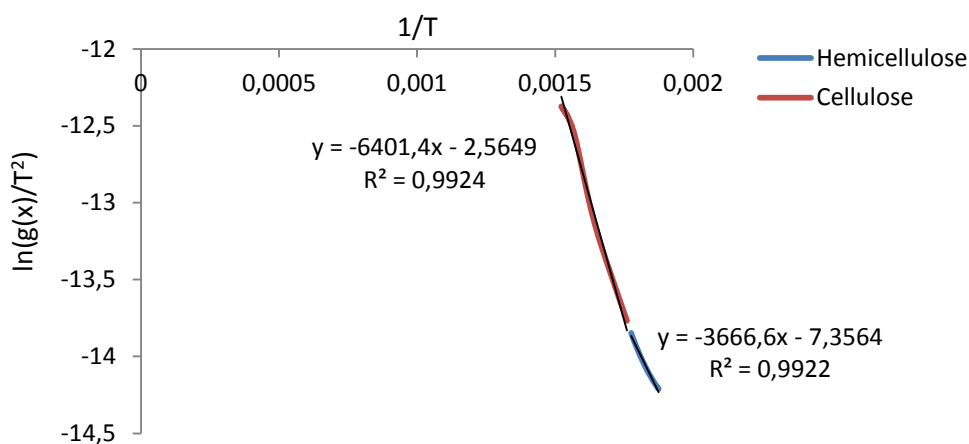


**Figure 6.15:** Plots obtained by Coats-Redfernd method for determination of activation energy for olive pomace at the heating rate of  $30\text{ }^{\circ}\text{C}\cdot\text{min}^{-1}$

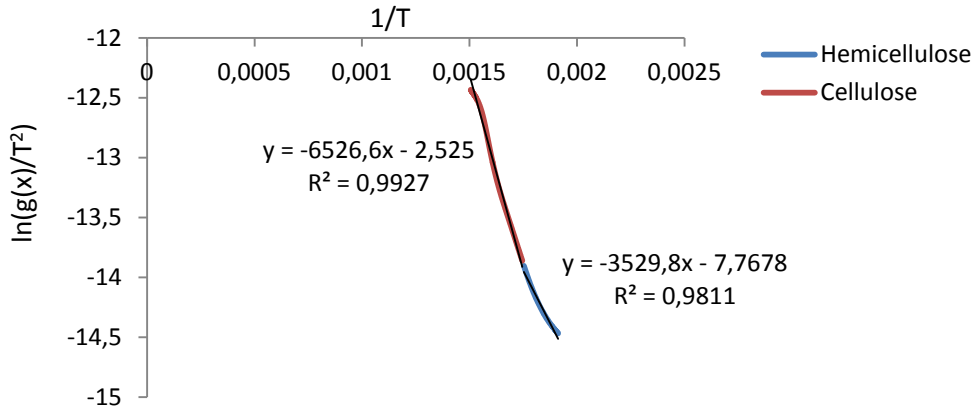


**Figure 6.16:** Plots obtained by Coats-Redfern method for determination of activation energy for olive pomace at the heating rate of 40 °C.min<sup>-1</sup>

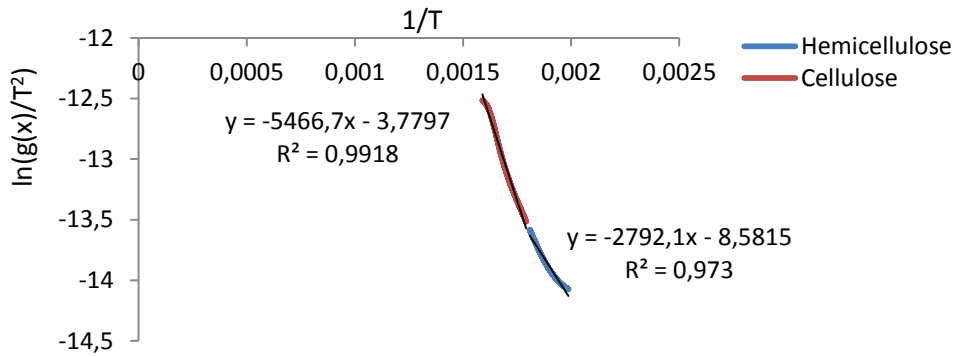


**Figure 6.17:** Plots obtained by Coats-Redfern method for determination of activation energy for olive pomace:ZSM-5(1:1) at the heating rate of 10 °C.min<sup>-1</sup>

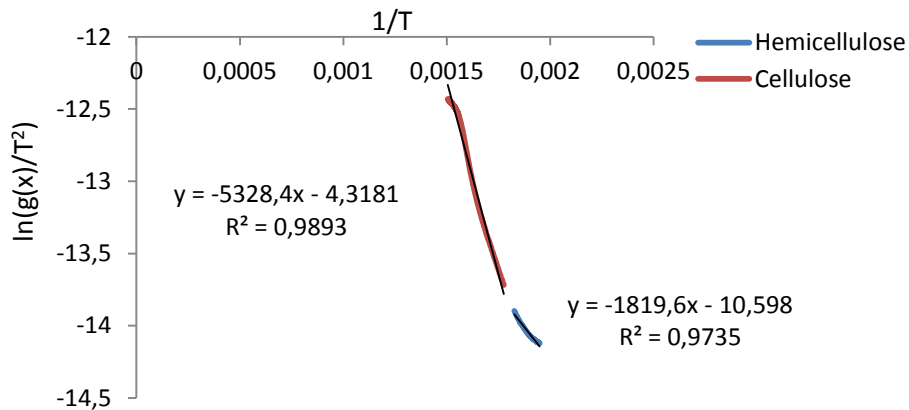


**Figure 6.18:** Plots obtained by Coats-Redfern method for determination of activation energy for olive pomace:ZSM-5(1:1) at the heating rate of 30 °C.min<sup>-1</sup>

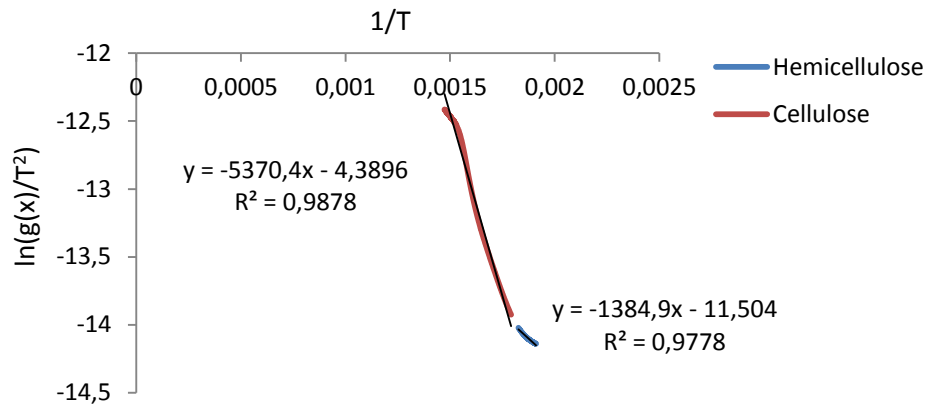


**Figure 6.19:** Plots obtained by Coats-Redfern method for determination of activation energy for olive pomace:ZSM-5(1:1) at the heating rate of  $40\text{ }^\circ\text{C}\cdot\text{min}^{-1}$

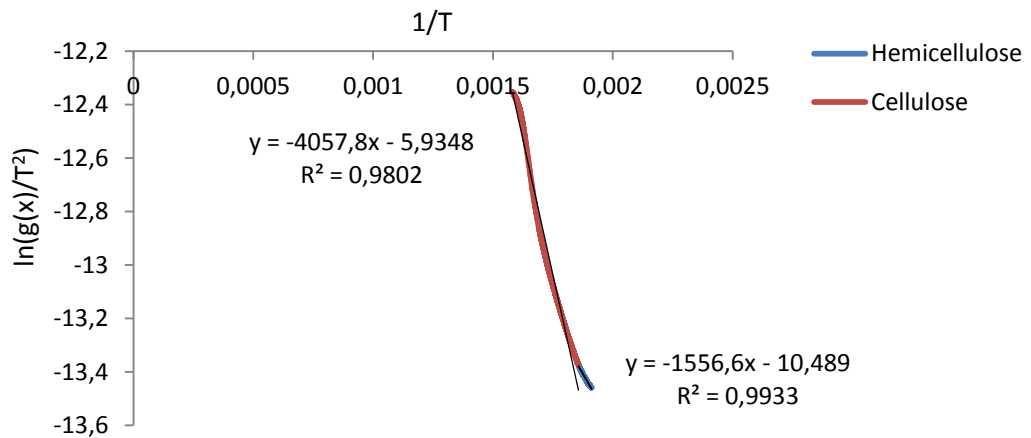


**Figure 6.20:** Plots obtained by Coats-Redfern method for determination of activation energy for olive pomace:ZSM-5(1:2) at the heating rate of  $10\text{ }^\circ\text{C}\cdot\text{min}^{-1}$

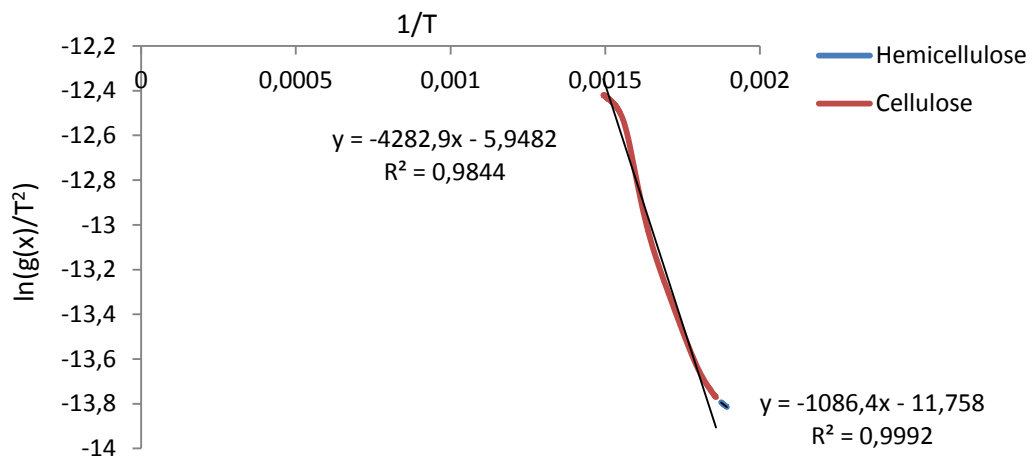


**Figure 6.21:** Plots obtained by Coats-Redfern method for determination of activation energy for olive pomace:ZSM-5(1:2) at the heating rate of  $30\text{ }^\circ\text{C}\cdot\text{min}^{-1}$

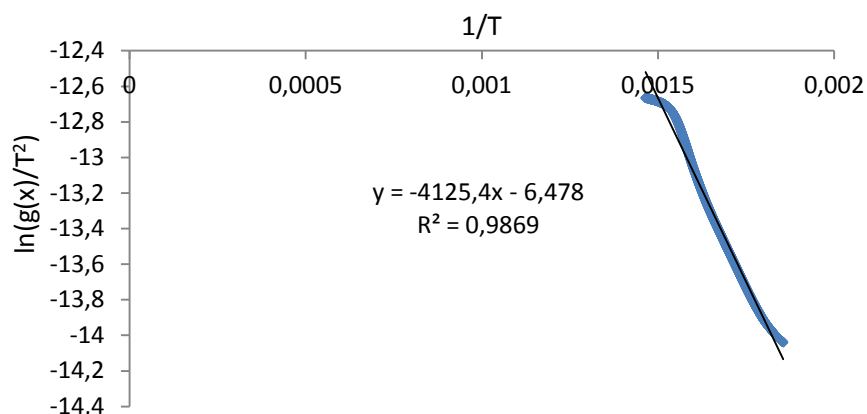


**Figure 6.22:** Plot obtained by Coats-Redfern method for determination of activation energy for olive pomace:ZSM-5(1:2) at the heating rate of 40 °C.min<sup>-1</sup>

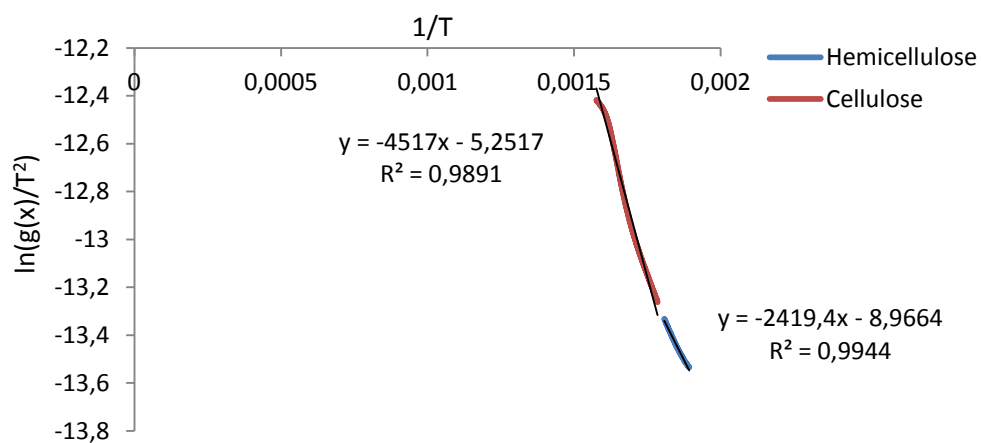


**Figure 6.23:** Plots obtained by Coats-Redfern method for determination of activation energy for olive pomace:ZSM-5(1:3) at the heating rate of 10 °C.min<sup>-1</sup>

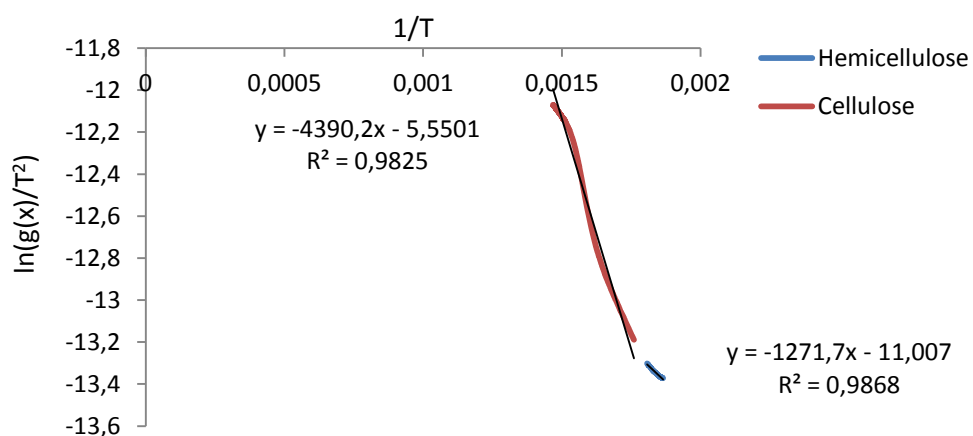


**Figure 6.24:** Plots obtained by Coats-Redfern method for determination of activation energy for olive pomace:ZSM-5(1:3) at the heating rate of 30 °C.min<sup>-1</sup>

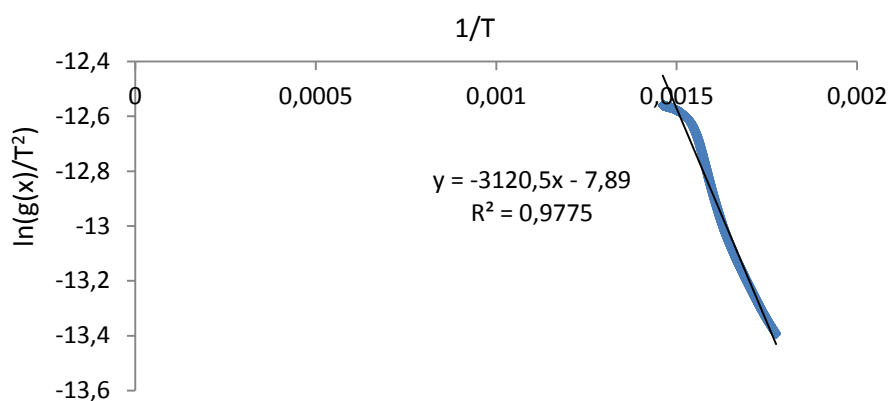


**Figure 6.25:** Plot obtained by Coats-Redfern method for determination of activation energy for olive pomace:ZSM-5(1:3) at the heating rate of 40 °C.min<sup>-1</sup>

#### 6.4 Effect of Catalyst to Product Yields

Table 6.3 shows the effect of biomass to catalyst ratio on conversion and product yields. Adding ZSM-5 to olive pomace did not significantly change the char yield and overall conversion. As expected, this suggested that low acidity ZSM-5 did not affect the overall conversion. On the other hand, several studies have shown that using ZSM-5 as catalyst for biomass conversion reduced bio-oil yield with increasing temperature [25]. However, the current pyrolysis system design for the experiments did not allow to collect the final product for yield calculations of each pyrolysis fractions. During the release of gaseous fraction of non-catalytic pyrolysis, grey colored smoke was visually observed, whereas, the gas released during the catalytic runs were colorless. This also indicates that ZSM-5 altered the composition of pyrolysis products.

**Table 6.3:** Product yields and conversion from olive pomace pyrolysis

Feedstock	Char (wt.%)	Liquid+Gas(wt.%)	Conversion(wt.%)
Olive pomace	26,7	73,2	73,2
Olive pomace: ZSM-5(1:1)	25,7	74,3	74,3
Olive pomace: ZSM-5(1:2)	24,1	75,9	75,9

Due to limitations that the tubular reactor did not allow us to insert enough feedstock for the catalytic run with the catalyst to biomass ratio of 1:3, that part of the experiments were excluded from the overall evaluation in terms of product yields and conversion.

## 6.5 Compositional Analysis of Bio-oil

The chemical composition of bio-oil was analysed using GC-MS. The GC-MS chromatogram for olive pomace bio-oil is shown in Figure 6.20. The names, chemical formulas and molecular weights of chemical compounds of corresponding labelled peaks are listed in Table 6.4 and Table 6.5. The compounds, which are listed, are detected in bio-oil dissolved in methanol and dichloromethane, respectively.

Olive pomace pyrolysis bio-oil is regarded as reference bio-oil with very complex mixtures of organic compounds of C<sub>5</sub>-C<sub>25</sub>. The methanol fraction of olive pomace bio-oil mostly consists of phenolic compounds, the peak corresponding the retention time at 6.55 (phenol,2-methoxy) in Figure 6.26 giving the highest abundance. Phenolic compounds, such as guaiacol and its derivatives, are important due to being thermally unstable. Reducing of these compounds is of high importance in terms of enhancing stability of bio-oil.

The dichloromethane fraction was mainly comprised of alkanes, alkyl aldehydes, and methyl esters of carboxylic acids. Especially syringol, guaiacol and its derivatives were found in high abundance in GC-MS chromatogram of reference bio-oil. Studies have shown that thermal bio-oil consists of levoglucosan as main compound [50]. However, holocellulose derived products, namely levoglucosan and furfural were not detected in any of the bio-oil samples for the current study. This suggested that above mentioned products were converted into other chemical compounds.



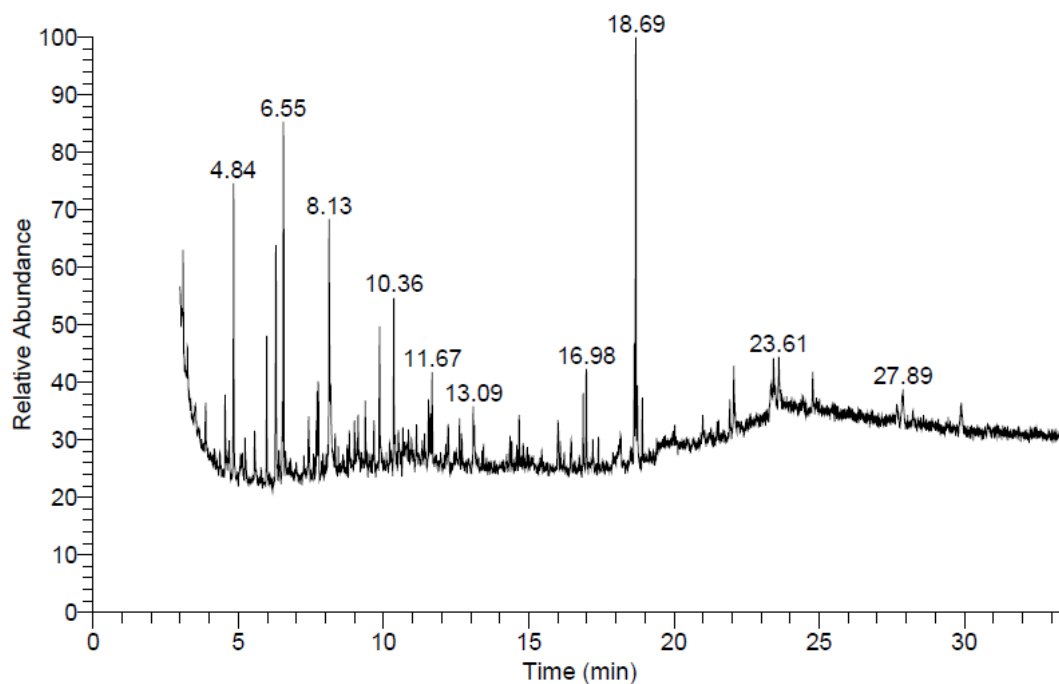


**Figure 6.26:** GC-MS spectrum of olive pomace bio-oil dissolved in methanol

In a study of Mihalcik *et al.* [25], ZSM-5 catalysts with different Si/Al ratios were compared and ZSM-5(280) was found to be less effective in eliminating oxygenated compounds compared to ZSM-5 zeolites of higher acidity. Furans were not detected thus indicating the cracking ability of ZSM-5, which is consistent with the results of our study. For the current study, the catalytic bio-oil derived from pyrolysis with biomass to catalyst ratio of 1:1 was comprised of organic compounds of C<sub>6</sub>-C<sub>25</sub>, whereas, with the biomass to catalyst ratio of 1:2 the bio-oil was of C<sub>6</sub>-C<sub>19</sub>.

It is interesting to note the varying effect of the different catalyst amounts on bio-oil composition. Figure 6.27 shows the methanol fraction of catalytic bio-oil derived from olive pomace with biomass to catalyst ratio of 1:1. Using ZSM-5 did not eliminate undesired products such as phenolics and ketones, however, addition of ZSM-5 to olive pomace pyrolysis decreased phenolic compounds in bio-oil significantly. Compared to reference bio-oil, the amount of compounds corresponding to the labelled peaks at retention time of 4.84, 6.55, 8.13 and 10.36 were decreased by considerable amounts. This suggests that the formation of phenol and its derivatives (guaiacol and syringol) was considerably affected by using ZSM-5 as catalyst.

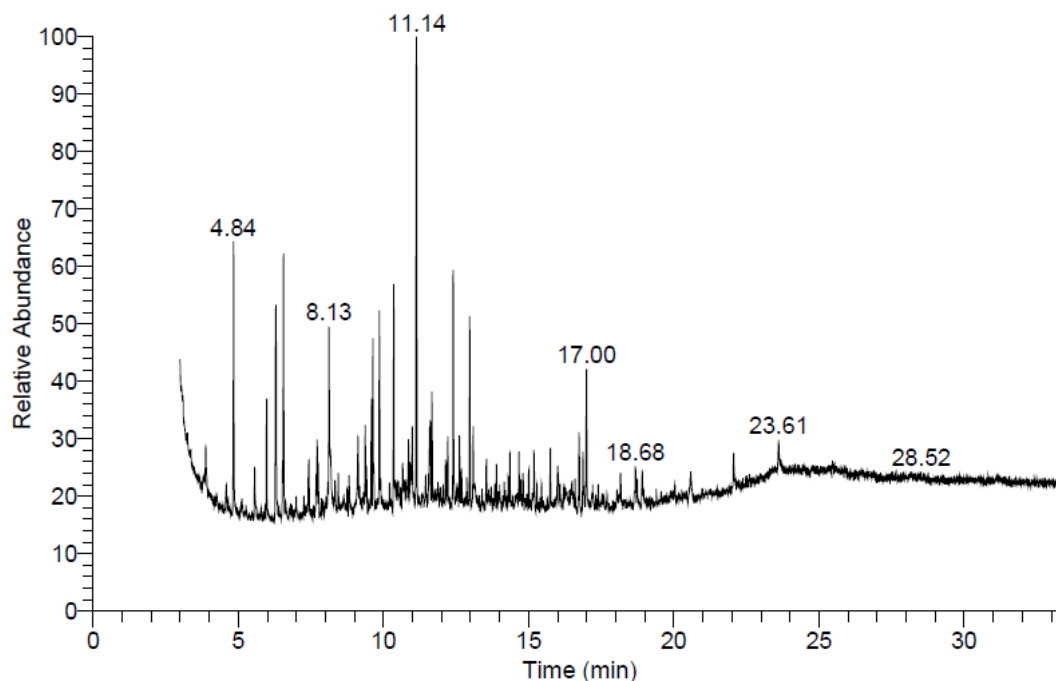


**Figure 6.27:** GC-MS spectrum of bio-oil with olive pomace: ZSM-5 mixture (1:1) dissolved in methanol

Phenolic compounds have kinetic diameter larger than that of ZSM-5 pore size suggesting that these compounds could not enter the pores of the catalyst, thus could only be converted at the external surface of ZSM-5, which contained only small amount of active acid sites. Hence, ZSM-5 reduced the amount of phenolics significantly that the surface activity of the zeolite can not be neglected. Oxygenated compounds such as trans-Isoeugenol, 2,3,5-trimethoxytoluene, phenol, 2,6-dimethoxy-4-(2-propenyl)- and, 4-isopropyl-1,3-cyclohexanedione were slightly reduced compared to reference bio-oil. As expected, the formation of aromatic hydrocarbons were favored in case of using ZSM-5. Mostly phenanthrene, naphthalene derivatives (methylnaphthalene, naphthalene,1-ethyl-, naphthalene, 1,6-dimethyl-, naphthalene, 2-(1-methylethyl)-), fluorene and its derivatives, methyl derivatives of indene were formed in result of olive pomace pyrolysis over ZSM-5.

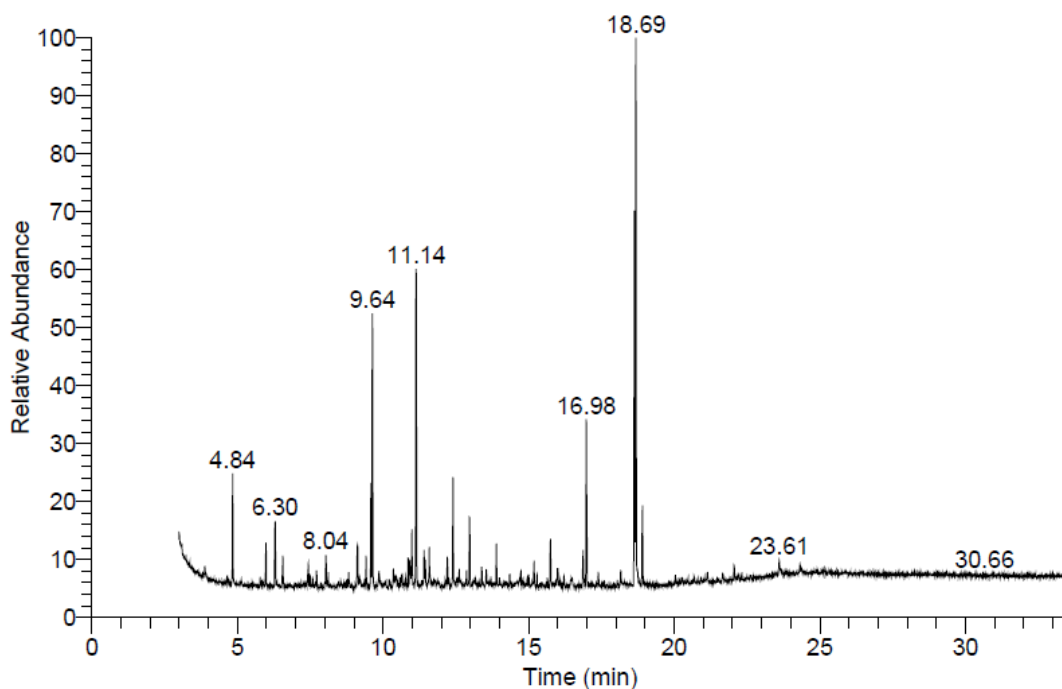


**Figure 6.28:** GC-MS spectrum of bio-oil with olive pomace: ZSM-5 mixture (1:2) dissolved in methanol

Compounds such as phenol-2-methoxy-, 2-methoxy-4-vinylphenol and phenol,2,6-dimethoxy were identified in GC-MS spectrum of olive pomace bio-oil with high abundance. As shown in Figures 6.27 and 6.28, as biomass to catalyst ratio increased to 1:2, there was no phenol,2,6-dimethoxy and 2-methoxy-4-vinylphenol peaks detected. Thus, this indicated that lignin derived products (syringol, guaiacol and its derivatives) were selectively converted into aromatics with increased catalyst addition. With biomass to catalyst ratio of 1:2, all the oxygenated compounds in bio-oil were eliminated excluding phenol, phenol,2-methyl-, phenol,4-methyl-, and phenol,2-methoxy- which were reduced significantly.

As shown in Figure 6.28, the primary products from the pyrolysis of olive pomace with ZSM-5 are naphthalene and its derivatives. In a study of Jae *et al.*, where the kinetic diameters of pyrolytic compounds and the pore size of ZSM-5 were compared, it was revealed that naphthalene was likely to be formed inside the pores of the catalyst at elevated temperatures above 600 °C [77]. It was due to decreased energetic barrier to diffusion and expansion of the pore size of ZSM-5 at elevated temperatures [111]. However, in the current system where the final operation temperature was kept constant at 550 °C, the formation of naphthalene and its

derivatives could be assumed to be at the external acid sites of ZSM-5. Because the pore size of ZSM-5 (5.6 Å) is smaller than the kinetic diameter of naphthalene (6.2 Å) [77] and its derivatives. This also suggested that, in case of using biomass to catalyst ratio of 1:2, the conversion of olive pomace over ZSM-5 was mostly affected by mass transfer limitations. Also, the formation of phenanthrene assumed to be occurred at the surface of the catalyst due to its larger kinetic diameter (6.96 Å) [77] compared to ZSM-5 pore size.

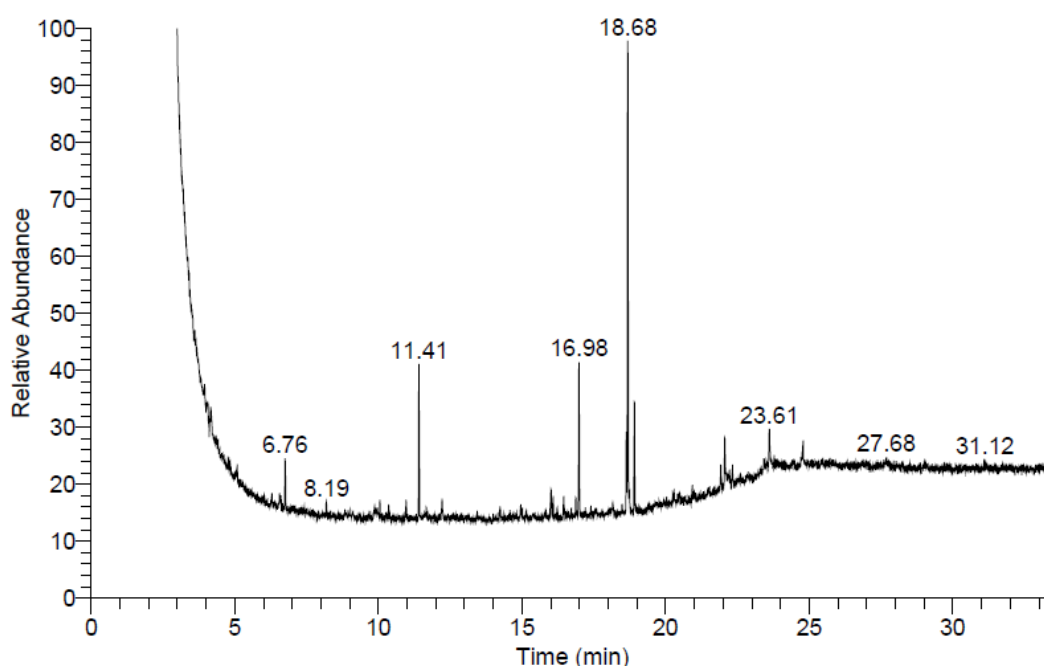


**Figure 6.29:** GC-MS spectrum of olive pomace bio-oil dissolved in DCM

The DCM (dichloromethane) fractions of reference bio-oil and catalytic bio-oil with the biomass to catalyst ratio of 1:1 are shown in Figure 6.29 and Figure 6.30. The DCM fraction of reference bio-oil mainly consist of oxygenated compounds such as methyl esters of carboxylic acids and nonanal (alkyl aldehyde), whereas the catalytic bio-oil is comprised of benzene derivatives and alkanes. Using ZSM-5 as catalyst completely eliminated the oxygenates in DCM fraction of olive pomace bio-oil resulting higher aromatic yield as shown in Table 6.5. Particularly, in Figure 6.30 the peak (5.09) corresponding benzene,1,2,4-trimethyl-, which is used as gasoline additive, is of high importance. These results confirms the shape selectivity effect of ZSM-5.

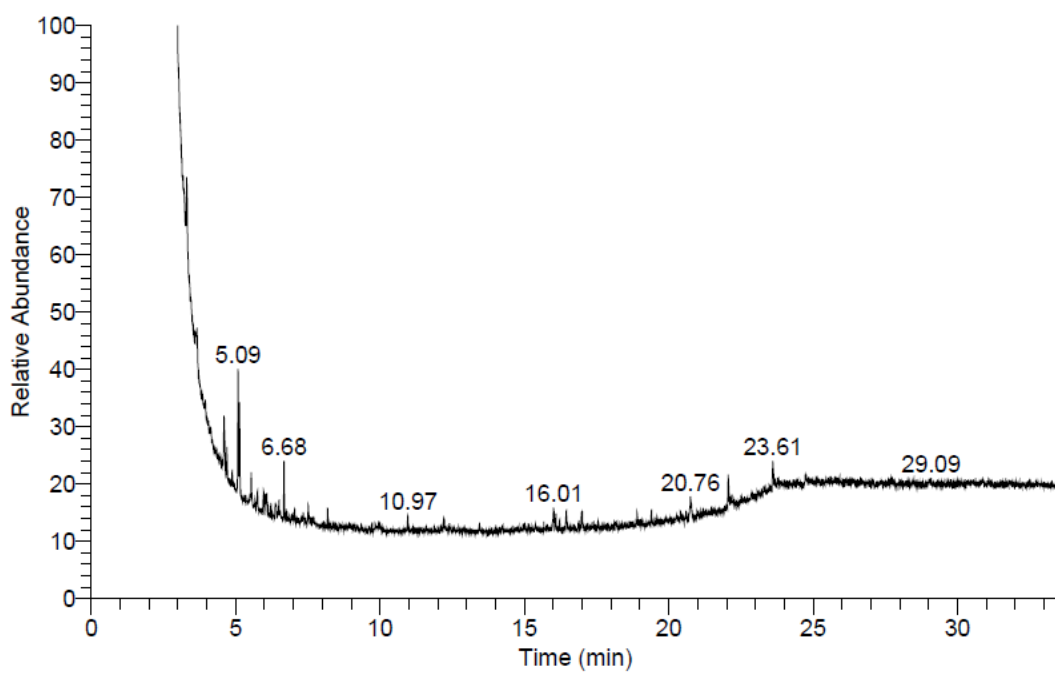


**Figure 6.30:** GC-MS spectrum of bio-oil with olive pomace: ZSM-5 mixture (1:1) dissolved in DCM

**Table 6.4:** Methanol fraction of olive pomace bio-oil with and without the addition of catalyst

<b>Retention Time</b>	<b>Compound Name</b>	<b>Formula</b>	<b>M.W (g/mol)</b>	<b>Reference Bio-oil</b>	<b>1:1</b>	<b>1:2</b>
3.89	Cyclopentanone	C <sub>5</sub> H <sub>8</sub> O	84.12	+	+	-
4.84	Phenol	C <sub>6</sub> H <sub>6</sub> O	94.11	+	+	+
5.57	4-Isopropyl-1,3-cyclohexanedione	C <sub>9</sub> H <sub>14</sub> O <sub>2</sub>	154.21	+	+	-
5.98	Phenol, 2-methyl-	C <sub>7</sub> H <sub>8</sub> O	108.14	+	+	+
6.30	Phenol, 4-methyl-	C <sub>7</sub> H <sub>8</sub> O	108.14	+	+	+
6.55	Phenol, 2-methoxy-	C <sub>7</sub> H <sub>8</sub> O <sub>2</sub>	124.14	+	+	+
7.43	Phenol, 2,4-dimethyl-	C <sub>8</sub> H <sub>10</sub> O	122.16	+	+	-
7.72	Phenol, 3-ethyl-	C <sub>8</sub> H <sub>10</sub> O	122.16	+	+	-
8.04	Naphthalene	C <sub>10</sub> H <sub>8</sub>	128.17	-	-	+
8.13	2-Cyclopenten-1-one, 3,4,5,5-tetramethyl-	C <sub>9</sub> H <sub>14</sub> O	138.21	+	+	-
9.13	1H-Indene, 1,3-dimethyl-	C <sub>11</sub> H <sub>12</sub>	144.21	-	+	+
9.38	7,7-dimethylbicyclo[3.3.0]octan-2-one	C <sub>10</sub> H <sub>16</sub> O	152.23	+	+	-
9.64	2-Methylnaphthalene	C <sub>11</sub> H <sub>10</sub>	142.20	-	+	+
9.86	2-Methoxy-4-vinylphenol	C <sub>9</sub> H <sub>10</sub> O <sub>2</sub>	150.17	+	+	-
10.36	Phenol, 2,6-dimethoxy-	C <sub>8</sub> H <sub>10</sub> O <sub>3</sub>	154.16	+	+	-
10.99	Naphthalene, 1-ethyl-	C <sub>12</sub> H <sub>12</sub>	156.22	-	+	+
11.14	Naphthalene, 1,6-dimethyl-	C <sub>15</sub> H <sub>18</sub>	198.30	-	+	+
11.67	trans-Isoeugenol	C <sub>10</sub> H <sub>12</sub> O <sub>2</sub>	164.20	+	+	-
12.41	Naphthalene, 2-(1-methylethyl)-	C <sub>13</sub> H <sub>14</sub>	170.25	-	+	+
12.62	2,3,5-Trimethoxytoluene	C <sub>10</sub> H <sub>14</sub> O <sub>3</sub>	182.22	+	+	-
12.97	Naphthalene, 2,3,6-trimethyl-	C <sub>13</sub> H <sub>14</sub>	170.25	-	-	+

(+) denotes that relevant compounds were detected in bio-oil samples

(-) denotes that relevant compounds were not detected in bio-oil samples

**Table 6.4:** Methanol fraction of olive pomace bio-oil with and with the addition of catalyst (continued)

<b>Retention Time</b>	<b>Compound Name</b>	<b>Formula</b>	<b>M.W (g/mol)</b>	<b>Reference Bio-oil</b>	<b>1:1</b>	<b>1:2</b>
13.09	1,4-Dimethoxy-2,3,6-trimethylbenzene	C <sub>11</sub> H <sub>16</sub> O <sub>2</sub>	180.24	+	+	-
13.89	9H-Fluorene	C <sub>13</sub> H <sub>10</sub>	166.22	-	+	+
14.67	Phenol, 2,6-dimethoxy-4-(2-propenyl)-	C <sub>11</sub> H <sub>14</sub> O <sub>3</sub>	194.23	+	+	-
15.19	9H-Fluorene, 1-methyl-	C <sub>14</sub> H <sub>12</sub>	180.24	-	+	-
15.75	Phenanthrene	C <sub>14</sub> H <sub>10</sub>	178.23	-	+	+
16.88	Benzene, (1-methyldodecyl)-	C <sub>19</sub> H <sub>32</sub>	260.46	+	+	-
16.98	Hexadecanoic acid, methyl ester	C <sub>17</sub> H <sub>34</sub> O <sub>2</sub>	270.45	+	-	+
17.00	1H-Indene, 7-phenyl-	C <sub>15</sub> H <sub>12</sub>	192.09	-	+	-
18.69	9-Octadecenoic acid, methyl ester, (E)-	C <sub>19</sub> H <sub>36</sub> O <sub>2</sub>	296.48	+	+	+
22.06	1H-Indene, 1-hexadecyl-2,3-dihydro-	C <sub>25</sub> H <sub>42</sub>	342.60	+	+	-

(+) denotes that relevant compounds were detected in bio-oil samples

(-) denotes that relevant compounds were not detected in bio-oil samples

**Table 6.5:** DCM fraction of olive pomace bio-oil with and without the addition of catalyst

<b>Retention Time</b>	<b>Compound Name</b>	<b>Formula</b>	<b>M.W (g/mol)</b>	<b>Reference Bio-oil</b>	<b>1:1</b>
<b>4.61</b>	Benzene, 1-ethyl-3-methyl-	$C_9H_{12}$	120.19	-	+
<b>5.09</b>	Benzene, 1,2,4-trimethyl-	$C_9H_{12}$	120.19	-	+
<b>6.76</b>	Nonanal	$C_9H_{18}O$	142.24	+	-
<b>8.19</b>	Dodecane	$C_{12}H_{26}$	170.33	+	+
<b>10.05</b>	Methyl 8-oxooctanoate	$C_9H_{16}O_3$	172.22	+	-
<b>11.41</b>	Nonanoic acid, 9-oxo-, methyl ester	$C_{10}H_{18}O_3$	186.25	+	-
<b>16.01</b>	Benzene, (1-pentyloctyl)-	$C_{19}H_{32}$	260.46	+	+
<b>16.98</b>	Hexadecanoic acid, methyl ester	$C_{17}H_{34}O_2$	270.45	+	-
<b>18.68</b>	9-Octadecenoic acid, methyl ester, (E)-	$C_{19}H_{36}O_2$	296.49	+	-
<b>18.91</b>	Methyl stearate	$C_{19}H_{38}O_2$	298.50	+	-

(+) denotes that relevant compounds were detected in bio-oil samples

(-) denotes that relevant compounds were not detected in bio-oil samples



## 7.CONCLUSION

Pyrolysis behavior and kinetics of olive pomace and olive pomace:ZSM-5 mixtures (1:1, 1:2 and 1:3) were investigated by thermogravimetric analysis. Both olive pomace pyrolysis and catalytic pyrolysis showed similar pyrolysis profile. At high heating rates and with catalyst, the decomposition of hemicellulose was not detected as a hump in the characteristic peak. Decomposition was seen as a one step reaction. Adding catalyst decreased the activation energy but did not change the peak temperatures. Reduction of energy consumption by decreasing the activation energy can be achieved. From DSC profiles, the pyrolysis of reaction was seen as endothermic.

Pyrolysis experiments were also performed in a tubular furnace system under atmospheric pressure 550 °C with a heating rate of 25 °C.min<sup>-1</sup>, for 15 min of operation at the final temperature of 550 °C. The purpose of the pyrolysis experiments using tubular furnace system for this study was to investigate the bio-oil quality in terms of deoxygenation by using ZSM-5 as catalyst. With biomass to catalyst ratio of 1:2, all the oxygenated compounds in bio-oil were eliminated. Also, phenol, phenol,2-methyl-, phenol,4-methyl-, and phenol,2-methoxy- were reduced significantly. This amount of catalyst addition favored mostly formation of naphthalene and its derivatives in methanol fraction, formation of benzene derivatives in DCM fraction. This shows the shape selectivity effect of ZSM-5 catalyst.

As a result of this study, following recommendations are suggested for further studies:

- In order to determine the physicochemical properties of bio-oil, a pyrolysis system, which allows to use higher amount of biomass for should be designed. Also, for higher liquid yield, a system design with higher heating rate should be considered.

- Apart from higher heating rate, low biomass to catalyst ratio is necessary to maximize the aromatic yield. Therefore, the optimum system design must allow for catalytic pyrolysis of olive pomace with high heating rate while maintaining a low biomass to catalyst ratio.
- Due to limitations of the current system, fresh catalyst samples were used for each pyrolysis experiments. Thus, deactivation of the catalyst could not be studied. For an economical design, catalyst recovery and regeneration steps should be added to the system.
- ZSM-5 is known to be an effective deoxygenating catalyst. In this study, a ZSM-5 with Si/Al ratio of 280 was used. ZSM-5 with different acidities, preferably higher acidity, in order for better selectivity in terms of deoxygenation and aromatization should be compared for further study.

## REFERENCES

- [1] **Thangalazhy-Gopakumar, S., Adhikari, S., Gupta, R., Tu, M., & Taylor, S.,** 2011: Production of hydrocarbon fuels from biomass using catalytic pyrolysis under helium and hydrogen environment, *Bioresource Technology*, **102**, 6742-6749.
- [2] **Chouchene, A., Jeguirim, M., Khairi, B., Zagrouba, F., & Trouvé, G.,** 2010: Thermal degradation of olive solid waste: Influence of particle size and oxygen concentration, *Resources, Conservation and Recycling*, **54**, 271-277.
- [3] **Garcia-Maraver, A., Salvachúa, D., & Martín, M.,** 2013: Analysis of the relation between the cellulose, hemicellulose and lignin content and the thermal behavior of residual biomass from olive trees, *Waste Management*, **33**, 2245-2249.
- [4] **Ounas, A., Aboulkas, A., El harfi, K., Bacaoui, A., & Yaacoubi, A.,** 2011: Pyrolysis of olive residue and sugar cane bagasse: Non-isothermal thermogravimetric kinetic analysis, *Bioresource Technology*, **102**, 11234-11238.
- [5] **Encinar, J.M., González, J.F., Martínez, G., & González, J.M.,** 2008: Two stages catalytic pyrolysis of olive oil waste, *Fuel Processing Technology*, **89**, 1448-1455.
- [6] **Seo, D.K., Park, S.S., Hwang, J., & Yu, T.-U.,** 2010: Study of the pyrolysis of biomass using thermo-gravimetric analysis (TGA) and concentration measurements of the evolved species, *Journal of Analytical and Applied Pyrolysis*, **89**, 66-73.
- [7] **Demiral, İ., & Şensöz, S.,** 2008: The effects of different catalysts on the pyrolysis of industrial wastes(olive and hazelnut bagasse), *Bioresource Technology*, **99**, 8002-8007.
- [8] **Balat, M., Balat, H., Balat, M., & Kırtay, E.,** 2009: Main routes for the thermo-conversion of biomass into fuels and chemicals. Part 1: Pyrolysis systems, *Energy Conversion and Management*, **50**, 3147-3157.
- [9] **García-Ibañez, P., Sánchez, M., & Cabanillas, A.,** 2006: Thermogravimetric analysis of olive-oil residue in air atmosphere, *Fuel Processing Technology*, **87**, 103-107.

- [10] **Jauhiainen, J., Conesa, J.A., Font, R., & Martín-Gullón, I.**, 2004: Kinetics of the pyrolysis and combustion of olive oil solid waste, *Journal of Analytical and Applied Pyrolysis*, **72**, 9-15.
- [11] **Özveren, U., & Özdoğan, Z.S.**, 2013: Investigation of the slow pyrolysis kinetics of olive oil pomace using thermo-gravimetric analysis coupled with mass spectrometry, *Biomass and Bioenergy*, 1-12.
- [12] **Başakçılardan-Kabakçı, S., & Aydemir, H.**, 2013: Pyrolysis of olive pomace and copyrolysis of olive pomace with refuse derived fuel, *Environmental Progress & Sustainable Energy*.
- [13] **International Olive Oil Council.**  
www.internationaloliveoil.org:http://www.internationaloliveoil.org/estaticos/view/131-world-olive-oil-figures, date retrieved December, 2013.
- [14] **Başkan, A. E.**, 2010: *Zeytinyağı işletmelerinin atıkları değerlendirme yolları*. T.C. Güney Marmara Kalkınma Ajansı T.C. Güney Marmara Kalkınma Ajansı.
- [15] **Bulushev, D. A., & Ross, J.R.H.**, 2011: Catalysis for conversion of biomass via pyrolysis and gasification: A review, *Catalysis Today*, **171**, 1-13.
- [16] **Bu, Q., Lei, H., Ren, S., Wang, L., Zhang, Q., Thang, J., Ruan, R.**, 2012: Production of phenols and biofuels by catalytic microwave pyrolysis of lignocellulosic biomass, *Bioresource Technology*, **108**, 274-279.
- [17] **Chattopadhyay, J., Kim, C., Kim, R., & Pak, D.**, 2009: Termogravimetric study on pyrolysis of biomass with Cu/Al<sub>2</sub>O<sub>3</sub> catalysts. *Journal of Industrial and Engineering Chemistry*, **15**, 72-76.
- [18] **Thangalazhy-Gopakumar, S., Adhikari, S., & Gupta, R.**, 2012: Catalytic pyrolysis of biomass over H+ZSM-5 under hydrogen pressure, *Energy Fuels*, **26**, 5300-5306.
- [19] **Zhou, L., Yang, H., Wu, H., Wang, M., & Cheng, D.**, 2013: Catalytic pyrolysis of rice husk by mixing with zinc oxide: Characterization of bio-oil and its rheological behavior, *Fuel Processing Technology*, **106**, 385-391.
- [20] **Pütün, E., Ateş, F., & Pütün, A.**, 2008: Catalytic pyrolysis of biomass in inert and steam atmospheres, *Fuel*, **87**, 815-824.
- [21] **Foster, A., Jae, J., Cheng, Y.-T., Huber, G., & Lobo, R.**, 2012: Optimizing the aromatic yield and distribution from catalytic fast pyrolysis of biomass over ZSM-5, *Applied Catalysis A: General*, **423**, (434), 154-161.
- [22] **Zabeti, M., Nguyen, T., Heeres, H., & Seshan, K.**, 2012: In situ catalytic pyrolysis of lignocellulose using alkali-modified amorphous silica alumina,

*Bioresource Technology*, **(118)**, 374-381.

- [23] **Mansur, D., Yoshikawa, T., Norinaga, K., Hayashi, J., Tago, T., & Masuda, T.**, 2013: Production of ketones from pyrolytic acid of woody biomass pyrolysis over an iron-oxide catalyst, *Fuel*, **(103)**, 130-134.
- [24] **Yu, Y., Li, X., Su, L., Zhang, Y., Wang, Y., & Zhang, H.**, 2012: The role of shape selectivity in catalytic fast pyrolysis of lignin with zeolite catalysts, *Applied Catalysis A: General*, **447-448**, 115-123.
- [25] **Mihalcik, D., Mullen, C., & Boateng, A.**, 2011: Screening acidic zeolites for catalytic fast pyrolysis of biomass and its components, *Journal of Analytical and Applied Pyrolysis*, **92**, 224-232.
- [26] **French, R., & Czernik, S.**, 2010: Catalytic pyrolysis of biomass for biofuels production. *Fuel Processing Technology*, **91**, 25-32.
- [27] **Iisa, K., Stanton, A., & Czernik, S.**, 2012: Production of hydrocarbon fuels from biomass by catalytic fast pyrolysis. *World Renewable Energy Forum*.
- [28] **Basu, P.**, 2010: Pyrolysis and Torrefaction. In *Biomass Gasification and Pyrolysis: Practical Design*. Burlington, USA: Academic Press.
- [29] **Pütün, E.**, 2010: Catalytic pyrolysis of biomass: Effect of pyrolysis temperature, sweeping gas flow rate and MgO catalyst, *Energy*, **35**, 2761-2766.
- [30] **Huang, W., Gong, F., Fan, M., Zhai, Q., Hong, C., & Li, Q.**, 2012: Production of light olefins by catalytic conversion of lignocellulosic biomass with HZSM-5 zeolite impregnated with 6 wt.% lanthanum, *Bioresource Technology*, **(121)**, 248-255.
- [31] **Encinar, J. M., Gonzalez, J. F., Martinez, G., & Roman, S.**, 2009: Catalytic pyrolysis of exhausted olive oil waste, *J. Anal. Appl. Pyrolysis*, **(85)**, 197-203.
- [32] **Uzun, B.B., & Sarioğlu, N.**, 2009: Rapid and catalytic pyrolysis of corn stalks. *Fuel Processing Technology*, **(90)**, 705-716.
- [33] **Asadullah, M., Zhang, S., & Li, C.-Z.**, 2010: Evaluation of structural features of chars from pyrolysis of biomass of different particle sizes. *Fuel Processing Technology*, **(91)**, 877-881.
- [34] **Aysu, T., & Küçük, M.**, 2014: Biomass pyrolysis in a fixed-bed reactor: Effects of pyrolysis parameters on product yields and characterization of products, *Energy*, **64**, 1002-1025.
- [35] **Luo, S., Yi, C., & Zhou, Y.**, 2013: Bio-oil production by pyrolysis of

- biomass using hot blast furnace slag, *Renewable Energy*, **(50)**, 373-377.
- [36] **Choi, H. S., Choi, Y. S., & Park, H. C.**, 2012: Fast pyrolysis characteristics of lignocellulosic biomass with varying, *Renewable Energy*, **(42)**, 131-135.
- [37] **Melligan, F., Hayes, M., Kwapinski, W., & Leahy, J.**, 2012: Hydro-Pyrolysis of Biomass and Online Catalytic Vapor Upgrading with Ni-ZSM-5 and Ni-MCM-41, *Energy Fuels*, **(26)**, 6080-6090.
- [38] **Stefanidis, S., Kalogiannis, K., Iliopoulou, E., Michailof, C., Pilavachi, P., & Lappas, A.**, 2014: A study of lignocellulosic biomass pyrolysis via the pyrolysis of cellulose, hemicellulose and lignin, *Journal of Analytical and Applied Pyrolysis*, **105**, 143-150.
- [39] **Haykiri-Acma, H., & Yaman, S.**, 2009: Thermogravimetric investigation on the thermal reactivity of biomass during slow pyrolysis, *International Journal of Green Energy*, **6** (4), 333-342.
- [40] **Collard, F.-X., Blin, J., Bensakhira, A., & Valette, J.**, 2012: Influence of impregnated metal on the pyrolysis conversion of biomass constituents, *Journal of Analytical and Applied Pyrolysis*, **(95)**, 213-226.
- [41] **Stenseng, M., Jensen, A., & Dam-Johansen, K.**, 2001: Investigation of biomass pyrolysis by thermogravimetric analysis and differential scanning calorimetry, *Journal of Analytical and Applied Pyrolysis*, **58** (59), 765-780.
- [42] **Bertero, M., de la Puente, G., & Sedran, U.**, 2012: Fuels from bio-oil: Bio-oil production from different residual sources, characterization and thermal conditioning, *Fuel*, **(95)**, 263-271.
- [43] **Mihalcik, D.J., Mullen, C.H., & Boateng, A.A.**, 2012: Screening acidic zeolites for catalytic fast pyrolysis of biomass and its components, *Journal of Analytical and Applied Pyrolysis*, **(92)**, 224-232.
- [44] **Nokkosmaki, M.I., Kuoppala, E.T., Leppamaki, E.A., & Krause, A.O.I.**, 2000: Catalytic conversion of biomass pyrolysis vapours with zinc oxide, *Journal of Analytical and Applied Pyrolysis*, **(55)**, 119-131.
- [45] **Iliopoulou, E.F., Stefanidis, S., Kalogiannis, K., Delimitis, A., Lappas, A., & Triantafyllidis, K.**, 2012: Catalytic upgrading of biomass pyrolysis vapors using transition metal-modified ZSM-5 zeolite, *Applied Catalysis B: Environmental*, **(127)**, 281-290.
- [46] **Zhang, H., Xiao, R., Jin, B., Shen, D., Chen, R., & Xiao, G.**, 2013: Catalytic fast pyrolysis of straw biomass in an internally interconnected fluidized bed to produce aromatics and olefins: Effect of different catalyst, *Bioresource Technology*, **(137)**, 82-87.

- [47] **Aho, A., Kumar, N., Eränen, K., Salmi, T., Hupa, M., & Murzin, D.,** 2007: Catalytic pyrolysis of biomass in a fluidized bed reactor: Influence of acidity of H-Beta Zeolite, *Process Safety and Environmental Protection*, **85** (B5), 473-480.
- [48] **Yildiz, G., Pronk, M., Djokic, M., van Geem, K., Ronsse, F., van Duren, R., et al.** 2013: Validation of a new set-up for continuous catalytic fast pyrolysis of biomass coupled with vapour phase upgrading, *Journal of Analytical and Applied Pyrolysis*, **103**, 343-351.
- [49] **Iliopoulou, E.F., Antonakou, E., Karakoulia, S., Vasalos, I., Lappas, A., & Triantafyllidis, K.,** 2007: Catalytic conversion of biomass pyrolysis products by mesoporous materials: Effect of steam stability and acidity of Al-MCM-41 catalysts, *Chemical Engineering Journal*, (**134**), 51-57.
- [50] **Abu Bakar, M.S., & Titiloye, J.O.,** 2012: Catalytic pyrolysis of rice husk for bio-oil production, *Journal of Analytical and Applied Pyrolysis* .
- [51] **Mante, O.D., & Agblevor, F.A.,** 2011: Catalytic conversion of biomass to bio-synchrude oil, *Biomass Conversion and Biorefinery*, **1**, 203-215.
- [52] **Nguyen, T.S., Zabeti, M., Lefferts, L., Brem, G., & Seshan, K.,** 2013: Conversion of lignocellulosic biomass to green fuel oil over sodium based catalysts, *Bioresource Technology*, **142**, 353-360.
- [53] **Wang, S., Guo, X., Liang, T., Zhou, Y., & Luo, Z.,** 2012: Mechanism research on cellulose pyrolysis by Py-GC/MS and subsequent density functional theory studies, *Bioresource Technology*, **104**, 722-728.
- [54] **Bai, X., Johnston, P., Sadula, S., & Brown, R.,** 2013: Role of levoglucosan physiochemistry in cellulose pyrolysis, *Journal of Analytical and Applied Pyrolysis*, **99**, 58-65.
- [55] **Xin, S., Yang, H., Chen, Y., Wang, X., & Chen, H.,** 2013: Assessment of pyrolysis polygeneration of biomass based on major components: Product characterization and elucidation of degradation pathways, *Fuel*, **113**, 266-273.
- [56] **Mante, O.D., Agblevor, F.A., Oyama, S.T., & McClung, R.,** 2014: Catalytic pyrolysis with ZSM-5 based additive as co-catalyst to Y-zeolite in two reactor configurations, *Fuel*, **117**, 649-659.
- [57] **Bertero, M., Gorostegui, H., Orrabalis, C., Guzmán, C., Calandri, E., & Sedran, U.,** 2013: Characterization of the liquid products in the pyrolysis of residual chañar and palm fruit biomasses, *Fuel* .
- [58] **Wang, D., Xiao, R., Zhang, H., & He, G.,** 2011: Comparison of catalytic pyrolysis of biomass with MCM-41 and CaO catalysts by using TGA-FTIR

- analysis, *Journal of Analytical and Applied Pyrolysis*, **89**, 171-177.
- [59] **Chen, G.**, 2003: Catalytic application to biomass pyrolysis in a fixed bed reactor, *Energy Sources*, **25**, 223-228.
- [60] **Duman, G., Pala, M., Ucar, S., & Yanik, J.**, 2013: Two-step pyrolysis of safflower oil cake, *Journal of Analytical and Applied Pyrolysis*, **103**, 352-361.
- [61] **Oasmaa, A., Elliott, D., & Korhonen, J.**, 2010: Acidity of biomass fast pyrolysis bio-oils, *Energy Fuels*, **24**, 6548-6554.
- [62] **Van de Beld, B., Holle, E., & Florjin, J.**, 2013: The use of pyrolysis oil and pyrolysis oil derived fuels in diesel engines for CHP applications, *Applied Energy*, **102**, 190-197.
- [63] **Chiaramonti, D., Bonini, M., Fratini, E., Tondi, G., Gartner, K., Bridgwater, A., et al.**, 2003: Development of emulsions from biomass pyrolysis liquid and diesel and their use in engines—Part 1: emulsion production, *Biomass and Bioenergy*, **25**, 85-99.
- [64] **Calabria, R., Chiariello, F., & Massoli, P.**, 2007: Combustion fundamentals of pyrolysis oil based fuels, *Experimental Thermal and Fluid Science*, **31**, 413-420.
- [65] **Yang, S., Hsu, T., Wu, C., Chen, K., Hsu, Y., & Li, Y.**, 2014: Application of biomass fast pyrolysis part II: The effects that bio-pyrolysis oil has on the performance of diesel engines, *Energy*, 1-9.
- [66] **Chiaramonti, D., Bonini, M., Fratini, E., Tondi, G., Gartner, K., Bridgwater, A., et al.**, 2003: Development of emulsions from biomass pyrolysis liquid and diesel and their use in engines—Part 2: tests in diesel engines, *Biomass and Bioenergy*, **25**, 101-111.
- [67] **Pelaez-Samaniego, M., Mesa-Pérez, J., Cortez, L., Rocha, J., Sanchez, C., & Marín, H.**, 2011: Use of blends of gasoline with biomass pyrolysis-oil derived fractions as fuels in an Otto engine, *Energy for Sustainable Development*, **15**, 376-381.
- [68] **Chiaramonti, D., Oasmaa, A., Solantausta, Y., & Peacocke, C.**, 2009: *The use of biomass derived fast pyrolysis liquids in power generation: Engines and turbines*, Technical Research Centre of Finland .
- [69] **Boucher, M.E., Chaala, A., & Roy, C.**, 2000: Bio-oils obtained by vacuum pyrolysis of softwood bark as a liquid fuel for gas turbines. Part I: Properties of bio-oil and its blends with methanol and a pyrolytic aqueous phase, *Biomass and Bioenergy*, **19**, 337-350.



- [70] **Juste, L., & Monfort, S.**, 2000: Preliminary test on combustion of wood derived fast pyrolysis oils in a gas turbine combustor, *Biomass and Bioenergy*, **19**, 119-128.
- [71] **Wang, C., Hao, Q., Lu, D., Jia, Q., Li, G., & Xu, B.**, 2008: Production of light aromatic hydrocarbons from biomass by catalytic pyrolysis, *Chinese Journal of Catalysis*, **29** (9), 907-912.
- [72] **Shadangi, K., & Mohanty, K.**, 2014: Production and characterization of pyrolytic oil by catalytic pyrolysis of Niger seed, *Fuel*, **126**, 109-115.
- [73] **Yorgun, S., & Şimşek, Y.**, 2008: Catalytic pyrolysis of *Miscanthus x giganteus* over activated alumina, *Bioresource Technology*, **99**, 8095-8100.
- [74] **Flanigen, E. M.**, 2001: Zeolites and Molecular Sieves: An Historical Perspective. H. van Bekkum, E.M. Flanigen, P. Jacobs, & J. Jansen (Eds). In *Introduction to Zeolite Science and Practice* (s. 11-12). Amsterdam: Elsevier.
- [75] **Payra, P., & Dutta, P.**, 2003: Zeolites: A Primer. S. Auerbach, K. Carrado, & P. Dutta (Eds) In, *Handbook of Zeolite Science and Technology* (s. 1-21). New York, USA: Marcel Dekker.
- [76] **Shen, Y., & Yoshikawa, K.**, 2013: Recent progresses in catalytic tar elimination during biomass gasification or pyrolysis-A review, *Renewable and Sustainable Energy Reviews*, **21**, 371-392.
- [77] **Jae, J., Tompsett, G., Foster, A., Hammond, K., Auerbach, S., Lobo, R., et al.**, 2011: Investigation into the shape selectivity of zeolite catalysts for biomass conversion, *Journal of Catalysis*, **279**, 257-268.
- [78] **McCusker, L.B., & Baerlocher, C.**, 2001: Zeolite Structures. P. Jacobs, E. Flanigen, J. Jansen, H. van Bekkum, P. Jacobs, E. Flanigen, J. Jansen, & H. van Bekkum (Eds). In, *Introduction to Zeolite Science and Practice* (s. 38-40). Amsterdam, Netherlands: Elsevier.
- [79] **Pattiya, A., Titiloye, J.O., & Bridgwater, A.V.**, 2008: Fast pyrolysis of cassava rhizome in the presence of catalysts. *Journal of Analytical and Applied Pyrolysis*, **81**, 72-79.
- [80] **Zheng, A., Zhao, Z., Chang, S., Huang, Z., Wu, H., Wang, X., et al.**, 2014: Effect of crystal size of ZSM-5 on the aromatic yield and selectivity from catalytic fast pyrolysis of biomass, *Journal of Molecular Catalysis A: Chemical*, **383-384**, 23-30.
- [81] **Shirazi, L., Jamshidi, E., & Ghasemi, M. R.**, 2008: The effect of Si/Al ratio of ZSM-5 zeolite on its morphology, acidity and crystal size, *Crystal Research Technology*, **43** (12), 1300-1306.

- [82] **Baerlocher, C., McCusker, L., & Olson, D.,** 2007: *Atlas of Zeolite Framework Types* (Sixth Revised Edition b.). Amsterdam, Netherlands: Elsevier.
- [83] **Carlson, T., Jae, J., Lin, Y.-C., Tompsett, G., & Huber, G.,** 2010: Catalytic fast pyrolysis of glucose with HZSM-5: The combined homogeneous and heterogeneous reactions, *Journal of Catalysis*, **270**, 110-124.
- [84] **Williams, P.T., & Horne, P.A.,** 1995: The influence of catalyst type on the composition of upgraded biomass pyrolysis oils, *Journal of Analytical and Applied Pyrolysis*, **31**, 39-61.
- [85] **Jae, J., Coolman, R., Mountziaris, T.J., & Huber, G.W.,** 2014: Catalytic fast pyrolysis of lignocellulosic biomass in a process development unit with continual catalyst addition and removal, *Chemical Engineering Science*, **108**, 33-46.
- [86] **Naqvi, S., Uemura, Y., & Bt Yusup, S.,** 2014: Catalytic pyrolysis of paddy husk in a drop type pyrolyzer for bio-oil production: The role of temperature and catalyst, *Journal of Analytical and Applied Pyrolysis*, **104**, 57-62.
- [87] **Zhang, M., Resende, F.L.P., & Moutsoglou, A.,** 2014: Catalytic fast pyrolysis of aspen lignin via Py-GC/MS, *Fuel*, **116**, 358-369.
- [88] **Murata, K., Liu, Y., Inaba, M., & Takahara, I.,** 2012: Catalytic fast pyrolysis of jatropha wastes, *Journal of Analytical and Applied Pyrolysis*, **94**, 75-82.
- [89] **Weitkamp, J., Ernst, S., & Puppe, L.,** 1999: Shape-Selective Catalysis in Zeolites. J. Weitkamp, & L. Puppe (Eds) In, *Catalysis and Zeolites: Fundamentals and Applications* (s. 327-370). Berlin, Germany: Springer-Verlag.
- [90] **Van Santen, R.,** 1994: Theory of Bronsted Acidity in Zeolites. J. Jansen, M. Stöcker, H. Karge, & J. Weitkamp (Eds) In, *Advanced Zeolite Science and Applications, Studies in Surface Science and Catalysis* (s. 273-294). Elsevier Science.
- [91] **Fogassy, G., Thegarid, N., Schuurman, Y., & Mirodatosa, C.,** 2011: From biomass to bio-gasoline by FCC co-processing: effect of feed composition and catalyst structure on product quality, *Energy & Environmental Science*, **(4)**, 5068-5076.
- [92] **Kim, J., Park, S., Jinho, J., Jeon, J.-K., Ko, C., Jeong, K.-E., et al.,** 2013: Catalytic pyrolysis of mandarin residue from the mandarin juice processing industry, *Bioresource Technology*, **(136)**, 431-436.

- [93] **Kerssens, M.M., Sprung, C., Whiting, G.T., & Weckhuysen, B.M.**, 2014: Selective staining of zeolite acidity: Recent progress and future perspectives on fluorescence microscopy, *Microporous and Mesoporous Materials*, (**189**), 136-143.
- [94] **Laredo, G.C., Quintana-Solórzano, R., Castillo, J.J., Armendáriz-Herrera, H., & Garcia-Gutier, J.L.**, 2013: Benzene reduction in gasoline by alkylation with propylene over MCM-22 zeolite with a different Brønsted/Lewis acidity ratios, *Applied Catalysis A: General*, (**454**), 37-45.
- [95] **Ateş, F., & Işıkdag, M.A.**, 2009: Influence of temperature and alumina catalyst on pyrolysis of corncob, *Fuel*, **88**, 1991-1997.
- [96] **Wang, P., Zhan, S., Yu, H., Xue, X., & Hong, N.**, 2010: The effects of temperature and catalysts on the pyrolysis of industrial wastes(herb residue), *Bioresource Technology*, **101**, 3236-3241.
- [97] **Smets, K., Roukaerts, A., Czech, J., Reggers, G., Schreurs, S., Carleer, R., et al.**, 2013: Slow catalytic pyrolysis of rapeseed cake: Product yield and characterization of the pyrolysis liquid, *Biomass and Bioenergy*, 1-11.
- [98] **Lehto, J., Oasmaa, A., Solantausta, Y., Kytö, M., & Chiaramonti, D.**, 2013: *Fuel oil quality and combustion of fast pyrolysis of bio-oils*, VTT Technical Research Centre of Finland, Espoo.
- [99] **Fan, Y., Cai, Y., Li, X., Yu, N., & Yin, H.**, 2014: Catalytic upgrading of pyrolytic vapors from the vacuum pyrolysis of rape straw over nanocrystalline HZSM-5 zeolite in a two-stagefixed-bed reactor, *Journal of Analytical and Applied Pyrolysis* .
- [100] **Azargohar, R., Jacobson, K., Powell, E., & Dalai, A.**, 2013: Evaluation of properties of fast pyrolysis products obtained from Canadian waste biomass, *Journal of Analytical and Applied Pyrolysis*, **104**, 330-340.
- [101] **Shadangi, K.P., & Mohanty, K.**, 2014: Comparison of yield and fuel properties of thermal and catalytic Mahua seed pyrolytic oil, *Fuel*, **117**, 372-380.
- [102] **Shadangi, K.P., & Mohanty, K.**, 2014: Thermal and catalytic pyrolysis of Karanja seed to produce liquid fuel, *Fuel*, **114**, 434-442.
- [103] **Yu, F., Gao, L., Wang, W., Zhang, G., & Ji, J.**, 2013: Bio-fuel production from the catalytic pyrolysis of soybean oil over Me-Al-MCM-41 (Me = La, Ni or Fe) mesoporous materials, *Journal of Analytical and Applied Pyrolysis*, **104**, 325-329.
- [104] **Hoekstra, E., Kersten, S., Tudos, A., Meier, D., & Hogendoorn, K.**, 2011: Possibilities and pitfalls in analyzing (upgraded) pyrolysis oil by size

exclusion chromatography (SEC), *Journal of Analytical and Applied Pyrolysis*, **91**, 76-88.

- [105] **Diebold, J.P., & Czernik, S.**, 1997: Additives to lower and stabilize the viscosity of pyrolysis oils during storage, *Energy & Fuels*, **11**, 1081-1091.
- [106] **Oasmaa, A., Leppämäki, E., Koponen, P., Levander, J., & Tapola, E.**, 1997: *Physcial characterisation of biomass-based pyrolysis liquids. Application of standard fuel oil analyses*. VTT Technical Centre of Finland, Espoo.
- [107] **Bartholomew, C.H.**, 2001: Mechanisms of catalyst deactivation, *Applied Catalysis A: General* , **212**, 17-60.
- [108] **Forzatti, P., & Lietti, L.**, 1999: Catalyst deactivation, *Catalysis Today* , **52**, 165-181.
- [109] **Sie, S.T.**, 2001: Consequences of catalyst deactivation for process design and operation, *Applied Catalysis A: General*, **212**, 129-151.
- [110] **Kahrizangi-Ebrahimi, R., & Abbasi, M.H.**, 2008: Evaluation of reliability of Coats-Redfern method for kinetic analysis of non-isothermal TGA, *Transactions of Nonferrous Metals Society of China*, **18**, 217-221.
- [111] **Carlson, T.R., Tompsett, G.A., Conner, W.C., & Huber, G.W.**, 2009: Aromatic production from catalytic fast pyrolysis of biomass-derived feedstocks, *Topics in Catalysis*, **52**, 241-252.

## **CURRICULUM VITAE**

**Name Surname:** Şeyma HACİBEKTAŞOĞLU

**Place and Date of Birth:** Üsküdar/ 9 August 1986

**Address:** Rüstem Paşa Mah. Çakıllı Sok. Mesken Ap. NO: 12/7 77200 YALOVA

**E-Mail:** seyma.hacibektasoglu@hotmail.com

**B.Sc.:** Kocaeli University, Chemical Engineering, 2010

## **PUBLICATIONS/PRESENTATIONS ON THE THESIS**

▪ **Hacibektaşoğlu Ş., Başakçılardan Kabakcı S.,** 2014: Zeytin Küspesinin Katalitik Piroлизine Ait Kinetiğinin İncelenmesi, *Enerji Tarımı ve Biyoyakıtlar 4. Ulusal Çalıştayı*, 28-29 Mayıs, Samsun, Türkiye.

